PTEP
Prog. Theor. Exp. Phys. **2014**, 083B04 (48 pages)
DOI: 10.1093/ptep/ptu113

One-loop radiative correction to Kaluza–Klein masses in S^2/Z_2 universal extra-dimensional model

Nobuhito Maru[1,*], Takaaki Nomura[2,*], and Joe Sato[3,*]

[1]*Department of Mathematics and Physics, Osaka City University, Osaka, 558-8585, Japan*
[2]*Department of Physics, National Cheng-Kung University, Tainan 701, Taiwan*
[3]*Department of Physics, Saitama University, Shimo-Okubo, Sakura-ku, Saitama 355-8570, Japan*
*E-mail: nmaru@sci.osaka-cu.ac.jp, nomura@mail.ncku.edu.tw, joe@phy.saitama-u.ac.jp

Received April 29, 2014; Revised July 23, 2014; Accepted July 23, 2014; Published August 21, 2014

We investigate a radiative correction to the masses of Kaluza–Klein (KK) modes in a universal extra-dimensional model defined on a six-dimensional spacetime with extra space as a two-sphere orbifold S^2/Z_2. We first define the Feynman rules which are necessary for the calculation. We then calculate the one-loop diagrams which contribute to the radiative corrections to the KK masses, and obtain one-loop corrections to masses for fermions, gauge bosons, and scalar bosons. We estimate the one-loop corrections to KK masses for the first KK modes of standard model particles as a function of momentum cut-off scale, and we determine the lightest KK particle which would be a promising candidate for dark matter.

Subject Index B33, B40, B43, B71

1. Introduction

The Standard Model (SM) has been well established. It has indeed passed the test of the accelerator experiments. It is, however, not a satisfactory theory for all physicists. There seem to be several flaws, e.g., the hierarchy problems, no candidate for dark matter (DM), and so on. With the fact that relic abundance of dark matter is well explained by a weakly interacting massive particle, these problems strongly indicate a new physics beyond the SM at TeV scale.

There are many candidates for such models, for example models with supersymmetry, little Higgs, extra dimensions, and so on. Since the Large Hadron Collider (LHC) experiment is now operating, which will explore physics at the TeV scale, it is urgent to investigate possible models at that scale.

Among these, the idea of a universal extra-dimensional (UED) model is very interesting [1,2]. The minimal version of UED has recently been studied very extensively. It is a model with one extra dimension defined on an orbifold S^1/Z_2. This orbifold is given by identifying the extra spatial coordinate y with $-y$ and hence there are fixed points $y = 0, \pi$. By this identification chiral fermions are obtained. It is shown that this model is free from the current experimental constraints if the scale of the extra dimension, $1/R$, which is the inverse of the compactification radius R, is larger than 400 GeV [1,3–11]. Dark matter can be explained by the first or second Kaluza–Klein (KK) mode [12–19], which is often the first KK photon, and this model can be discriminated from other models [20,21]. This model can also give plausible explanations for SM neutrino masses which are embedded in extended models [22].

In contrast with the UED models in five dimensions, UED models in six dimensions have interesting properties which would explain some problems in the SM. For example, in six dimensions, the

Funded by SCOAP[3]

number of generations of quarks and leptons is derived by anomaly cancellations [23], and proton stability is guaranteed by a discrete symmetry of a subgroup of six-dimensional Lorentz symmetry [24]. Candidates for UED models in a six-dimensional model are the one with extra dimensions of T^2, a torus [1], or the one with S^2, a sphere [25,26]. In these two classes of model, the latter is quite new and its phenomenology has been studied recently in Refs. [27–30].

Although we do not have experimental hints of the existence of extra dimensions at the moment, it is meaningful to explore non-minimal UED models. There are many kind of UED models and we should know the properties for different models to test them in experiments. For example, we can explore preferred KK mass scale by estimating the relic density of dark matter for each UED model using the KK mass spectrum and couplings, and it will suggest what values of KK masses we can expect to discover in collider experiments. Thus it is important to investigate properties of each UED model such as mass spectrum and couplings to examine the validity of the UED in experiments. Furthermore, S^2 has the structure of the simplest coset space SU(2)/U(1) and it has been applied in the Coset Space Unification scenario [31,32] to construct unified models. Thus it is worth investigating the radiative corrections to the mass spectrum of the KK modes even apart from UED models.

To study it in detail, first of all we have to calculate the quantum correction to the mass spectrum. It is well known that at tree level all the particles in the same Kaluza–Klein (KK) mode are degenerate in mass and therefore it is impossible to predict even a decay mode. It is hence inevitable to calculate the quantum correction to their mass to find its phenomenological consequences, say, collider signatures. This small correction relative to their tree mass is crucial since mass differences from it are "infinitely" large compared with at tree level, and hence it determines physics. In the five-dimensional model, radiative corrections to KK masses and couplings are discussed in [33] where the importance of choice of regulator is taken into account [34,35]. For the UED model, the authors of [36] have calculated the radiative corrections in S^1 and T^2. Also, the running Higgs self-couplings and Yukawa couplings are discussed in [37] for the T^2 UED and in [30] for S^2-based UED models. However, there is no calculation of the corrected KK masses for the S^2 model [25].

In models with a two-sphere, fermions cannot be massless because of the positive curvature and hence they have a mass of $O(1/R)$ [38,39]. We cannot overcome the theorem simply by the orbifolding of the extra spaces. In usual cases, we have no massless fermion on the curved space with positive curvature, but we know a mechanism to obtain a massless fermion on that space by introducing a non-trivial background gauge field [40,41]. The non-trivial background gauge field can cancel the spin connection term in the covariant derivative. As a result, a massless fermion naturally appears. Furthermore, we note that the background gauge field configuration is energetically favorable since the background gauge kinetic energy lowers the total energy. In order to realize chiral fermions, the orbifolding is required, for instance. Unfortunately it makes the calculation of the quantum correction very difficult.

In this paper, we study a new type of UED with S^2/Z_2 extra dimensions. We treat this theory as a cut-off theory. We show Feynmann rules for it and calculate the quantum correction as a function of the cut-off. By this we show the mass spectrum for the theory and offer a basis for studying phenomenology, such as LHC physics.

The paper is organized as follows. In Sect. 2, we recapitulate the model [25]. We then specify the Feynman rules for propagators and vertices on the six-dimensional spacetime with the S^2/Z_2 extra space. In Sect. 3, we discuss the one-loop calculation for KK mass correction and derive formulas to estimate corrected KK masses. In Sect. 4, we estimate the corrected first KK masses for each SM

particle and determine the lightest KK particle of the model. Section 5 is devoted to the summary and discussions.

2. S^2/Z_2 UED model

In this section, we first review the universal extra dimensions defined on the six-dimensional spacetime which has extra space as a two-sphere orbifold S^2/Z_2 [25]. We then define Feynman rules relevant to our calculation.

2.1. Structure of the model

The model is defined on the six-dimensional spacetime M^6 which has extra dimensional space compactified as the two-sphere orbifold S^2/Z_2. The coordinates of M^6 are denoted by $X^M = (x^\mu, y^\theta = \theta, y^\phi = \phi)$, where x^μ and $\{\theta, \phi\}$ are the M^4 coordinates and the S^2 spherical coordinates, respectively. The orbifold is defined by identifying the point (θ, ϕ) with $(\pi - \theta, -\phi)$.

The spacetime index M runs over $\mu \in \{0, 1, 2, 3\}$ and $\alpha \in \{\theta, \phi\}$. The metric of M^6 can be written as

$$g_{MN} = \begin{pmatrix} \eta_{\mu\nu} & 0 \\ 0 & -g_{\alpha\beta} \end{pmatrix}, \tag{1}$$

where $\eta_{\mu\nu} = \mathrm{diag}(1, -1, -1, -1)$ and $g_{\alpha\beta} = \mathrm{diag}(R^2, R^2 \sin^2\theta)$ are metrics of M^4 and S^2/Z_2 with a radius R, respectively, with the radius of S^2/Z_2 as R.

We introduce a gauge field $A_M(x, y) = (A_\mu(x, y), A_\alpha(x, y))$, SO(1,5) chiral fermions $\Psi_\pm(x, y)$, and the complex scalar field $H(x, y)$ as the SM Higgs field. The chiral fermion is defined by the action of the SO(1,5) chiral operator $\Gamma_7 = \gamma_5 \otimes \sigma_3$, where σ_i $(i = 1, 2, 3)$ are Pauli matrices and γ_5 is the SO(1,3) chiral operator, such that

$$\Gamma_7 \Psi_\pm(x, y) = \pm \Psi_\pm(x, y), \tag{2}$$

so that the chiral projection operator is given by $\Gamma_\pm = (1 \pm \Gamma_7)/2$. The boundary conditions for each field can be defined as

$$\Psi_\pm^{(\pm\gamma_5)}(x, \pi - \theta, -\phi) = \pm \Upsilon_5 \Psi_\pm^{(\pm\gamma_5)}(x, \theta, \phi), \tag{3}$$

$$A_\mu(x, \pi - \theta, -\phi) = A_\mu(x, \theta, \phi), \tag{4}$$

$$A_\alpha(x, \pi - \theta, -\phi) = -A_\alpha(x, \theta, \phi), \tag{5}$$

$$H(x, \pi - \theta, -\phi) = H(x, \theta, \phi), \tag{6}$$

where $\Upsilon_5 = \gamma_5 \otimes I_2$ with I_2 being the 2×2 identity, requiring the invariance of an action in six dimensions under the Z_2 transformation.

The gauge symmetry of the model is $G = \mathrm{SU}(3) \times \mathrm{SU}(2) \times \mathrm{U}(1)_Y \times \mathrm{U}(1)_X$ defined on the six-dimensional spacetime with gauge-coupling constants g_{6a} in six dimensions where the index $a = \{X, 1, 2, 3\}$ distinguishes the gauge symmetries $\mathrm{U}(1)_X$, $\mathrm{U}(1)_Y$, SU(2), and SU(3). The extra $\mathrm{U}(1)_X$ is introduced, which is associated with a background gauge field A_ϕ^B given by [41–43],

$$A_\phi^B = \hat{Q}_X \cos\theta, \tag{7}$$

where $\hat{Q}_X$ is the $\mathrm{U}(1)_X$ charge operator, in order to obtain massless chiral fermions in four dimensions. We then assign the $\mathrm{U}(1)_X$ charge $\hat{Q}_X = \frac{1}{2}$ to fermions as the simplest case in which massless

Table 1. The fermion contents in the model where the representations under gauge symmetry, SO(1,5) chirality, and the boundary conditions are shown.

	$Q(x, y)$	$U(x, y)$	$D(x, y)$	$L(x, y)$	$E(x, y)$
(SU(3), SU(2))(U(1)$_Y$, U(1)$_X$)	$(3, 2)\left(\frac{1}{6}, \frac{1}{2}\right)$	$(3, 1)\left(\frac{3}{2}, \frac{1}{2}\right)$	$(3, 1)\left(-\frac{1}{3}, \frac{1}{2}\right)$	$(1, 2)\left(-\frac{1}{2}, \frac{1}{2}\right)$	$(1, 1)\left(-1, \frac{1}{2}\right)$
SO(1,5) chirality	$-$	$+$	$+$	$-$	$+$
Boundary condition	$-$	$+$	$+$	$-$	$+$

SM fermions appear in four dimensions. Fermions in six dimensions are thus introduced as in Table 1 with zero modes corresponding to SM fermions. Then the action of our model in six dimensions is written as:

$$
\begin{aligned}
S_{6D} = & \int \mathrm{d}x^4 R^2 \sin\theta \mathrm{d}\theta \mathrm{d}\phi [(\bar{Q}, \bar{U}, \bar{D}, \bar{L}, \bar{E}) \mathrm{i}\Gamma^M D_M (Q, U, D, L, E)^T \\
& - g^{MN} g^{KL} \sum_a \frac{1}{4(g_{6a})^2} Tr[F_{aMK} F_{aNL}] \\
& - \frac{R^2}{2\xi (g_{6a})^2} \left[(\partial_\mu A^\mu)^2 + \frac{\xi^2}{R^4 \sin^2\theta} \left(\partial_\theta (\sin\theta A_\theta) + \frac{1}{\sin\theta} \partial_\phi A_\phi \right) \right. \\
& \left. - \frac{2\xi}{R^2 \sin\theta} (\partial_\mu A^\mu) \left(\partial_\theta (\sin\theta A_\theta) + \frac{1}{\sin\theta} \partial_\phi A_\phi \right) \right] \\
& + \bar{c} \left(\partial^\mu D_\mu + \frac{\xi}{R^2 \sin\theta} \partial_\theta (\sin\theta D_\theta) + \frac{\xi}{R^2 \sin^2\theta} \partial_\phi (D_\phi) \right) c \\
& + (D^M H)^\dagger (D_M H) - \mu^2 H^\dagger H + \frac{\lambda_6}{4} (H^\dagger H)^2 \\
& + [Y_u Q \bar{U} H^* + Y_d Q \bar{D} H + Y_e L \bar{E} H + \mathrm{h.c.}]], \qquad (8)
\end{aligned}
$$

where the Γ^M in the first line in the right-hand side are gamma matrices in six dimensions defined as $\Gamma^M = \{\gamma^\mu \otimes I_2, \gamma_5 \otimes \mathrm{i}\sigma_1, \gamma_5 \otimes \mathrm{i}\sigma_2\}$ with the four-dimensional Gamma matrices γ^μ, the third to the fourth lines are gauge-fixing terms with the gauge-fixing parameter ξ, the fifth line corresponds to a ghost term for the non-Abelian gauge group, the sixth line denotes a Lagrangian for the Higgs field, and the last line denotes Yukawa interactions with Yukawa couplings $Y_{u,d,e}$ in six dimensions.

We note here that the U(1)$_X$ gauge symmetry should be broken to avoid a massless gauge boson. In [25], we discussed that the U(1)$_X$ symmetry is anomalous and is broken at the quantum level, so that its gauge boson should be heavy at the UV cut-off scale. However, it is also discussed that if U(1)$_X$ is broken at high scale, the classical monopole configuration is changed by the mass term of the gauge boson, and the spontaneous compactification mechanism is spoiled [26,44]. Thus it would be necessary to introduce some mechanism to recover the monopole configuration. As another possibility, we can consider a lower breaking scale of U(1)$_X$ than the compactification scale if U(1)$_X$ is not anomalous, introducing suitable fermion content. This case will give a Z' boson which would be relatively light, and it can accommodate observed data if the gauge coupling of U(1)$_X$ is small enough. Also, its first KK mode will be heavier than the lightest KK mode of SM particles since the zero mode is not massless and quantum correction would be small due to small coupling, and it will not be a DM candidate consistent with our analysis below. In this paper, we will not discuss further the U(1)$_X$ issue since it is beyond the scope of our discussion.

The KK masses for each particle are obtained from the kinetic terms in Eq. (8), by expanding fields on six dimensions using KK mode functions. The fermions $\Psi_{\pm}^{(\pm\gamma_5)}$ are expanded in terms of the eigenfunctions of the Dirac operator on S^2 which are given as

$$\Psi_{\ell m(\neq 0)}(\theta,\phi)=\begin{pmatrix}\tilde{\alpha}_{\ell m}(z,\phi)\\ \tilde{\beta}_{\ell m}(z,\phi)\end{pmatrix}=\frac{e^{\ell m\phi}}{\sqrt{2\pi}}\begin{pmatrix}C_{\tilde{\alpha}}^{\ell m}(1-z)^{\frac{1}{2}|m|}(1+z)^{\frac{1}{2}|m|}P_{\ell-|m|}^{(|m|,|m|)}(z)\\ C_{\tilde{\beta}}^{\ell m}(1-z)^{\frac{1}{2}|m+1|}(1+z)^{\frac{1}{2}|m-1|}P_{\ell-|m|}^{(|m+1|,|m-1|)}(z)\end{pmatrix}, \tag{9}$$

$$\Psi_{\ell 0}(\theta,\phi)=\begin{pmatrix}\tilde{\alpha}_{\ell 0}(z)\\ \tilde{\beta}_{\ell-10}(z)\end{pmatrix}=\frac{1}{\sqrt{2\pi}}\begin{pmatrix}C_{\tilde{\alpha}}^{\ell 0}P_{\ell}^{(0,0)}(z)\\ C_{\tilde{\beta}}^{\ell-10}\sqrt{1-z^2}P_{\ell-1}^{(1,1)}(z)\end{pmatrix}, \tag{10}$$

where $P_{\ell}^{(m,n)}(z)$ is a Jacobi polynomial with $z=\cos\theta$, $C_{\tilde{\alpha}(\tilde{\beta})}^{\ell m}$ are the normalization constants determined by $\int d\Omega\tilde{\alpha}^*\tilde{\alpha}(\tilde{\beta}^*\tilde{\beta})=1$, and the indices $\{\ell,m\}$ correspond to angular momentum quantum numbers on the two-sphere specifying KK modes [25,39]. These mode functions satisfy

$$i\hat{D}\Psi_{\ell m}=-\frac{1}{R}\left[\sigma_1\left(\partial_\theta+\frac{\cos\theta}{2}\right)+\sigma_2\left(\frac{1}{\sin\theta}\partial_\phi+\hat{Q}_X\cot\theta\right)\right]\Psi_{\ell m}=M_\ell\Psi_{\ell m}, \tag{11}$$

where $M_\ell=\frac{\sqrt{\ell(\ell+1)}}{R}$, corresponding to KK mass, and $i\hat{D}$ is the Dirac operator on S^2/Z_2 with the background gauge field in Eq. (7). They also satisfy the completeness relation

$$\sum_{\ell=0}^{\infty}\sum_{m=-\ell}^{\ell}\Psi_{\ell m}(z,\phi)\Psi_{\ell m}^{\dagger}(z',\phi')=\delta(z-z')\delta(\phi-\phi'). \tag{12}$$

A fermion $\Psi_{+}^{(\pm\gamma_5)}(x,\theta,\phi)$ on $M^4\times S^2/Z_2$, satisfying boundary condition Eq. (3), is expanded as

$$\Psi_{+}^{(\pm\gamma_5)}(x,\theta,\phi)=\sum_{\ell m}\frac{1}{\sqrt{2}}\begin{pmatrix}[\tilde{\alpha}_{\ell m}(\theta,\phi)\pm\tilde{\alpha}_{\ell m}(\pi-\theta,-\phi)]P_R\psi_{\ell m}(x)\\ [\tilde{\beta}_{\ell m}(\theta,\phi)\mp\tilde{\beta}_{\ell m}(\pi-\theta,-\phi)]P_L\psi_{\ell m}(x)\end{pmatrix}, \tag{13}$$

where $\psi_{\ell m}$ shows an SO(1,3) Dirac fermion, $P_{L(R)}$ are chiral projection operators in four dimensions, and $\{P_L,P_R\}$ are interchanged in the right-hand side for $\Psi_{-}^{(\pm\gamma_5)}(x,\theta,\phi)$. Then the kinetic and KK mass terms for KK modes are given in terms of $\psi_{\ell m}$ such that

$$\begin{aligned}&\int d\Omega\Psi_{\pm}^{(\pm\gamma_5)}(x,\theta,\phi)i\Gamma^M\partial_M\Psi_{\pm}^{(\pm\gamma_5)}(x,\theta,\phi)\\ &\quad=\sum_{\ell m}\epsilon_{\ell m}\left[\bar{\psi}_{\ell m}(x)i\gamma^\mu\partial_\mu\psi_{\ell m}(x)\pm M_\ell\bar{\psi}_{\ell m}(x)\gamma_5\psi_{\ell m}(x)\right],\end{aligned} \tag{14}$$

where $\epsilon_{\ell m}$ is 0 for $\{\ell=\text{odd},m=0\}$ and unity for other modes. We also need to take into account Yukawa couplings of Higgs zero mode and fermion non-zero KK modes to obtain the mass spectrum of the KK particles after the electroweak symmetry breaking. The Yukawa coupling with Higgs zero mode H^{00} is written as

$$L_Y=\sum_{\ell m}\frac{Y}{\sqrt{4\pi R^2}}\left[\bar{\psi}_{\ell m}^F(x)H^{00}(x)P_L\psi_{\ell m}^f(x)+\bar{\psi}_{\ell m}^F(x)H^{00}(x)P_R\psi_{\ell m}^f(x)\right]+\text{h.c.}, \tag{15}$$

where $\psi^F = Q, L$ correspond to SU(2) doublets and $\psi^f = U, D, E$ correspond to SU(2) singlets. After the zero-mode Higgs getting a vacuum expectation value (VEV), we have the mass term of the KK modes in the form

$$L_{\psi\,\mathrm{mass}} = \begin{pmatrix} \bar{\psi}^F_{\ell m} & \bar{\psi}^f_{\ell m} \end{pmatrix} \begin{pmatrix} M_\ell & m_{\mathrm{SM}} \\ m_{\mathrm{SM}} & -M_\ell \end{pmatrix} \begin{pmatrix} \psi^F_{\ell m} \\ \psi^f_{\ell m} \end{pmatrix}, \tag{16}$$

where m_{SM} expresses the masses in the SM, and the mass spectrum is obtained by diagonalizing the mass matrix.

The four-dimensional components of gauge fields $A_\mu(x, \theta, \phi)$ are expanded in terms of a linear combination of spherical harmonics, satisfying boundary condition Eq. (4), such that

$$A_\mu(x, \theta, \phi) = \sum_{\ell m} Y^+_{\ell m}(\theta, \phi) A_{\ell m \mu}(x), \tag{17}$$

where $Y^+_{\ell m}(\theta, \phi) = (\mathrm{i})^{\ell+m}[Y_{\ell m}(\theta, \phi) + (-1)^\ell Y_{\ell -m}(\theta, \phi)]/\sqrt{2}$ for $m \neq 0$ and $Y^+_{\ell 0}(\theta) = Y_{\ell 0}(\theta)(0)$ for $m = 0$ with $\ell =$ even(odd), respectively. Then the kinetic and KK mass terms for the KK modes are obtained as

$$\begin{aligned} &\int \mathrm{d}\Omega \left[-\frac{1}{4} F^{\mu\nu}(x, \theta, \phi) F_{\mu\nu}(x, \theta, \phi) - \frac{1}{2} g^{\mu\alpha} g^{\nu\beta} F_{\mu\alpha}(x, \theta, \phi) F_{\mu\beta}(x, \theta, \phi) \right] \\ &\supset \int \mathrm{d}\Omega \left[-\frac{1}{4} F^{\mu\nu}(x, \theta, \phi) F_{\mu\nu}(x, \theta, \phi) + \frac{1}{2} A^\mu(x, \theta, \phi) \hat{L}^2 A_\mu(x, \theta, \phi) \right] \\ &= \sum_{\ell m} \epsilon_{\ell m} \left[-\frac{1}{4} F^{\mu\nu}_{\ell m}(x) F_{\ell m \mu\nu}(x) + \frac{1}{2} M^2_\ell A^\mu_{\ell m}(x) A_{\ell m \mu}(x) \right], \end{aligned} \tag{18}$$

where $\hat{L}^2 = -(1/\sin\theta)\partial_\theta(\sin\theta\,\partial_\theta) - (1/\sin^2\theta)\partial^2_\phi$ is the square of the angular momentum operator and $\epsilon_{\ell m}$ is the same as in Eq. (14). After electroweak symmetry breaking, the KK modes of the $W^\pm$ and Z bosons also obtain the contribution of SM mass $m^2_W W^{+\ell m}_\mu W^{\mu -\ell m}$ and $m^2_Z Z^{\ell m}_\mu Z^{\mu \ell m}$ respectively.

The Lagrangian quadratic in $\{A_\theta, A_\phi\}$ is given by

$$\begin{aligned} L_{A_\theta, A_\phi\ \mathrm{quadratic}} = \frac{1}{2g^2} \sin\theta \Bigg[&(\partial_\mu A_\theta)(\partial^\mu A_\theta) + (\partial_\mu \tilde{A}_\phi)(\partial^\mu \tilde{A}_\phi) \\ &- \frac{1}{R^2 \sin^2\theta}((\partial_\theta \sin\theta \tilde{A}_\phi) - (\partial_\phi A_\theta))^2 - \frac{\xi}{R^2 \sin^2\theta}((\partial_\theta \sin\theta A_\theta) + \partial_\phi \tilde{A}_\phi)^2 \Bigg], \end{aligned} \tag{19}$$

where $\tilde{A}_\phi = A_\phi/\sin\theta$ and the second line in the right-hand side corresponds to a gauge-fixing term. This Lagrangian is not diagonal for $\{A_\theta, A_\phi\}$ so that we carry out the substitution

$$A_\theta(x, \theta, \phi) = \partial_\theta \phi_2(x, \theta, \phi) - \frac{1}{\sin\theta} \partial_\phi \phi_1(x, \theta, \phi), \tag{20}$$

$$\frac{A_\phi(x, \theta, \phi)}{\sin\theta} = \partial_\theta \phi_1(x, \theta, \phi) + \frac{1}{\sin\theta} \partial_\phi \phi_2(x, \theta, \phi), \tag{21}$$

to diagonalize the quadratic terms. Then the quadratic terms become

$$L_{A_\theta, A_\phi\ \mathrm{quadratic}} = \frac{1}{g^2} \sin\theta \left[\partial_\mu \phi_1 \partial^\mu (\hat{L}^2 \phi_1) + \partial_\mu \phi_2 \partial^\mu (\hat{L}^2 \phi_2) - \frac{1}{R^2}(\hat{L}^2 \phi_1)^2 - \frac{\xi}{R^2}(\hat{L}^2 \phi_1)^2 \right]. \tag{22}$$

Thus the mode functions for the extra-dimensional components' gauge field ϕ_i is given as

$$\tilde{Y}_{\ell m}(\theta,\phi) = \frac{1}{\sqrt{\ell(\ell+1)}} Y_{\ell m}(\theta,\phi), \tag{23}$$

where the factor of $1/\sqrt{\ell(\ell+1)}$ is required for normalization due to the extra $\hat{L}^2$ factor in Eq. (22). Then $\phi_i(\theta,\phi,x)$ is expanded as

$$\phi_i(x,\theta,\phi) = \sum_{\ell m} \tilde{Y}^+_{\ell m}(\theta,\phi)\phi_{i\ell m}(x), \tag{24}$$

taking into account the boundary condition Eq. (5). Therefore, KK mass terms for ϕ_i are obtained as

$$\begin{aligned}
&\frac{1}{2}\int \mathrm{d}\Omega \Bigg[\partial_\mu\phi_1(x,\theta,\phi)\partial^\mu(\hat{L}^2\phi_1(x,\theta,\phi)) + \partial_\mu\phi_2(x,\theta,\phi)\partial^\mu(\hat{L}^2\phi_2(x,\theta,\phi)) \\
&\quad - \frac{1}{R^2}(\hat{L}^2\phi_1)^2 - \frac{\xi^2}{R^2}(\hat{L}^2\phi_2)^2 \Bigg] \\
&\quad = \sum_{\ell m} \epsilon_{\ell m} \Big[\partial_\mu\phi_{1\ell m}\partial^\mu\phi_{1\ell m} + \partial_\mu\phi_{2\ell m}\partial^\mu\phi_{2\ell m} - M_\ell^2\phi_{1\ell m}\phi_{1\ell m} - \xi M_\ell^2\phi_{2\ell m}\phi_{2\ell m} \Big],
\end{aligned} \tag{25}$$

where $\epsilon_{\ell m}$ is 0 for $\{\ell = \text{odd}, m = 0\}$ and unity for other modes, the gauge-fixing parameter ξ is taken as 1 in our analysis applying the Feynman–t'Hooft gauge, and the KK modes of ϕ_2 are interpreted as Nambu–Goldstone (NG) bosons. These NG bosons will be eaten by KK modes of four-dimensional components of the gauge field giving their longitudinal component. After electroweak symmetry breaking, KK modes corresponding to extra components for $W^\pm$ and Z fields obtain the contribution of SM mass $m_W^2 W_{1,2}^{+\ell m} W_{1,2}^{-\ell m}$ and $m_Z^2 Z_{1,2}^{\ell m} Z_{1,2}^{\ell m}$, respectively.

The mode function for the scalar field is also given by the spherical harmonics $Y_{\ell m}(\theta,\phi)$, and $H(x,\theta,\phi)$ on $M^4 \times S^2/Z_2$ is expanded as

$$H(x,\theta,\phi) = \sum_{\ell m} Y^+_{\ell m}(\theta,\phi) H_{\ell m}(x), \tag{26}$$

taking into account the boundary condition Eq. (6). Thus the kinetic and KK mass terms are obtained as

$$\begin{aligned}
&\int \mathrm{d}\Omega \Big[\partial^\mu H^\dagger(x,\theta,\phi)\partial_\mu H(x,\theta,\phi) - \hat{L}^2 H^\dagger(x,\theta,\phi) H(x,\theta,\phi) \Big] \\
&\quad = \sum_{\ell m} \epsilon_{\ell m} \Big[\partial^\mu H^\dagger_{\ell m}\partial_\mu H_{\ell m} - M_\ell^2 H^\dagger_{\ell m} H_{\ell m} \Big],
\end{aligned} \tag{27}$$

and we also have SM Higgs mass contribution $m_H^2 (H^{\ell m})^\dagger H^{\ell m}$. Therefore, the KK masses are given, in general, at tree level, as

$$m_\ell^2 = \frac{\ell(\ell+1)}{R^2} + m_{\mathrm{SM}}^2, \tag{28}$$

which is characterized by angular momentum number ℓ but independent of m. Also, the KK parity is defined as $(-1)^m$ for each KK particle due to discrete Z_2' symmetry of $(\theta,\phi) \to (\theta,\phi+\pi)$, which is understood as the symmetry under the exchange of two fixed points on the S^2/Z_2 orbifold, $\left(\frac{\pi}{2},0\right)$ and $\left(\frac{\pi}{2},\pi\right)$. Thus we can confirm the stability of the lightest KK particle with odd parity.

2.2. *Propagators on the six dimensions with S^2/Z_2 extra space*

Here we discuss the Feynman rules for propagators and vertices on $M^4 \times S^2/Z_2$ for a fermion and a gauge boson. We first consider propagators on $M^4 \times S^2$ and then derive the rules after orbifolding taking into account the boundary conditions of fields on S^2/Z_2. The propagator of fermion $S_F(x - x', z - z', \phi - \phi') = \langle \Psi(x, \theta, \phi)\bar{\Psi}(x, \theta, \phi)\rangle$ on $M^4 \times S^2$, here Ψ being a Dirac fermion, is defined as an inverse matrix of the Dirac operator on six dimensions:

$$\mathrm{i}\Gamma^M \partial_M = \mathrm{i}\Gamma^\mu \partial_\mu + \mathrm{i}\Gamma^\alpha \partial_\alpha, \tag{29}$$

where the $\mathrm{i}\Gamma^\alpha \partial_\alpha = \gamma_5 \otimes \mathrm{i}\hat{D}$ are the extra-dimensional components of the Dirac operator in six dimensions, with $\mathrm{i}\hat{D}$ given in Eq. (11). Then the propagator should satisfy

$$\mathrm{i}\Gamma^M \partial_M S_F(x - x', z - z', \phi - \phi') = \frac{\mathrm{i}}{R^2}\delta^{(4)}(x - x')\delta(z - z')\delta(\phi - \phi'), \tag{30}$$

where the R^2 factor on the right-hand side is included to compensate mass dimensions. Then $S_F(x - x', z - z', \phi - \phi')$ can be written, using the mode function in Eqs. (9) and (10), as

$$\begin{aligned} S_F(x - x', z - z', \phi - \phi') = \sum_{\ell=0}^{\infty}\sum_{m=-\ell}^{\ell}\int \frac{\mathrm{d}^4 p}{(2\pi)^4}\frac{\mathrm{i}}{\Gamma^\mu p_\mu + \mathrm{i}\Upsilon_5 M_\ell}\frac{\Psi_{\ell m}(z, \phi)}{R} \\ \times \frac{\Psi^\dagger_{\ell m}(z', \phi')}{R}\mathrm{e}^{-\mathrm{i}p\cdot(x-x')}, \end{aligned} \tag{31}$$

where we can confirm that it satisfies Eq. (30) applying Eq. (11) and the completeness condition Eq. (12) for mode functions. The propagator on $M^4 \times S^2/Z_2$ is obtained in terms of the linear combination $\Psi^{(\pm\gamma_5)}(x, z, \phi) = (\Psi(x, z, \phi) \pm \Upsilon_5\Psi(x, -z, -\phi))/2$, satisfying the boundary condition Eq. (3), such that

$$\begin{aligned} &\tilde{S}_F^{(\pm\gamma_5)}(x - x', z - z', \phi - \phi') \\ &\quad = \langle \Psi^{(\pm\gamma_5)}(x, \theta, \phi)\bar{\Psi}^{(\pm\gamma_5)}(x, \theta, \phi)\rangle \\ &\quad = \frac{1}{4}\Big[\langle \Psi(x, z, \phi)\bar{\Psi}(x', z', \phi')\rangle \mp \langle \Psi(x, z, \phi)\bar{\Psi}(x', -z', -\phi')\rangle\Upsilon_5 \\ &\qquad \pm \Upsilon_5\langle \Psi(x, -z, -\phi)\bar{\Psi}(x', z', \phi')\rangle - \Upsilon_5\langle \Psi(x, -z, -\phi)\bar{\Psi}(x', -z', -\phi')\rangle\Upsilon_5\Big], \end{aligned} \tag{32}$$

where each $\langle \Psi\bar{\Psi}\rangle$ is given by Eq. (31). Then it can be simplified as

$$\begin{aligned} \tilde{S}_F^{(\pm\gamma_5)}(x - x', z - z', \phi - \phi') = \frac{1}{2}\sum_{\ell=0}^{\infty}\sum_{m,m'=-\ell}^{\ell}\int \frac{\mathrm{d}^4 p}{(2\pi)^4}\left[\frac{\mathrm{i}\delta_{mm'}}{\Gamma^\mu p_\mu + \mathrm{i}\Upsilon_5 M_l} \mp \frac{(-1)^{\ell+m}\mathrm{i}\delta_{-mm'}}{\Gamma^\mu p_\mu + \mathrm{i}\Upsilon_5 M_\ell}\Upsilon_5\right] \\ \times \frac{\Psi_{\ell m}(z, \phi)}{R}\frac{\Psi^\dagger_{\ell m'}(z', \phi')}{R}\mathrm{e}^{-\mathrm{i}p\cdot(x-x')}, \end{aligned} \tag{33}$$

where the sign factor $(-1)^{\ell+m}$ is derived from the relation $\Psi_{\ell m}(-z, -\phi) = (-1)^{\ell+m}\Psi_{\ell-m}(z, \phi)$. This propagator has a similar structure to the minimal UED case except for the sign factor [36,45].

The propagator of the gauge boson, $D_F^{\mu\nu}(x-x', z-z', \phi-\phi')$, on $M^4 \times S^2$ is defined to satisfy

$$\left[\partial_\mu \partial^\mu + \frac{1}{R^2}\hat{L}^2\right] D_F^{\mu\nu}(x-x', z-z', \phi-\phi') = \frac{\mathrm{i}g^{\mu\nu}}{R^2}\delta^{(4)}(x-x')\delta(z-z')\delta(\phi-\phi'), \tag{34}$$

in Feynman–t'Hooft gauge, where the operator in the left-hand side comes from the kinetic term shown in Eq. (18). Then the propagator is expressed by spherical harmonics as

$$D_F^{\mu\nu}(x-x', z-z', \phi-\phi') = \sum_{\ell=0}^{\infty}\sum_{m=-\ell}^{\ell}\int \frac{\mathrm{d}^4 p}{(2\pi)^4}\frac{-\mathrm{i}g^{\mu\nu}}{p^2 - M_\ell^2}\frac{Y_{\ell m}(z,\phi)}{R}\frac{Y_{\ell m}^*(z',\phi')}{R}\mathrm{e}^{-\mathrm{i}p\cdot(x-x')}, \tag{35}$$

which satisfies Eq. (34) with the completeness relation of spherical harmonics. The propagator on $M^4 \times S^2/Z_2$ is obtained by taking into account the boundary condition Eq. (4) as the case of fermion propagator. Substituting $Y_{\ell m}(\theta,\phi)$ in the linear combination $(Y_{\ell m}(\theta,\phi) + Y_{\ell m}(\pi-\theta,-\phi))/2$, satisfying the boundary condition, we obtain

$$\begin{aligned}\tilde{D}_F^{\mu\nu}(x-x', z-z', \phi-\phi') = \frac{1}{2}\sum_{\ell=0}^{\infty}\sum_{m,m'=-\ell}^{\ell}\int \frac{\mathrm{d}^4 p}{(2\pi)^4}\frac{-\mathrm{i}g^{\mu\nu}}{p^2 - M_\ell^2}\left[\delta_{mm'} + (-1)^\ell \delta_{-mm'}\right] \\ \times \frac{Y_{\ell m}(z,\phi)}{R}\frac{Y_{\ell m'}^*(z',\phi')}{R}\mathrm{e}^{-\mathrm{i}p\cdot(x-x')},\end{aligned} \tag{36}$$

where the factor of $(-1)^\ell$ is derived from the relation $Y_{\ell m}(\pi-\theta,-\phi) = (-1)^\ell Y_{\ell -m}(\theta,\phi)$.

The propagators for $\phi_{1,2}$, the linear combination of the extra-dimensional component of gauge field $A_{\theta,\phi}$, are similarly given as four-dimensional components which satisfy

$$\left[\partial_\mu \partial^\mu + \frac{1}{R^2}\hat{L}^2\right]\hat{L}^2 D_F^{ex}(x-x', z-z', \phi-\phi') = -\frac{\mathrm{i}}{R^2}\delta^{(4)}(x-x')\delta(z-z')\delta(\phi-\phi'), \tag{37}$$

where the minus sign in the right-hand side comes from the minus sign in the $\theta\theta$ and $\phi\phi$ components of the metric g_{MN}, and the extra $\hat{L}^2$ factor comes from the left-hand side of Eq. (25) due to the substitutions of Eqs. (20) and (21). Thus the propagators before and after orbifolding are obtained as

$$D_F^{ex}(x-x', z-z', \phi-\phi') = \sum_{\ell=0}^{\infty}\sum_{m,m'=-\ell}^{\ell}\int \frac{\mathrm{d}^4 p}{(2\pi)^4}\frac{\mathrm{i}}{p^2 - M_\ell^2}\frac{\tilde{Y}_{\ell m}(z,\phi)}{R}\frac{\tilde{Y}_{\ell m'}^*(z',\phi')}{R}\mathrm{e}^{-\mathrm{i}p\cdot(x-x')}, \tag{38}$$

$$\begin{aligned}\tilde{D}_F^{ex}(x-x', z-z', \phi-\phi') = \frac{1}{2}\sum_{\ell=0}^{\infty}\sum_{m,m'=-\ell}^{\ell}\int \frac{\mathrm{d}^4 p}{(2\pi)^4}\frac{\mathrm{i}}{p^2 - M_\ell^2}\left[\delta_{mm'} + (-1)^\ell \delta_{-mm'}\right] \\ \times \frac{\tilde{Y}_{\ell m}(z,\phi)}{R}\frac{\tilde{Y}_{\ell m'}^*(z',\phi')}{R}\mathrm{e}^{-\mathrm{i}p\cdot(x-x')},\end{aligned} \tag{39}$$

where $\tilde{Y}_{\ell m} = Y_{\ell m}/\sqrt{\ell(\ell+1)}$, for both ϕ_1 and ϕ_2 in the Feynman–t'Hooft gauge, and the propagator on $M^4 \times S^2/Z_2$ is obtained in the same way as for four-dimensional components using $(\tilde{Y}_{\ell m}(\theta,\phi) + \tilde{Y}_{\ell m}(\pi-\theta,-\phi))/2$ for mode functions.

The propagator for the scalar boson is obtained similarly to the gauge boson case as

$$D_F(x-x',z-z',\phi-\phi') = \sum_{\ell=0}^{\infty}\sum_{m=-\ell}^{\ell}\int \frac{\mathrm{d}^4p}{(2\pi)^4}\frac{\mathrm{i}}{p^2-M_\ell^2}\frac{Y_{\ell m}(z,\phi)}{R}\frac{Y^*_{\ell m}(z',\phi')}{R}\mathrm{e}^{-\mathrm{i}p\cdot(x-x')}. \quad (40)$$

This propagator satisfies the condition

$$\left[\partial_\mu\partial^\mu + \frac{1}{R^2}\hat{L}^2\right]D_F(x-x',z-z',\phi-\phi') = -\frac{\mathrm{i}}{R^2}\delta^{(4)}(x-x')\delta(z-z')\delta(\phi-\phi'). \quad (41)$$

Then, after orbifolding, we obtain

$$\begin{aligned}\tilde{D}_F(x-x',z-z',\phi-\phi') = \frac{1}{2}\sum_{\ell=0}^{\infty}\sum_{m=-\ell}^{\ell}\sum_{m'=-\ell}^{\ell}\int\frac{\mathrm{d}^4p}{(2\pi)^4}\frac{\mathrm{i}}{p^2-M_\ell^2}[\delta_{mm'}+(-1)^\ell\delta_{-mm'}]\\ \times\frac{Y_{\ell m}(z,\phi)}{R}\frac{Y^*_{\ell m'}(z',\phi')}{R}\mathrm{e}^{-\mathrm{i}p\cdot(x-x')}. \quad (42)\end{aligned}$$

2.3. *Vertices on the six dimensions with S^2/Z_2 extra space*

The Feynman rules for the vertices in the model, along with the propagators, are obtained in terms of mode functions. As an example, we consider a gauge interaction of a chiral fermion $\Psi_\pm^{(\pm\gamma_5)}$ written by

$$\int \mathrm{d}^4x d\Omega g_{6a}\bar{\Psi}_\pm^{(\pm\gamma_5)}\Gamma^\mu T_i^a A_\mu^i\Psi_\pm^{(\pm\gamma_5)} = \int \mathrm{d}^4x\mathrm{d}\Omega g_{6a}\bar{\Psi}^{(\pm\gamma_5)}\Gamma^\mu T_i^a A_\mu^i\frac{1\pm\Gamma_7}{2}\Psi^{(\pm\gamma_5)}, \quad (43)$$

where the T^as are generators of a gauge symmetry. When the fields $\bar{\Psi}^{(\pm\gamma_5)}$, $\Psi^{(\pm\gamma_5)}$, and A_μ on the interaction make contractions, applying the propagators of Ψ and A_μ given in Eqs. (33) and (36), we get the propagators on momentum space:

$$\frac{1}{2}\left[\frac{\mathrm{i}\delta_{mm'}}{\Gamma^\mu p_\mu+\mathrm{i}\Upsilon_5 M_l}\mp\frac{(-1)^{\ell+m}\mathrm{i}\delta_{-mm'}}{\Gamma^\mu p_\mu+\mathrm{i}\Upsilon_5 M_\ell}\Upsilon_5\right], \quad (44)$$

$$\frac{1}{2}\frac{-\mathrm{i}g^{\mu\nu}}{k^2-M_\ell^2}\left[\delta_{mm'}+(-1)^\ell\delta_{-mm'}\right], \quad (45)$$

and the mode functions $\Psi_{\ell m}(z,\phi)(\Psi^\dagger_{\ell m}(z,\phi))$ and $Y_{\ell m}(z,\phi)$ are left as a vertex factor. Thus the vertex factor of $\psi_{\ell_1 m_1}A^i_{\ell_2 m_2}\psi_{\ell_3 m_3}$ coupling for each combination of KK modes is derived as

$$\begin{aligned}&\mathrm{i}\frac{g_{6a}}{R}T_i^a\int\mathrm{d}\Omega\Psi^\dagger_{\ell_1 m_1}(z,\phi)Y_{\ell_2 m_2}(z,\phi)\Gamma^\mu\frac{1\pm\Gamma_7}{2}\Psi_{\ell_3 m_3}(z,\phi)\\ &=\mathrm{i}\frac{g_{6a}}{R}T_i^a\left[\left(\int\mathrm{d}\Omega\tilde{\alpha}^*_{\ell_1 m_1}Y_{\ell_2 m_2}\tilde{\alpha}_{\ell_3 m_3}\right)\gamma^\mu P_{R(L)}+\left(\int\mathrm{d}\Omega\tilde{\beta}^*_{\ell_1 m_1}Y_{\ell_2 m_2}\tilde{\beta}_{\ell_3 m_3}\right)\gamma^\mu P_{L(R)}\right]\\ &\equiv\mathrm{i}\frac{g_{6a}}{R}T_i^a\gamma^\mu\left[I^\alpha_{\ell_1 m_1;\ell_2 m_2;\ell_3 m_3}P_{R(L)}+I^\beta_{\ell_1 m_1;\ell_2 m_2;\ell_3 m_3}P_{L(R)}\right], \quad (46)\end{aligned}$$

where the integration in the right-hand side is over S^2/Z_2, the mode functions for fermions are given in Eq. (9) and (10), and indices of T_a are understood to be contracted with KK fermions $\psi_{\ell_1 m_1}$ and $\psi_{\ell_3 m_3}$. Other vertex factors are derived in the same way and the full list of the vertex factors in the model is given in Appendix A.

3. One-loop quantum correction of KK masses

In this section, we derive one-loop corrections to the KK mass M_ℓ which does not include the SM mass $m_{\rm SM}$, being purely obtained from the extra-dimensional kinetic term, by calculating relevant one-loop diagrams. Readers who are interested in our results might skip this section discussing the technical details.

3.1. Correction to KK masses of fermions

The one-loop diagrams relevant to correction of KK masses of fermions are given as Figs. 1 and 2, where the corresponding quantum numbers $\{\ell, m\}$ are shown for each external and internal line. Figure 1 shows the virtual gauge boson contributions, including both four-dimensional components and extra-dimensional components, and Fig. 2 shows the virtual Higgs boson contribution. Here we discuss the one-loop diagram Fig. 1 with virtual A_μ for the external $\Psi_+^{(\pm\gamma_5)}$ case to show the structure of the quantum correction. We can calculate the diagram by applying the propagators Eqs. (33) and (36) and vertex Eq. (46), such that

$$\begin{aligned}
-\mathrm{i}\Sigma^{\text{Fig.1}}(p;\ell m;\ell' m') = \frac{1}{4R^2}\sum_{\ell_1=0}^{\ell_{\max}}\sum_{\ell_2=0}^{\ell_{\max}}\sum_{m_1=-\ell_1}^{\ell_1}\sum_{m_1'=-\ell_1}^{\ell_1}\int_\Lambda\frac{\mathrm{d}^4k}{(2\pi)^4}\\
\times\left[\frac{-\mathrm{i}}{(p-k)^2-M_{\ell_2}^2}(\delta_{m_1-m,m_1'-m'}+(-1)^{\ell_2}\delta_{-(m_1-m),m_1'-m'})\right.\\
\times(\mathrm{i}g_{6a}T^a\gamma^\mu)[I^\alpha_{\ell_1 m_1';\ell_2 m_1'-m';\ell' m'}P_R+I^\beta_{\ell_1 m_1';\ell_2 m_1'-m';\ell' m'}P_L]\\
\times\frac{\mathrm{i}}{\not{k}+\mathrm{i}\gamma_5 M_{\ell_1}}(\delta_{m_1,m_1'}\mp(-1)^{\ell_1+m_1}\delta_{-m_1,m_1'}\gamma_5)\\
\left.\times(\mathrm{i}g_{6a}T^a\gamma_\mu)[I^\alpha_{\ell m;\underline{\ell_2 m_1-m};\ell_1 m_1}P_R+I^\beta_{\ell m;\underline{\ell_2 m_1-m};\ell_1 m_1}P_L]\right],
\end{aligned}\tag{47}$$

where P_L and P_R on the right-hand side will be interchanged for $\Psi_-^{(\pm\gamma_5)}$ and the underline for the KK numbers in the vertex factor $I^{\alpha(\beta)}_{\ell m;\underline{\ell_2 m_1-m};\ell_1 m_1}$ shows that the corresponding spherical harmonics are conjugate: $Y^*_{\ell_2 m_1-m}$. The quantum numbers ℓ_1, ℓ_2, m_1, and m_1' are associated with the KK modes in the loop which are summed over. In this paper we employ, for all one-loop diagram calculations, the cut-off Λ for four-momentum integration and $\ell_{\max}$ for the angular momentum sum, in order to

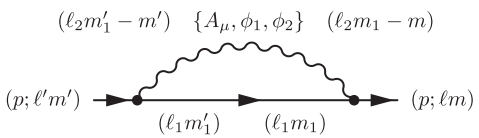

Fig. 1. One-loop diagram for correction to KK masses of fermion with virtual gauge bosons including extra-dimensional components.

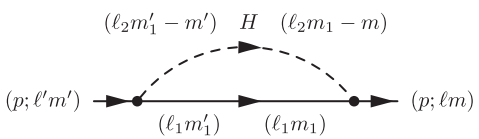

Fig. 2. One-loop diagram for correction to KK masses of fermion with virtual Higgs bosons.

regularize the loop diagram. Summing over m'_1, the products of the Kronecker delta and the vertex factors I^x ($x = \alpha$ or β) are arranged as

$$\begin{aligned}
&\sum_{m'_1}(\delta_{m_1-m,m'_1-m'} + (-1)^{\ell_2}\delta_{-(m_1-m),m'_1-m'})(\delta_{m_1,m'_1} \pm (-1)^{\ell_1+m_1}\delta_{-m_1,m'_1}\gamma_5) \\
&\quad \times I^x_{\ell_1 m'_1;\ell_2 m'_1-m';\ell' m'} I^{x'}_{\ell m;\underline{\ell_2 m_1-m};\ell_1 m_1} \\
&= (\delta_{m,m'} \pm (-1)^{\ell'+m}\delta_{-m,m'}\gamma_5) I^x_{\ell_1 m_1;\ell_2 m_1-m;\ell' m} I^{x'}_{\ell m;\ell_2 m-m_1;\ell_1 m_1} \\
&\quad + (-1)^{\ell_2}(\delta_{2m_1,m+m'} \pm (-1)^{\ell'+m}\delta_{2m_1,m-m'}\gamma_5) I^x_{\ell_1 m_1;\ell_2-m_1+m;\ell' 2m_1-m} I^{x'}_{\ell m;\ell_2 m-m_1;\ell_1 m_1}, \quad (48)
\end{aligned}$$

where we used the relation $I^x_{\ell_1-m_1;\ell_2-m_2;\ell_3-m_3} = (-1)^{\ell_1+\ell_2+\ell_3+m_1+m_3} I^x_{\ell_1 m_1;\ell_2 m_2;\ell_3 m_3}$ obtained from the definition of the vertex factor given in Eq. (46). The first term in the right-hand side of Eq. (48) corresponds to bulk contribution conserving KK-number m, and the second term corresponds to the boundary contribution violating the conservation of the KK-number m. Thus the one-loop diagram contribution can be separated into bulk and boundary contributions such that

$$-\mathrm{i}\Sigma^{\text{Fig.1}}(p;\mu;\ell m;\ell' m') = -\mathrm{i}\Sigma^{\text{Fig.1}}_{\text{bulk}}(p;\ell m;\ell' m') - \mathrm{i}\Sigma^{\text{Fig.1}}_{\text{bound}}(\mu;\ell m;\ell' m'), \quad (49)$$

where bulk contribution is proportional to m conserving Kronecker deltas $\{\delta_{m,m'}, \delta_{-m,m'}\}$, and the boundary contribution is proportional to m violating Kronecker deltas $\{\delta_{2m_1,m+m'}, \delta_{2m_1,m-m'}\}$. As usual we combine denominators in the momentum integral using Feynman parameter α, and carry out Wick rotation. The momentum integral becomes

$$\begin{aligned}
&\int_\Lambda \frac{\mathrm{d}^4 k}{(2\pi)^4} \frac{1}{\left[(p-k)^2 - M^2_{\ell_2}\right]\left[k^2 - M^2_{\ell_1}\right]} \\
&\quad = \frac{\mathrm{i}}{(4\pi)^2}\int_0^1 \mathrm{d}\alpha \int_0^{\Lambda^2} \frac{k_E^2 \mathrm{d}k_E^2}{\left[k_E^2 - \alpha(1-\alpha)p^2 + M^2_{\ell_1}(1-\alpha) + M^2_{\ell_2}\alpha\right]^2}, \quad (50)
\end{aligned}$$

where we performed the substitution $k - \alpha p \to k$, k_E is a Euclidean 4-momentum, and the integration over k_E^2 is regularized by cut-off Λ. We estimate the momentum integration numerically, taking cut-off Λ as a parameter for bulk contribution, while we only left the leading log-divergent part with renormalization scale μ for a boundary contribution such that

$$\int_0^{\Lambda^2} \frac{k_E^2 \mathrm{d}k_E^2}{\left[k_E^2 - \alpha(1-\alpha)p^2 + M^2_{\ell_1}(1-\alpha) + M^2_{\ell_2}\alpha\right]^2} \to \log\left(\frac{\Lambda^2}{\mu^2}\right), \quad (51)$$

assuming a vanishing contribution at the cut-off scale Λ. Then, after arranging the terms, Eq. (47) is organized as

$$\begin{aligned}
-\mathrm{i}\Sigma^{\text{Fig.1}}_{\text{bulk}}(p;\ell m;\ell' m') &= \Big[\not{p}\Big(\mathrm{i}\Sigma^{\text{Fig.1},L}_{\text{bulk}}(p;\ell m;\ell' m')P_L + \mathrm{i}\Sigma^{\text{Fig.1},R}_{\text{bulk}}(p;\ell m;\ell' m')P_R\Big) \\
&\quad + \mathrm{i}\gamma_5\Big(\mathrm{i}\tilde{\Sigma}^{\text{Fig.1},L}_{\text{bulk}}(p;\ell m;\ell' m')P_L + \mathrm{i}\tilde{\Sigma}^{\text{Fig.1},R}_{\text{bulk}}(p;\ell m;\ell' m')P_R\Big)\Big] \quad (52) \\
-\mathrm{i}\Sigma^{\text{Fig.1}}_{\text{bound}}(p;\ell m;\ell' m') &= \Big[\not{p}\Big(\mathrm{i}\Sigma^{\text{Fig.1},L}_{\text{bound}}(\mu;\ell m;\ell' m')P_L + \mathrm{i}\Sigma^{\text{Fig.1},R}_{\text{bound}}(\mu;\ell m;\ell' m')P_R\Big) \\
&\quad + \mathrm{i}\gamma_5\Big(\mathrm{i}\tilde{\Sigma}^{\text{Fig.1},L}_{\text{bound}}(\mu;\ell m;\ell' m')P_L + \mathrm{i}\tilde{\Sigma}^{\text{Fig.1},R}_{\text{bound}}(\mu;\ell m;\ell' m')P_R\Big)\Big], \quad (53)
\end{aligned}$$

where the coefficients $\Sigma^{L(R)}$ and $\tilde{\Sigma}^{L(R)}$ correspond to the terms proportional to $\not{p}$ and $\mathrm{i}\gamma_5$ respectively, associated with $P_{L(R)}$. These coefficients are explicitly given by

$$\mathrm{i}\Sigma^{\mathrm{Fig.1},L(R)}_{\mathrm{bulk}}(p;\ell m;\ell' m') = \mathrm{i}\frac{g_{6a}^2}{64\pi^2 R^2}(T^a)^2 \sum_{\ell_1=0}^{\ell_{\max}}\sum_{\ell_2=0}^{\ell_{\max}}\sum_{m_1=-\ell_1}^{\ell_1}\int_0^1 \mathrm{d}\alpha \int_0^{\Lambda^2}\frac{x\,\mathrm{d}x}{[x+\Delta]^2}(-1)^{m_1-m} \times 2\alpha I^{\beta(\alpha)}_{\ell_1 m_1;\ell_2 m_1-m;\ell' m} I^{\beta(\alpha)}_{\ell m;\ell_2 m-m_1;\ell_1 m_1}\left(\delta_{m,m'} \pm (-1)^{\ell'+m}\delta_{-m,m'}\gamma_5\right), \tag{54}$$

$$\mathrm{i}\tilde{\Sigma}^{\mathrm{Fig.1},L(R)}_{\mathrm{bulk}}(p;\ell m;\ell' m') = \mathrm{i}\frac{g_{6a}^2}{64\pi^2 R^2}(T^a)^2 \sum_{\ell_1=0}^{\ell_{\max}}\sum_{\ell_2=0}^{\ell_{\max}}\sum_{m_1=-\ell_1}^{\ell_1}\int_0^1 \mathrm{d}\alpha \int_0^{\Lambda^2}\frac{x\,\mathrm{d}x}{[x+\Delta]^2}(-1)^{m_1-m} \times 4M_{\ell_1} I^{\alpha(\beta)}_{\ell_1 m_1;\ell_2 m_1-m;\ell' m} I^{\beta(\alpha)}_{\ell m;\ell_2 m-m_1;\ell_1 m_1}\left(\delta_{m,m'} \pm (-1)^{\ell'+m}\delta_{-m,m'}\gamma_5\right), \tag{55}$$

$$\mathrm{i}\Sigma^{\mathrm{Fig.1},L(R)}_{\mathrm{bound}}(\mu;\ell m;\ell' m') = \mathrm{i}\frac{g_{6a}^2}{64\pi^2 R^2}(T^a)^2 \sum_{\ell_1=0}^{\ell_{\max}}\sum_{\ell_2=0}^{\ell_{\max}}\sum_{m_1=-\ell_1}^{\ell_1}(-1)^{m_1-m+\ell_2}\log\left(\frac{\Lambda^2}{\mu^2}\right) \times I^{\beta(\alpha)}_{\ell_1 m_1;\ell_2-m_1+m;\ell' 2m_1-m} I^{\beta(\alpha)}_{\ell m;\ell_2 m-m_1;\ell_1 m_1} \times \left(\delta_{2m_1,m+m'} \pm (-1)^{\ell'+m}\delta_{2m_1,m-m'}\gamma_5\right), \tag{56}$$

$$\mathrm{i}\tilde{\Sigma}^{\mathrm{Fig.1},L(R)}_{\mathrm{bound}}(\mu;\ell m;\ell' m') = \mathrm{i}\frac{g_{6a}^2}{64\pi^2 R^2}(T^a)^2 \sum_{\ell_1=0}^{\ell_{\max}}\sum_{\ell_2=0}^{\ell_{\max}}\sum_{m_1=-\ell_1}^{\ell_1}(-1)^{m_1-m+\ell_2}\log\left(\frac{\Lambda^2}{\mu^2}\right) \times 4M_{\ell_1} I^{\alpha(\beta)}_{\ell_1 m_1;\ell_2-m_1+m;\ell' 2m_1-m} I^{\beta(\alpha)}_{\ell m;\ell_2 m-m_1;\ell_1 m_1} \times \left(\delta_{2m_1,m+m'} \pm (-1)^{\ell'+m}\delta_{2m_1,m-m'}\gamma_5\right), \tag{57}$$

where $\Delta = -\alpha(1-\alpha)p^2 + (1-\alpha)M_{\ell_1}^2 + \alpha M_{\ell_2}^2$. We also note that there appear sign factors of $(-1)^{\{\ell,m\}}$ from propagators in the S^2/Z_2 orbifold and vertices, which lead to different sign contributions from each KK mode in the loop. Then the contributions depend on $\ell_{\max}$ differently for even or odd $\ell_{\max}$, as we will see below. Also, we can numerically check that external ℓ and m are conserved so that the $\ell = \ell'$ and $m = m'$ cases give non-zero contribution, which is satisfied for other diagrams. The other diagrams are also calculated in the same manner, and we list the contributions from each diagram in Table A4. Therefore, we obtain one-loop level correction to the Lagrangian such that

$$\begin{aligned}\delta L_{1-\mathrm{loop}} =\ & \Sigma^L_{\mathrm{bulk}}(p^2;\ell m;\ell m)\bar{\psi}_{\ell m L}\mathrm{i}\gamma^\mu\partial_\mu\psi_{\ell m L} + \Sigma^R_{\mathrm{bulk}}(p^2;\ell m;\ell m)\bar{\psi}_{\ell m R}\mathrm{i}\gamma^\mu\partial_\mu\psi_{\ell m R} \\ & + \frac{1}{2}\Big[\tilde{\Sigma}^L_{\mathrm{bulk}}(p^2;\ell m;\ell m) + \tilde{\Sigma}^R_{\mathrm{bulk}}(p^2;\ell m;\ell m)]\bar{\psi}_{\ell m}\mathrm{i}\gamma_5\psi_{\ell m}\Big] \\ & + \Sigma^L_{\mathrm{bound}}(\mu;\ell m;\ell m)\bar{\psi}_{\ell m L}\mathrm{i}\gamma^\mu\partial_\mu\psi_{\ell m L} + \Sigma^R_{\mathrm{bound}}(\mu;\ell m;\ell m)\bar{\psi}_{\ell m R}\mathrm{i}\gamma^\mu\partial_\mu\psi_{\ell m R} \\ & + \frac{1}{2}\Big[\tilde{\Sigma}^L_{\mathrm{bound}}(\mu;\ell m;\ell m) + \tilde{\Sigma}^R_{\mathrm{bound}}(\mu;\ell m;\ell m)]\bar{\psi}_{\ell m}\mathrm{i}\gamma_5\psi_{\ell m}\Big],\end{aligned} \tag{58}$$

where each coefficient $\Sigma^{L(R)}_{\mathrm{bulk}}$, $\Sigma^{L(R)}_{\mathrm{bound}}$, $\tilde{\Sigma}^{L(R)}_{\mathrm{bulk}}$, and $\tilde{\Sigma}^{L(R)}_{\mathrm{bound}}$ is understood as the sum of the corresponding contributions from all diagrams.

To obtain one-loop corrections to KK mass, we take into account a renormalization condition for each KK mode. The kinetic and KK mass terms of each KK mode of a fermion are given in Eq. (14).

Defining, as a renormalization of fields, $\psi_{R(L)} \to \sqrt{Z_{R(L)}}\psi_{R(L)} = \sqrt{1+\delta_{R(L)}}\psi_{R(L)}$, the terms in Eq. (14) become

$$\bar{\psi}_{L\ell m}\mathrm{i}\gamma^\mu\partial_\mu\psi_{L\ell m} + \bar{\psi}_{R\ell m}\mathrm{i}\gamma^\mu\partial_\mu\psi_{R\ell m} + \mathrm{i}M_\ell\bar{\psi}_{L\ell m}\gamma_5\psi_{R\ell m} + \mathrm{i}M_\ell\bar{\psi}_{R\ell m}\gamma_5\psi_{L\ell m}$$
$$\delta_L\bar{\psi}_{L\ell m}\mathrm{i}\gamma^\mu\partial_\mu\psi_{L\ell m} + \delta_R\bar{\psi}_{R\ell m}\mathrm{i}\gamma^\mu\partial_\mu\psi_{R\ell m} + \frac{1}{2}(\delta_L+\delta_R)(\mathrm{i}M_\ell\bar{\psi}_{L\ell m}\gamma_5\psi_{R\ell m} + \mathrm{i}M_\ell\bar{\psi}_{R\ell m}\gamma_5\psi_{L\ell m}), \tag{59}$$

where we have taken up to the first order in $\delta_{R(L)}$, which corresponds to the counter terms. Thus the contribution from these counter terms is shown by

$$\text{counter terms}(p;\ell m) = \mathrm{i}\not{p}[\delta_L P_L + \delta_R P_R] + \mathrm{i}(\mathrm{i}\gamma_5 M_\ell)(P_L+P_R)\frac{1}{2}[\delta_L+\delta_R]. \tag{60}$$

Then we employ the renormalization conditions at cut-off scale Λ as

$$\left(\mathrm{i}\delta_L + \mathrm{i}\Sigma^L_{\text{bulk}}(p^2;\ell m;\ell m)\right)|_{p^2=-\Lambda^2, M^2_{\ell max}=\Lambda^2} = 0, \tag{61}$$
$$\left(\mathrm{i}\delta_R + \mathrm{i}\Sigma^R_{\text{bulk}}(p^2;\ell m;\ell m)\right)|_{p^2=-\Lambda^2, M^2_{\ell max}=\Lambda^2} = 0, \tag{62}$$

which corresponds to the requirement that the kinetic term has canonical form at the cut-off scale, and the counter terms $\delta_{R(L)}$ are determined from these conditions. Combining contributions from the one-loop diagrams and the counter terms, we obtain the corrected kinetic and KK mass terms such that

$$\begin{aligned}\delta L = {}& \delta_L\bar{\psi}_{L\ell m}\mathrm{i}\gamma^\mu\partial_\mu\psi_{L\ell m} + \delta_R\bar{\psi}_{R\ell m}\mathrm{i}\gamma^\mu\partial_\mu\psi_{R\ell m} \\ & + \frac{1}{2}(\delta_L+\delta_R)(\bar{\psi}_{L\ell m}\mathrm{i}M_\ell\gamma_5\psi_{R\ell m} + \bar{\psi}_{R\ell m}\mathrm{i}M_\ell\gamma_5\psi_{L\ell m}) + \delta L_{1-\text{loop}}.\end{aligned} \tag{63}$$

Therefore, normalizing the kinetic terms by

$$\psi_{R(L)\ell m} \to \left(1 + \Sigma^{R(L)}_{\text{bulk}}(p^2;\ell m;\ell m) + \Sigma^{R(L)}_{\text{bound}}(\mu;\ell m;\ell m) + \delta_{R(L)}\right)^{-\frac{1}{2}}\psi_{R(L)\ell m}, \tag{64}$$

we obtain the corrected KK mass of

$$\begin{aligned}\tilde{M}_{\ell m} \simeq {}& M_\ell + \frac{1}{2}\left[(\tilde{\Sigma}^L_{\text{bulk}} + \tilde{\Sigma}^R_{\text{bulk}})(p^2;\ell m;\ell m) + (\tilde{\Sigma}^L_{\text{bound}} + \tilde{\Sigma}^R_{\text{bound}})(\mu;\ell m;\ell m)\right] \\ & - \frac{1}{2}M_\ell\left[(\Sigma^L_{\text{bulk}} + \Sigma^R_{\text{bulk}})(p^2;\ell m;\ell m) + (\Sigma^L_{\text{bound}} + \Sigma^R_{\text{bound}})(\mu;\ell m;\ell m)\right] \\ \equiv {}& M_\ell + (\delta M)^\psi_{\ell m}\end{aligned} \tag{65}$$

for each KK mode of fermions, where we have taken the first order of Σ and δ in the right-hand side.

3.2. Correction to KK masses of gauge boson

The one-loop diagrams corresponding to corrections to KK masses of gauge bosons are given in Figs. 3–7 for both four-dimensional components and extra-dimensional components in external lines, where corresponding quantum numbers $\{\ell, m\}$ are shown for each external and internal line. Figure 3 shows the fermion loop, Figs. 4 and 5 show Higgs boson loops from 3-point and 4-point gauge interactions respectively, and Figs. 6 and 7 show the gauge boson loops from 3-point and 4-point self-interactions respectively. These diagrams are calculated in the same manner as the case of KK mass of

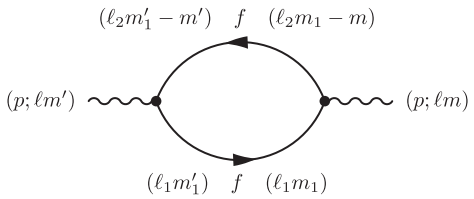

Fig. 3. One-loop diagram for correction to KK masses of gauge bosons $\{A_\mu, \phi_1, \phi_2\}$ with virtual fermions.

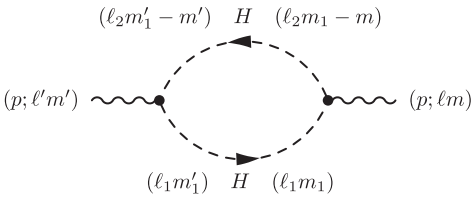

Fig. 4. One-loop diagram for correction to KK masses of gauge bosons $\{A_\mu, \phi_1, \phi_2\}$ with virtual Higgs bosons.

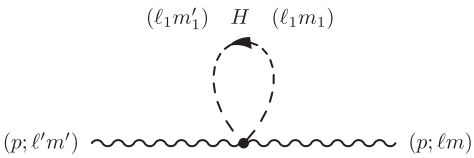

Fig. 5. One-loop diagram for correction to KK masses of gauge bosons $\{A_\mu, \phi_1, \phi_2\}$ with virtual Higgs bosons.

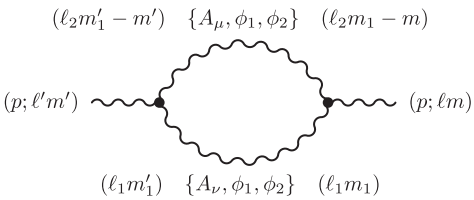

Fig. 6. One-loop diagram for correction to KK masses of gauge bosons $\{A_\mu, \phi_1, \phi_2\}$ with virtual gauge bosons including extra components.

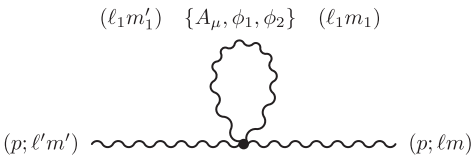

Fig. 7. One-loop diagram for correction to KK masses of gauge bosons $\{A_\mu, \phi_1, \phi_2\}$ with virtual gauge bosons including extra components.

fermions, and we summarize the results in Appendix B. Separating bulk and boundary contributions, we can organize the one-loop diagram contributions generally as

$$\mathrm{i}\Pi_{\mu\nu}(p^2;\mu;\ell m;\ell m) = \mathrm{i}\Pi^{\mathrm{bulk}}_{\mu\nu}(p^2;\ell m;\ell m) + \mathrm{i}\Pi^{\mathrm{bound}}_{\mu\nu}(p^2;\mu;\ell m;\ell m), \tag{66}$$

$$\begin{aligned}\mathrm{i}\Pi^{\mathrm{bulk(bound)}}_{\mu\nu}(p^2(p^2;\mu);\ell m;\ell m) &= (p^2 g_{\mu\nu} - p_\mu p_\nu)\mathrm{i}\Pi_{\mathrm{bulk(bound)}}(p^2(p^2;\mu);\ell m;\ell m) \\ &\quad + g_{\mu\nu}\mathrm{i}\tilde{\Pi}_{\mathrm{bulk(bound)}}(p^2(p^2;\mu);\ell m;\ell m),\end{aligned} \tag{67}$$

where we also separated the terms proportional to $(p^2 g_{\mu\nu} - p_\mu p_\nu)$ contributing the correction of the kinetic term of A_μ and the terms proportional to $g_{\mu\nu}$ in the right-hand side of second line. The contributions to the coefficients of $\Pi(\tilde{\Pi})$ from each diagram are summarized in Tables A5 and B1. Thus the correction to the Lagrangian is

$$\begin{aligned}\delta L_{1\text{loop}} = &\frac{1}{4}\Pi_{\text{bulk}}(p^2;\ell m;\ell m)F^{\mu\nu}_{lm}F_{\ell m\mu\nu} + \frac{1}{2}\tilde{\Pi}_{\text{bulk}}(p^2;\ell m;\ell m)A^\mu_{\ell m}A_{\ell m\mu}\\ &+\frac{1}{4}\Pi_{\text{bound}}(p^2;\mu;\ell m;\ell m)F^{\mu\nu}_{lm}F_{\ell m\mu\nu} + \frac{1}{2}\tilde{\Pi}_{\text{bound}}(p^2;\mu;\ell m;\ell m)A^\mu_{\ell m}A_{\ell m\mu},\end{aligned} \tag{68}$$

where $\Pi(\tilde{\Pi})$s in the right-hand side are understood as the sum of the corresponding contributions from all diagrams.

As in the fermion case, we consider the renormalization condition to obtain one-loop corrections to KK masses for KK gauge bosons. The kinetic and KK mass terms of each KK mode of the gauge boson are given in Eq. (18). Defining as a renormalization of the gauge field, $A_\mu \to \sqrt{Z_3}A_\mu = \sqrt{1+\delta_3}A_\mu$, these terms become

$$-\frac{1}{4}F^{\mu\nu}_{\ell m}F_{\ell m\mu\nu} + \frac{1}{2}M^2_\ell A^\mu_{\ell m}A_{\ell m\mu} - \frac{1}{4}\delta_3 F^{\mu\nu}_{\ell m}F_{\ell m\mu\nu} + \frac{1}{2}\delta_3 M^2_\ell A^\mu_{\ell m}A_{\ell m\mu}, \tag{69}$$

where we have taken up to the first order in δ_3 corresponding to counter terms. Thus the contribution from these counter terms is

$$\text{counter term}(p^2;\ell m) = -\mathrm{i}(p^2 g_{\mu\nu} - p_\mu p_\nu)\delta_3 + \mathrm{i}M^2_\ell\delta_3. \tag{70}$$

Then we employ the renormalization condition at cut-off scale Λ as

$$(\Pi_{\text{bulk}}(p^2;\ell m;\ell m) - \delta_3)\,|_{p^2=-\Lambda^2, M^2_{\ell max}=\Lambda^2} = 0, \tag{71}$$

which requires the canonical form of kinetic term at the cut-off scale as in the fermion case, and the counter term δ_3 is determined by the condition. Combining contributions from one-loop diagrams and counter terms, we obtain the one-loop corrections to kinetic and KK mass terms such that

$$\delta L = -\frac{1}{4}\delta_3 F^{\mu\nu}_{\ell m}F_{\ell m\mu\nu} + \frac{1}{2}\delta_3 A^\mu_{\ell m}\hat{L}^2 A_{\ell m\mu} + \delta L_{1-\text{loop}}. \tag{72}$$

Therefore, normalizing the kinetic terms by

$$A^\mu_{\ell m} \to \left(1 - \Pi_{\text{bulk}}(p^2;\ell m;\ell m) - \Pi_{\text{bound}}(p^2;\mu;\ell m;\ell m) + \delta_3\right)^{-\frac{1}{2}} A^\mu_{\ell m}, \tag{73}$$

we obtain one-loop corrections to KK mass

$$\begin{aligned}\tilde{M}^2_\ell &= M^2_\ell + \tilde{\Pi}_{\text{bulk}}(p^2;\ell m;\ell m) + \tilde{\Pi}_{\text{bound}}(p^2;\mu;\ell m;\ell m) + M^2_\ell\big[\Pi_{\text{bulk}}(p^2;\ell m;\ell m)\\ &\quad + \Pi_{\text{bound}}(p^2;\mu;\ell m;\ell m)\big],\\ &\equiv M^2_\ell + (\delta M^2)^{A_\mu}_{\ell m},\end{aligned} \tag{74}$$

for each KK mode of gauge bosons, where we have taken the first order in Π and δ_3 in the right-hand side.

The extra-dimensional components of gauge fields $A_{\theta,\phi}$ are considered as scalar fields in four dimensions, and the KK mass eigenstates are given by ϕ_i which are defined as Eqs. (20) and (21). Then the kinetic and KK mass terms of ϕ_i are in the same form as those of the scalar field. For ϕ_i,

we write the contributions from one-loop diagrams to corrections of diagonal mass terms $\phi_i\phi_i$ such that

$$\mathrm{i}\Theta^{(i)}(p^2;\mu;\ell m;\ell m') = \mathrm{i}\Theta^{(i)}_{\mathrm{bulk}}(p^2;\mu;\ell m;\ell m') + \mathrm{i}\Theta^{(i)}_{\mathrm{bound}}(p^2;\mu;\ell m;\ell m'), \tag{75}$$

$$\begin{aligned}\mathrm{i}\Theta^{(i)}_{\mathrm{bulk(bound)}}(p^2(p^2;\mu);\ell m;\ell m') &= p^2\mathrm{i}\Theta^{(i)}_{\mathrm{bulk(bound)}}(p^2=0(p^2=0;\mu);\ell m;\ell m') \\ &\quad - \mathrm{i}\tilde{\Theta}^{(i)}_{\mathrm{bulk(bound)}}(p^2=0(p^2=0;\mu);\ell m;\ell m'),\end{aligned} \tag{76}$$

where the bulk and the boundary contributions are separated, and each numerical factor can be calculated in the same manner as the above cases. The right-hand side of Eq. (76) corresponds to the expansion in terms of p^2, and we omit $p^2=0$ in $\Theta(\tilde{\Theta})$ hereafter. We note that there are contributions to off-diagonal $\phi_1\phi_2$ terms. However, these contributions are negligibly small compared to the diagonal terms, and we just ignore these contributions in this paper. The contributions to these coefficients $\Theta(\tilde{\Theta})$ from each diagram are summarized in Tables B2, B3, B4, and B5. Thus the correction to the Lagrangian is

$$\begin{aligned}\delta L_{1\mathrm{loop}} &= \Theta^{(i)}_{\mathrm{bulk}}(\ell m;\ell m)\partial_\mu\phi_{i\ell m}\partial^\mu\phi_{i\ell m} - \tilde{\Theta}^{(i)}_{\mathrm{bulk}}(\ell m;\ell m)\phi_{i\ell m}\phi_{i\ell m} \\ &\quad + \Theta^{(i)}_{\mathrm{bound}}(\mu;\ell m;\ell m)\partial_\mu\phi_{i\ell m}\partial^\mu\phi_{i\ell m} - \tilde{\Theta}^{(i)}_{\mathrm{bound}}(\mu;\ell m;\ell m)\phi_{i\ell m}\phi_{i\ell m},\end{aligned} \tag{77}$$

where the Θs in the right-hand side are understood as the sum of the corresponding contributions from all diagrams.

Then we consider the renormalization condition to obtain the one-loop corrections to KK masses for $\phi_{1,2}$. Defining as a renormalization of fields $\phi_i \to \sqrt{Z_3^{(i)}}\phi_i = \sqrt{1+\delta_3^{(i)}}\phi_i$, these terms become

$$\begin{aligned}&\partial_\mu\phi_{1\ell m}\partial^\mu\phi_{1\ell m} + \partial_\mu\phi_{2\ell m}\partial^\mu\phi_{2\ell m} - M_\ell^2\phi_{1\ell m}\phi_{1\ell m} - M_\ell^2\phi_{2\ell m}\phi_{2\ell m} \\ &\quad + \delta_3^{(1)}\partial_\mu\phi_{1\ell m}\partial^\mu\phi_{1\ell m} + \delta_3^{(2)}\partial_\mu\phi_{2\ell m}\partial^\mu\phi_{2\ell m} - \delta_3^{(1)}M_\ell^2\phi_{1\ell m}\phi_{1\ell m} - \delta_3^{(2)}M_\ell^2\phi_{2\ell m}\phi_{2\ell m},\end{aligned} \tag{78}$$

where we have taken up to the first order of $\delta_3^{(i)}$ corresponding to counter terms. Thus the contribution from the counter terms is

$$\text{counter term}(p^2;\ell m) = \mathrm{i}p^2\delta_3^{(i)} - \mathrm{i}M_\ell^2\delta_3^{(i)}. \tag{79}$$

Then we employ the renormalization condition at cut-off scale Λ as

$$(\Theta_{\mathrm{bulk}}(\ell m;\ell m) + \delta_3^{(i)})\,|_{M^2_{\ell max}=\Lambda^2} = 0 \tag{80}$$

in the same way as in the four-dimensional component case, and the counter term $\delta_3^{(i)}$ is determined by the condition. Combining contributions from the one-loop diagrams and counter terms, we obtain the one-loop corrections to kinetic and KK mass terms as

$$\delta L = \delta_3^{(i)}\partial_\mu\phi_{i\ell m}\partial^\mu\phi_{i\ell m} - M_\ell^2\delta_3^{(i)}\phi_{i\ell m}\phi_{i\ell m} + \delta L_{1-\mathrm{loop}}. \tag{81}$$

Therefore, normalizing the kinetic terms by

$$\phi_{i\ell m} \to \left(1 + \Theta_{\mathrm{bulk}}(\ell m;\ell m) + \Theta_{\mathrm{bound}}(\mu;\ell m;\ell m) + \delta_3^{(i)}\right)^{-\frac{1}{2}}\phi_{i\ell m}, \tag{82}$$

we obtain the one-loop corrections to KK mass

$$\begin{aligned}\tilde{M}^2_{\ell m} &= M_\ell^2 + \tilde{\Theta}_{\mathrm{bulk}}(\ell m;\ell m) + \tilde{\Theta}_{\mathrm{bound}}(\mu;\ell m;\ell m) - M_\ell^2\left[\Theta_{\mathrm{bulk}}(\ell m;\ell m) + \Theta_{\mathrm{bound}}(\mu;\ell m;\ell m)\right] \\ &\equiv M_\ell^2 + (\delta M^2)^{\phi_i}_{\ell m},\end{aligned} \tag{83}$$

for each KK mode of ϕ_i, where we took the first order of Θ and δ in the right-hand side.

3.3. Correction to KK masses of scalar boson

The one-loop diagrams corresponding to correction to KK masses of the Higgs boson are given in Figs. 8–11, where corresponding quantum numbers $\{\ell, m\}$ are shown for each external and internal line. Figures 8 and 9 show the gauge boson loops including both four-dimensional components and extra-dimensional components from 4-point and 3-point gauge interactions. Figures 10 and 11 show the fermion and the Higgs boson loop contributions, respectively. Quantum correction to the KK masses of the scalar boson can be organized in the same way as that of ϕ_i such that

$$\mathrm{i}\Xi(p^2;\mu;\ell m;\ell m') = \mathrm{i}\Xi_{\text{bulk}}(p^2;\ell m;\ell m') + \mathrm{i}\Xi_{\text{bound}}(p^2;\mu;\ell m;\ell m'), \tag{84}$$

$$\begin{aligned}\mathrm{i}\Xi_{\text{bulk(bound)}}(p^2(p^2;\mu);\ell m;\ell m') &= p^2\mathrm{i}\Xi_{\text{bulk(bound)}}(p^2=0(p^2=0;\mu);\ell m;\ell m') \\ &\quad - \mathrm{i}\tilde{\Xi}_{\text{bulk(bound)}}(p^2=0(p^2=0;\mu);\ell m;\ell m'),\end{aligned} \tag{85}$$

where we list the contribution from each diagram in Tables B6 and B7. The right-hand side of Eq. (85) corresponds to the expansion in terms of p^2, as in the previous case, and we omit $p^2 = 0$ in $\Xi(\tilde{\Xi})$

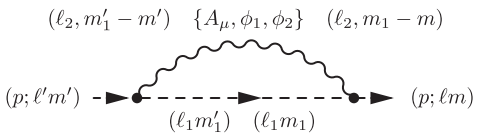

Fig. 8. One-loop diagram for correction to KK masses of Higgs bosons with virtual gauge bosons including extra components.

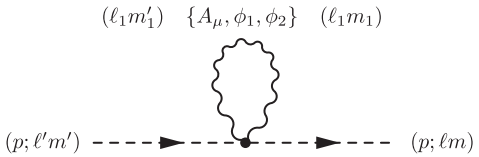

Fig. 9. One-loop diagram for correction to KK masses of Higgs bosons with virtual gauge bosons including extra components.

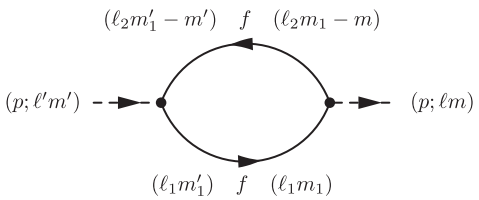

Fig. 10. One-loop diagram for correction to KK masses of Higgs bosons with virtual fermions.

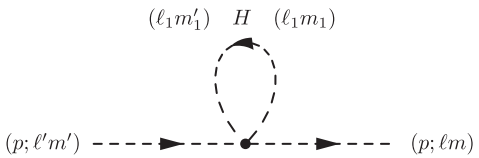

Fig. 11. One-loop diagram for correction to KK masses of Higgs bosons with virtual Higgs bosons.

hereafter. Thus the correction to the Lagrangian is

$$\begin{aligned}\delta L_{1\text{loop}} = {} & \Xi^{(i)}_{\text{bulk}}(\ell m;\ell m)\partial_\mu H^\dagger_{\ell m}\partial^\mu H_{\ell m} - \tilde{\Xi}^{(i)}_{\text{bulk}}(\ell m;\ell m)H^\dagger_{\ell m}H_{\ell m} \\ & + \Xi^{(i)}_{\text{bound}}(\mu;\ell m;\ell m)\partial_\mu H^\dagger_{\ell m}\partial^\mu H_{i\ell m} - \tilde{\Xi}^{(i)}_{\text{bound}}(\mu;\ell m;\ell m)H^\dagger_{\ell m}H_{\ell m},\end{aligned} \tag{86}$$

where the $\Xi(\tilde{\Xi})$s in the right-hand side are understood as the sum of the corresponding contributions from all diagrams.

The renormalization condition and one-loop corrections to KK mass are also discussed as in the case of ϕ_i. Repeating the same procedures as in the case of ϕ_i, we obtain counter terms

$$\delta_H \partial_\mu H^\dagger_{\ell m}\partial^\mu H_{\ell m} - M^2_\ell \delta_H H^\dagger_{\ell m}H_{\ell m}, \tag{87}$$

by the renormalization of field $H \to \sqrt{Z_H}H = \sqrt{1+\delta_H}$. We then apply the renormalization condition

$$(\Xi_{\text{bulk}}(\ell m;\ell m) - \delta_H)\,|_{M^2_{\ell max}=\Lambda^2} = 0, \tag{88}$$

at cut-off scale Λ, requiring the canonical form of the kinetic term at the cut-off scale. Then we carry out the normalization of fields,

$$H_{\ell m} \to (1 + \Xi_{\text{bulk}}(\ell m;\ell m) + \Xi_{\text{bound}}(\mu;\ell m;\ell m) + \delta_H)^{-\frac{1}{2}}\, H_{\ell m}, \tag{89}$$

as in the above cases. Therefore we obtain the one-loop corrections to KK mass

$$\begin{aligned}\tilde{M}^2_{\ell m} &= M^2_\ell + \tilde{\Xi}_{\text{bulk}}(\ell m;\ell m) + \tilde{\Xi}_{\text{bound}}(\mu;\ell m;\ell m) - M^2_\ell\big[\Xi_{\text{bulk}}(\ell m;\ell m) + \Xi_{\text{bound}}(\mu;\ell m;\ell m)\big] \\ &\equiv M^2_\ell + (\delta M^2)^H_{\ell m},\end{aligned} \tag{90}$$

for each KK mode of teh scalar boson, where we have taken the first order in Ξ and δ in the right-hand side.

4. KK mass spectrum and LKP

In this section, we estimate the one-loop corrections to KK masses for the first KK modes of SM fermions shown in Table 1, SM gauge bosons, and the Higgs boson. In estimating these corrections, we take the renormalization scale μ and the external momentum p^2 to be the first KK mass $\mu^2 = 2/R^2$ and $p^2 = -2/R^2$ respectively, and four-momentum cut-off scale Λ as a parameter. Then the angular momentum cut-off $\ell_{\max}$ is taken to be the maximum integer satisfying $\sqrt{\ell_{\max}(\ell_{\max}+1)}/R \le \Lambda$. We specify the lightest KK particle, which is expected to be the dark matter candidate.

To estimate the one-loop corrections to KK masses for SM fermions, we need to calculate coefficients $\Sigma(\tilde{\Sigma})$ in Eq. (58) from one-loop diagrams. For each fermion in Table 1, the coefficients $\Sigma(\tilde{\Sigma})$

obtain contributions from each diagram such that

$$\Sigma(Q) = \Sigma^{QG_\mu}_{\text{Fig.1}} + \Sigma^{QW_\mu}_{\text{Fig.1}} + \Sigma^{QB_\mu}_{\text{Fig.1}} + \sum_{i=1,2}\left[\Sigma^{QG_i}_{\text{Fig.1}} + \Sigma^{QW_i}_{\text{Fig.1}} + \Sigma^{QB_i}_{\text{Fig.1}}\right] + \Sigma^{QH}_{\text{Fig.2}} \tag{91}$$

$$\Sigma(U) = \Sigma^{UG_\mu}_{\text{Fig.1}} + \Sigma^{UB_\mu}_{\text{Fig.1}} + \sum_{i=1,2}\left[\Sigma^{UG_i}_{\text{Fig.1}} + \Sigma^{UB_i}_{\text{Fig.1}}\right] + \Sigma^{UH}_{\text{Fig.2}} \tag{92}$$

$$\Sigma(D) = \Sigma^{DG_\mu}_{\text{Fig.1}} + \Sigma^{DB_\mu}_{\text{Fig.1}} + \sum_{i=1,2}\left[\Sigma^{DG_i}_{\text{Fig.1}} + \Sigma^{DB_i}_{\text{Fig.1}}\right] + \Sigma^{DH}_{\text{Fig.2}} \tag{93}$$

$$\Sigma(L) = \Sigma^{LW_\mu}_{\text{Fig.1}} + \Sigma^{LB_\mu}_{\text{Fig.1}} + \sum_{i=1,2}\left[\Sigma^{LW_i}_{\text{Fig.1}} + \Sigma^{LB_i}_{\text{Fig.1}}\right] + \Sigma^{LH}_{\text{Fig.2}} \tag{94}$$

$$\Sigma(E) = \Sigma^{EB_\mu}_{\text{Fig.1}} + \sum_{i=1,2}\left[\Sigma^{EB_i}_{\text{Fig.1}}\right] + \Sigma^{EH}_{\text{Fig.2}}, \tag{95}$$

where the $\tilde{\Sigma}$s are given in the same way, and the terms on the right-hand side are the contributions from the different loop diagrams with particles running in the loop shown as superscripts: the G_μ, W_μ, and B_μ denote the SU(3), SU(2), and U(1)$_Y$ gauge fields respectively; the G_i, W_i, and B_i denote corresponding extra-dimensional components ϕ_i; and the H denotes the Higgs boson. Here we take into account the contribution from the Higgs loop only for fermions in the third generation since the Yukawa couplings for the first and the second generations are small. The contributions to each coefficient are obtained from Table A4, applying the corresponding gauge couplings g_{6a} and $(T^a)^2$ factor regarding the particles inside the loop: $g_{6a=1,2,3}$ for U(1)$_Y$, SU(2), and SU(3) gauge coupling; and $(T^a)^2 = \{Y^2, C_2(N), C_2(N)\}$, where $C_2(N) = (N^2-1)/2N$, for the fundamental representation. We also note that each gauge coupling, Yukawa coupling and the Higgs self-coupling in six dimensions $\{g_{6a}, Y_{u,d,e}, \lambda_6\}$ is related to that in four dimensions, as $g_a(y_{u,e,d}) = g_{6a}(Y_{u,d,e})/\sqrt{4\pi R^2}$ and $\lambda = \lambda_6/(4\pi R^2)$ since the factor $4\pi R^2$ comes from the surface area of S^2 and the $1/\sqrt{4\pi}$ factor comes from the mode functions for the zero mode.

The mass matrix for fermion Eq. (16) is corrected by quantum correction as

$$L_{m_f} = \begin{pmatrix} \bar{\psi}^F_{\ell m} \\ \bar{\psi}^f_{\ell m} \end{pmatrix}^T \begin{pmatrix} M_\ell + (\delta M)^F_{\ell m} & m_{\text{SM}} - \frac{1}{2} m_{\text{SM}} \delta N_{\ell m;\Lambda} \\ m_{\text{SM}} - \frac{1}{2} m_{\text{SM}} \delta N_{\ell m;\Lambda} & -(M_\ell + (\delta M)^f_{\ell m}) \end{pmatrix} \begin{pmatrix} \psi^F_{\ell m} \\ \psi^f_{\ell m} \end{pmatrix}, \tag{96}$$

where $(\delta M)^{f(F)}_{\ell m}$ is given by Eq. (65) and indices $F(f)$ show the corresponding fermion coming from the SU(2) doublet(singlet). Here we write the one-loop correction to KK mass $(\delta M)^{f(F)}_{\ell m}$ as a product of $1/R$ and the dimensionless numerical factor $\Delta^{f(F)}_{\ell m;\Lambda}$ which depends on $\{\ell, m\}$ and Λ, such as

$$(\delta M)^{f(F)}_{\ell m} = \Delta^{f(F)}_{\ell m;\Lambda} \frac{1}{R}, \tag{97}$$

and we list the numerical factor $\Delta^{f(F)}_{\ell m;\Lambda}$ in Table 2 for the first KK mode. The corrections to off-diagonal components are induced by normalization of field Eq. (64) such that

$$\delta N_{\ell m;\Lambda} = (\Sigma^L_{\text{bulk}} + \Sigma^L_{\text{bound}})^F(p^2;\mu;\ell m;\ell m) + \delta^F_L + (\Sigma^R_{\text{bulk}} + \Sigma^R_{\text{bound}})^f(p^2;\mu;\ell m;\ell m) + \delta^f_R, \tag{98}$$

Table 2. The numerical coefficients $\Delta_{\ell m}^{f(F)}$ in Eq. (97) for $\ell = 1, |m| = 1$ as a function of $\ell_{\max}$, where $b_{L(R)}$ and $t_{L(R)}$ are the KK b quark and KK top quark from the SU(2) doublet(singlet).

$\ell_{\max}$	2	3	4	5
$\Delta_{11,\Lambda}^{E_R}$	0.00232	0.00726	0.00650	0.0167
$\Delta_{11,\Lambda}^{L_L}$	0.00635	0.0199	0.0178	0.0455
$\Delta_{11,\Lambda}^{Q_L}$	0.0418	0.110	0.126	0.242
$\Delta_{11,\Lambda}^{U_R}$	0.0370	0.116	0.104	0.265
$\Delta_{11,\Lambda}^{D_R}$	0.0362	0.113	0.101	0.259
$\Delta_{11,\Lambda}^{b_L}$	0.0418	0.133	0.116	0.304
$\Delta_{11,\Lambda}^{b_R}$	0.0345	0.113	0.100	0.261
$\Delta_{11,\Lambda}^{t_L}$	0.0434	0.136	0.120	0.310
$\Delta_{11,\Lambda}^{t_R}$	0.0362	0.118	0.103	0.272

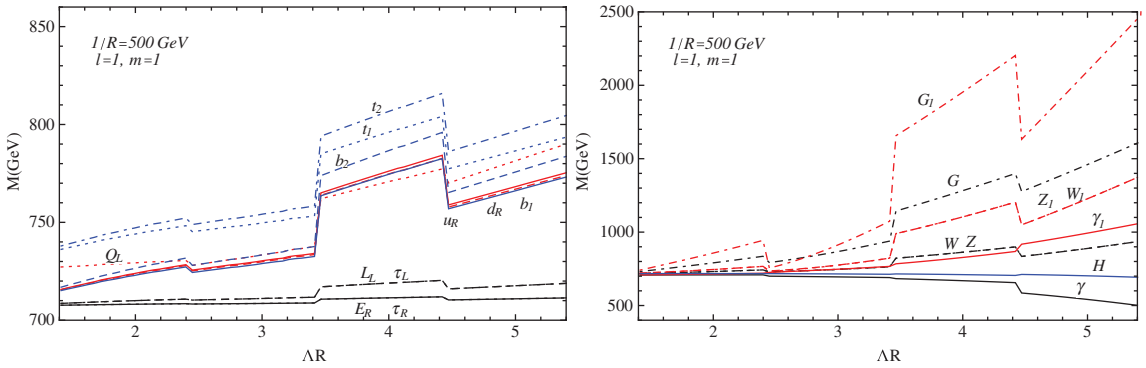

Fig. 12. The KK masses for the first KK modes at the one-loop level. The left panel shows the KK masses for fermions and the right panel shows those of gauge bosons as functions of ΛR. The angular momentum cut-off $\ell_{\max}$ is taken as the maximum integer satisfying $\sqrt{\ell_{\max}(\ell_{\max}+1)}/R \leq \Lambda$.

where we have taken the first order of $\{\Sigma, \delta\}$, and the values of $\delta N_{\ell m;\Lambda}$ are shown in Table 4 for the first KK mode. We thus obtain the KK mass eigenvalues

$$\tilde{m}_{\ell m}^{f_1} = \frac{1}{2}\Big[(\delta M)_{\ell m}^{f} - (\delta M)_{\ell m}^{F} + 2\sqrt{M_\ell^2 + m_{\rm SM}^2}\Big[1 + \frac{M_\ell((\delta M)_{\ell m}^{f} + (\delta M)_{\ell m}^{F}) - m_{\rm SM}\delta N_{\ell m;\Lambda}}{M_\ell^2 + m_{\rm SM}^2}\Big]\Big], \tag{99}$$

$$\tilde{m}_{\ell m}^{f_2} = -\frac{1}{2}\Big[(\delta M)_{\ell m}^{f} - (\delta M)_{\ell m}^{F} - 2\sqrt{M_\ell^2 + m_{\rm SM}^2}\Big[1 + \frac{M_\ell((\delta M)_{\ell m}^{f} + (\delta M)_{\ell m}^{F}) - m_{\rm SM}\delta N_{\ell m;\Lambda}}{M_\ell^2 + m_{\rm SM}^2}\Big]\Big], \tag{100}$$

for each KK mode of fermions, where we have taken the first order of $\{\delta M, \delta N\}$ in the right-hand side. The one-loop corrections to masses of the first KK modes for each fermion are shown in Table 5 and the left panel of Fig. 12.

To estimate the one-loop corrections to KK masses for four-dimensional gauge bosons, we need to calculate the coefficients Π in Eq. (68) from the one-loop diagrams. For each gauge boson, the

coefficients $\Pi(\tilde{\Pi})$ obtain contributions from each diagram such that

$$\Pi(G_\mu) = \sum_f \Pi^{ff}_{\text{Fig.3}} + \Pi^{HH}_{\text{Fig.4}} + \Pi^{H}_{\text{Fig.5}} + \Pi^{G_\mu G_\mu}_{\text{Fig.6}} + \Pi^{G_\mu}_{\text{Fig.7}} + \sum_{i=1,2} \Pi^{G_\mu G_i}_{\text{Fig.6}} + \sum_{i=1,2} \Pi^{G_i}_{\text{Fig.7}} + \sum_{i,j=1,2} \Pi^{G_i G_j}_{\text{Fig.6}} + \Pi^{c_G c_G}_{\text{Fig.4}}, \tag{101}$$

$$\Pi(W_\mu) = \sum_f \Pi^{ff}_{\text{Fig.3}} + \Pi^{HH}_{\text{Fig.4}} + \Pi^{H}_{\text{Fig.5}} + \Pi^{W_\mu W_\mu}_{\text{Fig.6}} + \Pi^{W_\mu}_{\text{Fig.7}} + \sum_{i=1,2} \Pi^{W_\mu W_i}_{\text{Fig.6}} + \sum_{i=1,2} \Pi^{W_i}_{\text{Fig.7}} + \sum_{i,j=1,2} \Pi^{W_i W_j}_{\text{Fig.6}} + \Pi^{c_W c_W}_{\text{Fig.4}}, \tag{102}$$

$$\Pi(B_\mu) = \sum_f \Pi^{ff}_{\text{Fig.3}} + \Pi^{HH}_{\text{Fig.4}} + \Pi^{H}_{\text{Fig.5}}, \tag{103}$$

where the $\tilde{\Pi}$s are given in the same way, each term in the right-hand side gives the contributions from different loop diagrams with particles running in the loop shown as superscript, and $c_{G,W}$ are ghost fields corresponding to G_μ and W_μ respectively. The contributions to each coefficient are obtained from Tables A5 and B1. For a U(1)$_Y$ gauge field B_μ and an SU(2) gauge field W^3_μ, the mass matrix at the one-loop level is given as

$$\begin{pmatrix} B_{\ell m\mu} \\ W^3_{\ell m\mu} \end{pmatrix}^T \begin{pmatrix} M^2_\ell + (\delta M^2)^B_{\ell m} + \frac{1}{4}g_1^2 v^2(1+\delta N^B) & \frac{1}{4}g_1 g_2 v^2\left(1+\frac{1}{2}\delta N^W + \frac{1}{2}\delta N^B\right) \\ \frac{1}{4}g_1 g_2 v^2\left(1+\frac{1}{2}\delta N^W + \frac{1}{2}\delta N^B\right) & M^2_\ell + (\delta M^2)^W_{\ell m} + \frac{1}{4}g_1^2 v^2(1+\delta N^W) \end{pmatrix} \times \begin{pmatrix} B^\mu_{\ell m} \\ W^{3\mu}_{\ell m} \end{pmatrix}, \tag{104}$$

where $(\delta M^2)^B_{\ell m}$ and $(\delta M^2)^W_{\ell m}$ are given by Eq. (74) with coefficients $\Pi(\tilde{\Pi})$ of Eqs. (102) and (103) for B_μ and W^i_μ respectively. Here we write $(\delta M^2)^{A_\mu}_{\ell m}$ as a product of $1/R^2$ and a numerical factor as in the fermion case, where $A_\mu = \{B_\mu, W_\mu, G_\mu\}$, such as

$$(\delta M^2)^{A_\mu}_{\ell m} = \Delta^{A_\mu}_{\ell m;\Lambda} \frac{1}{R^2}, \tag{105}$$

and we list the numerical factors $\Delta^{A_\mu}_{\ell m;\Lambda}$ in Table 3 for the first KK mode. The correction to non-diagonal elements is induced by renormalization of field Eq. (73) such that

$$\delta N^{W_\mu, B_\mu}_{\ell m;\Lambda} = \Pi_{\text{bulk}}(W, B)(p^2; \ell m; \ell m) + \Pi_{\text{bound}}(W, B)(p^2; \mu; \ell m; \ell m) - \delta_3(W, B), \tag{106}$$

where we have taken up to the first order in Π, and the values of $\delta N^{W,B}$ are shown in Table 4 for the first KK mode. Diagonalizing the mass matrix, we obtain the KK masses of KK-photon and KK-Z boson at one-loop level such that

$$\tilde{m}^2_{\gamma^\ell_\mu} \simeq M^2_\ell + \frac{1}{2}m_Z^2 + \frac{1}{2}\left[(\delta M^2)^B_{\ell m} + (\delta M^2)^W_{\ell m} - (m_Z^2 - m_W^2)\delta N^{B^\mu}_{\ell m;\Lambda} - m_W^2 \delta N^{W^\mu}_{\ell m;\Lambda}\right] - \frac{1}{2}\sqrt{((\delta M^2)^B_{\ell m} - (\delta M^2)^W_{\ell m})^2 + m_Z^4}, \tag{107}$$

Table 3. The numerical coefficients $\Delta_{\ell m}^{A_\mu,\phi_1}$ in Eqs. (105) and (115) for $\ell = 1$, $|m| = 1$ as a function of $\ell_{\max}$.

$\ell_{\max}$	2	3	4	5
$\Delta_{11,\Lambda}^{B_\mu}$	−0.0467	−0.141	−0.637	−1.128
$\Delta_{11,\Lambda}^{W_\mu}$	0.100	0.677	0.758	2.57
$\Delta_{11,\Lambda}^{G_\mu}$	0.513	3.23	4.52	13.6
$\Delta_{11,\Lambda}^{B_1}$	0.120	0.453	1.36	2.86
$\Delta_{11,\Lambda}^{W_1}$	0.118	1.89	2.38	10.2
$\Delta_{11,\Lambda}^{G_1}$	0.283	8.98	8.65	46.6
$\Delta_{11,\Lambda}^{H}$	−0.0064	−0.0167	−0.0362	−0.0269

Table 4. The numerical coefficients $\delta N_{\ell m;\Lambda}^{\psi,A,\phi_1,H}$ in Eqs. (98), (106), (116), and (123) for $\ell = 1$, $|m| = 1$ as a function of $\ell_{\max}$. Here the coefficients of only the third generation of fermions are shown.

$\ell_{\max}$	2	3	4	5
$\delta N_{11;\Lambda}^{\tau}$	0.00237	0.00223	0.00400	0.00274
$\delta N_{11;\Lambda}^{b}$	0.0229	0.0276	0.0397	0.0356
$\delta N_{11;\Lambda}^{t}$	0.0244	0.0301	0.0432	0.0404
$\delta N_{11;\Lambda}^{B_\mu}$	−0.0036	−0.0098	−0.0154	−0.0250
$\delta N_{11;\Lambda}^{W_\mu}$	−0.0014	−0.0067	−0.0129	−0.0240
$\delta N_{11;\Lambda}^{B_1}$	−0.00267	−0.000777	−0.00622	−0.000748
$\delta N_{11;\Lambda}^{W_1}$	−0.00532	−0.00152	−0.0124	−0.00149
$\delta N_{11;\Lambda}^{H}$	−0.00364	−0.00662	−0.0151	−0.0232

$$\tilde{m}_{Z_\mu^\ell}^2 \simeq M_\ell^2 + \frac{1}{2}m_Z^2 + \frac{1}{2}\left[(\delta M^2)_{\ell m}^B + (\delta M^2)_{\ell m}^W - (m_Z^2 - m_W^2)\delta N_{\ell m;\Lambda}^{B^\mu} - m_W^2 \delta N_{\ell m;\Lambda}^{W^\mu}\right] + \frac{1}{2}\sqrt{((\delta M^2)_{\ell m}^B - (\delta M^2)_{\ell m}^W)^2 + m_Z^4}, \tag{108}$$

where we ignored terms proportional to $\delta N_G^{B,W}$ in the square root in the second line of the right-hand side for both equations due to the smallness of the factor. For the KK modes of the $W^\pm$ bosons and gluon, the one-loop corrections to the KK masses are

$$(\tilde{m}_\ell^{W_\mu^\pm})^2 = M_\ell^2 + m_W^2 + (\delta M^2)_{\ell m}^W + m_W^2 \delta N_{\ell m;\Lambda}^{W^\mu}, \tag{109}$$

$$(\tilde{m}_\ell^G)^2 = M_\ell^2 + (\delta M^2)_{\ell m}^G, \tag{110}$$

where $(\delta M^2)_{\ell m}^G$ is given by Eq. (74) with coefficients Eq. (101). The corrected masses of the first KK modes for each gauge boson are shown in Table 5 and the right panel of Fig. 12.

To estimate the one-loop corrections to the KK masses for physical extra-dimensional components of gauge fields ϕ_1, we need to calculate the coefficients $\Theta(\tilde{\Theta})$ in Eq. (77) from one-loop diagrams.

Table 5. The one-loop correction to the masses of the first KK modes ($\ell = 1, |m| = 1$) for each cut-off scale where $\ell_{\max} = 2, 3, 4, 5$ are taken as reference values. Here we have taken the inverse of the S^2/Z_2 radius as $1/R = 500\,\text{GeV}$, where the tree-level first KK mass corresponds to $\sqrt{2}/R \simeq 707\,\text{GeV}$.

$\ell_{\max}$	2	3	4	5
$\tilde{m}_{11}(E_R)$ (GeV)	708.3	710.7	710.4	715.4
$\tilde{m}_{11}(L_L)$ (GeV)	710.3	717.1	716.0	729.9
$\tilde{m}_{11}(\tau_1)$ (GeV)	708.3	710.7	710.4	715.4
$\tilde{m}_{11}(\tau_2)$ (GeV)	710.3	717.1	716.0	729.9
$\tilde{m}_{11}(d_R)$ (GeV)	725.2	763.8.4	757.8	836.8
$\tilde{m}_{11}(u_R)$ (GeV)	725.6	765.0	758.9	839.6
$\tilde{m}_{11}(Q_L)$ (GeV)	728.0	762.1	770.1	827.9
$\tilde{m}_{11}(b_1)$ (GeV)	724.4	763.6	756.9	837.7
$\tilde{m}_{11}(b_2)$ (GeV)	728.0	773.9	765.2	859.3
$\tilde{m}_{11}(t_1)$ (GeV)	745.2	785.0	777.4	860.1
$\tilde{m}_{11}(t_2)$ (GeV)	748.9	794.0	786.1	879.2
$\tilde{m}_{11}(\gamma)$ (GeV)	701.4	684.7	587.2	428.4
$\tilde{m}_{11}(Z)$ (GeV)	727.7	820.7	833.0	1071.
$\tilde{m}_{11}(W)$ (GeV)	729.0	822.1	834.2	1072.
$\tilde{m}_{11}(G)$ (GeV)	792.8	1144.	1276.	1973.
$\tilde{m}_{11}(\gamma_1)$ (GeV)	727.9	785.7	919.0	1105.
$\tilde{m}_{11}(Z_1)$ (GeV)	733.6	988.9	1049.	1746.
$\tilde{m}_{11}(W_1)$ (GeV)	732.3	990.0	1050.	1746.
$\tilde{m}_{11}(G_1)$ (GeV)	755.4	1656.	1632.	3485.
$\tilde{m}_{11}(H)$ (GeV)	717.1	715.3	711.7	713.3

For each gauge boson, the coefficients $\Theta(\tilde{\Theta})$ obtain contributions from each diagram such that

$$\Theta(G_1) = \sum_f \Theta^{(1)ff}_{\text{Fig.3}} + \Theta^{(1)HH}_{\text{Fig.4}} + \Theta^{(1)H}_{\text{Fig.5}} + \Theta^{(1)G_\mu G_\mu}_{\text{Fig.6}} + \Theta^{(1)G_\mu}_{\text{Fig.7}} + \sum_{a=1,2} \Theta^{(1)G_\mu G_a}_{\text{Fig.6}} + \sum_{a=1,2} \Theta^{(1)G_a}_{\text{Fig.7}} + \sum_{a,b=1,2} \Theta^{(1)G_a G_b}_{\text{Fig.6}} + \Theta^{(1)c_G c_G}_{\text{Fig.4}}, \tag{111}$$

$$\Theta(W_1) = \sum_f \Theta^{(1)ff}_{\text{Fig.3}} + \Theta^{(1)HH}_{\text{Fig.4}} + \Theta^{(1)H}_{\text{Fig.5}} + \Theta^{(1)W_\mu W_\mu}_{\text{Fig.6}} + \Theta^{(1)W_\mu}_{\text{Fig.7}} + \sum_{a=1,2} \Theta^{(1)W_\mu W_a}_{\text{Fig.6}} + \sum_{a=1,2} \Theta^{(1)W_a}_{\text{Fig.7}} + \sum_{a,b=1,2} \Theta^{(1)W_a W_b}_{\text{Fig.6}} + \Theta^{(1)c_W c_W}_{\text{Fig.4}}, \tag{112}$$

$$\Theta(B_1) = \sum_f \Theta^{(1)ff}_{\text{Fig.3}} + \Theta^{(1)HH}_{\text{Fig.4}} + \Theta^{(1)H}_{\text{Fig.5}}, \tag{113}$$

where the $\tilde{\Theta}$s are given in the same way, and each term in the right-hand side gives the contributions from different loop diagrams with particles running in the loop shown as superscript. The contributions to each coefficient are obtained from Tables B2 and B3. The one-loop corrections to KK masses for ϕ_1 are obtained similarly to the four-dimensional case. For B_1 and W_1^3, the corrected mass matrix

is given as

$$\begin{pmatrix} B_{1\ell m} \\ W^3_{1\ell m} \end{pmatrix}^T \begin{pmatrix} M_\ell^2 + (\delta M^2)^{B_1}_{\ell m} + \frac{1}{4}g_1^2 v^2 (1 + \delta N^{B_1}_{\ell m;\Lambda}) & \frac{1}{4}g_1 g_2 v^2 \left(1 + \frac{1}{2}\delta N^{W_1}_{\ell m;\Lambda} + \frac{1}{2}\delta N^{B_1}_{\ell m;\Lambda}\right) \\ \frac{1}{4}g_1 g_2 v^2 \left(1 + \frac{1}{2}\delta N^{W_1}_{\ell m;\Lambda} + \frac{1}{2}\delta N^{B_1}_{\ell m;\Lambda}\right) & M_\ell^2 + (\delta M^2)^{W_1}_{\ell m} + \frac{1}{4}g_1^2 v^2 \left(1 + \delta N^{W_1}_{\ell m;\Lambda}\right) \end{pmatrix} \times \begin{pmatrix} B_{1\ell m} \\ W^3_{1\ell m} \end{pmatrix}, \tag{114}$$

where $\tilde{M}^2_{B_{1\ell m}}$ and $\tilde{M}^2_{W_{1\ell m}}$ are given by Eq. (83) with coefficients in Eqs. (112) and (113) for B_i and W_i respectively. Here we write $(\delta M^2)^{\phi_1}_{\ell m}$ in the same form as Eq. (105), where $\phi_1 = \{B_1, W_1, G_1\}$, as

$$(\delta M^2)^{\phi_1}_{\ell m} = \Delta^{\phi_1}_{\ell m} \frac{1}{R^2}, \tag{115}$$

and we list the numerical factor $\Delta^{\phi_1}_{\ell m}$ in Table 2 for the first KK mode. The correction to off-diagonal elements is induced by the renormalization of field Eq. (82) such that

$$\delta N^{W_1,B_1}_{\ell m;\Lambda} = -\Theta_{\rm bulk}(W,B)(\ell m;\ell m) - \Theta_{\rm bound}(W,B)(\mu;\ell m;\ell m) - \delta^{(1)}_3(W,B), \tag{116}$$

where we have taken up to the first order of $\Theta(\tilde{\Theta})$, and the values of $\delta N^{W_1,B_1}_{\ell m;\Lambda}$ are shown in Table 4 for the first KK mode. Diagonalizing the mass matrix, we obtain the one-loop corrections to KK masses of extra-dimensional components KK-photon and KK-Z boson such that

$$\tilde{m}^2_{\gamma^\ell_1} \simeq M_\ell^2 + \frac{1}{2}m_Z^2 + \frac{1}{2}\left[(\delta M^2)^{B_1}_{\ell m} + (\delta M^2)^{W_1}_{\ell m} - (m_Z^2 - m_W^2)\delta N^{B_1}_{\ell m;\Lambda} - m_W^2 \delta N^{W_1}_{\ell m;\Lambda}\right] - \frac{1}{2}\sqrt{((\delta M^2)^{B_1}_{\ell m} - (\delta M^2)^{W}_{\ell m})^2 + m_Z^4}, \tag{117}$$

$$\tilde{m}^2_{Z^\ell_1} \simeq M_\ell^2 + \frac{1}{2}m_Z^2 + \frac{1}{2}\left[(\delta M^2)^{B_1}_{\ell m} + (\delta M^2)^{W_1}_{\ell m} - (m_Z^2 - m_W^2)\delta N^{B_1}_{\ell m;\Lambda} - m_W^2 \delta N^{W_1}_{\ell m;\Lambda}\right] + \frac{1}{2}\sqrt{((\delta M^2)^{B_1}_{\ell m} - (\delta M^2)^{W_1}_{\ell m})^2 + m_Z^4}, \tag{118}$$

where we ignored the terms proportional to $\delta N^{B,W}_\phi$ in the square root in the second line of the right-hand side for both equations due to the smallness of the factor. For the KK modes of the $W^\pm$ bosons and gluon, the one-loop corrections to KK masses are

$$(\tilde{m}^{W^\pm_1}_\ell)^2 = M_\ell^2 + m_W^2 + (\delta M^2)^{W_1}_{\ell m} + m_W^2 \delta N^{W_1}_{\ell m;\Lambda}, \tag{119}$$

$$(\tilde{m}^{G_1}_\ell)^2 = M_\ell^2 + (\delta M^2)^{G_1}_{\ell m}, \tag{120}$$

where $(\delta M^2)^{G_1}_{\ell m}$ is given by Eq. (83) with coefficients in Eq. (111). The one-loop corrections to the masses of the first KK modes for each ϕ_1 are shown in Table 5 and the right panel of Fig. 12.

To estimate the one-loop corrections to KK masses for the SM Higgs boson, we need to calculate the coefficients $\Xi(\tilde{\Xi})$ in Eq. (86) from one-loop diagrams. The coefficients $\Xi(\tilde{\Xi})$ obtain contributions from each diagram such that

$$\Xi(H) = \sum_f \Xi^{ff}_{\rm Fig.10} + \Xi^{H}_{\rm Fig.11} + \Xi^{W_\mu H}_{\rm Fig.8} + \Xi^{B_\mu H}_{\rm Fig.8} + \Xi^{W_\mu}_{\rm Fig.9} + \Xi^{B_\mu}_{\rm Fig.9} + \sum_i \Xi^{W_i}_{\rm Fig.9} + \sum_i \Xi^{B_i}_{\rm Fig.9} + \sum_i \Xi^{W_i H}_{\rm Fig.8} + \sum_i \Xi^{B_i H}_{\rm Fig.8}, \tag{121}$$

where $\tilde{\Xi}$ is given in the same way, and each term in the right-hand side gives the contributions from different loop diagrams with particles propagating inside the loop shown as superscript. The one-loop corrections to KK masses for the KK Higgs boson are also obtained in a similar way such that

$$(\tilde{m}_\ell^H)^2 = M_\ell^2 + m_h^2 + (\delta M^2)_{\ell m}^H + m_h^2 \delta N_{\ell m;\Lambda}^H, \tag{122}$$

where the fourth term on the right-hand side is induced by normalization of field Eq. (89) such that

$$\delta N_{\ell m;\Lambda}^H = -\Xi_{\rm bulk}(\ell m;\ell m) - \Xi_{\rm bound}(\mu;\ell m;\ell m) - \delta_3^H, \tag{123}$$

taking up to the first order of Ξ, and the values of δN^H are shown in Table 4. The $(\delta M^2)_{\ell m}^H$ is also written as Eq. (105) such that

$$(\delta M^2)_{\ell m}^H = \Delta_{\ell m;\Lambda}^H \frac{1}{R^2}, \tag{124}$$

and we list the numerical factor $\Delta_{\ell m;\Lambda}^H$ in Table 2. Also, the one-loop corrections to the masses of the first KK modes for Higgs bosons are shown in Table 5 and the right panel of Fig. 12.

Table 5 shows the one-loop corrections to the KK mass of the first KK modes $\ell = 1, |m| = 1$ for each SM particle where we take the cut-off $\ell_{\rm max} = 2, 3, 4, 5$ as a reference value. From the table we can see that the first KK photon has the lightest KK mass for any cut-off scale. The first KK photon is thus a promising candidate of the dark matter in the model. The smallest correction to the KK photon mass is due to the negative contributions from fermion loops while the non-Abelian gauge bosons obtain large contributions from the loops associated with self-interactions. We also find that negative contributions from fermion loops to the KK masses of ϕ_1 tend to be less effective compared with the case of four-dimensional components, and the one-loop corrections to the KK masses become larger than those of four-dimensional components. We show the cut-off scale dependence of the first KK masses in Fig. 12, where we ignored the SM masses of e, μ, u, d, s, c and write E_R, L, u_R, d_R, Q_L for the SU(2) singlet charged lepton, doublet lepton, singlet quarks, and doublet quarks respectively. We also note that zig-zag-shaped lines appear in Fig. 12 where the discontinuity of the plot corresponds to an increase of $\ell_{\rm max}$ at $\Lambda R = \sqrt{\ell_{\rm max}(\ell_{\rm max}+1)}$ and the corrected masses tend to be small for even $\ell_{\rm max}$ compared to odd. This tendency is due to the sign factor of $(-1)^{\{\ell,m\}}$ which appears from propagator and vertices on S^2/Z_2 and gives a different sign contribution from each KK mode in the loops, as mentioned below Eq. (57). Since the number of negative and positive sign contributions is different for the even or odd $\ell_{\rm max}$ cases, the corrected mass depends on $\ell_{\rm max}$ differently for the even or odd cases. The quantum corrections tend to be large for the large cut-off scale since the six-dimensional loop expansion parameter $\epsilon = \frac{g_a^2}{32\pi^2}(R\Lambda)^2$ becomes large. This indicates that the perturbation is not reliable and we cannot take a large cut-off scale, which is a generic feature of non-renormalizable theories.

5. Summary and discussions

We have investigated the quantum correction of Kaluza–Klein masses in the S^2/Z_2 universal extra-dimensional model in order to determine the lightest KK particle which would be the dark matter candidate.

We first derived the Feynman rules for propagators and vertices on the six-dimensional spacetime $M^4 \times S^2/Z^2$. We then calculated the one-loop diagrams relevant to one-loop corrections to the KK masses with the Feynman rules. The contributions from the one-loop diagrams can be separated into the bulk contribution conserving KK number m and the boundary contribution violating KK number

conservation, which is a similar structure to the minimal UED case. In calculating these diagrams, we introduced the cut-off for both 4-momentum integration and angular momentum sum inside a loop by defining the 4-momentum cut-off scale Λ and the angular momentum number cut-off $\ell_{\max}$. Thus the bulk contribution is estimated with cut-off scale Λ as an upper bound of momentum integration while the boundary contribution is estimated by taking the leading log-divergent part assuming vanishing contribution at the cut-off scale. The contributions from the one-loop diagrams are then organized in the form of Eqs. (58), (68), (77), and (86) for fermions, gauge bosons, extra-dimensional components gauge bosons, and scalar bosons respectively, and the explicit forms of the contributions are summarized in Tables A4, A5, B1, B2, B3, B5, B6, and B7. Taking into account the renormalization conditions, we finally obtained the formulas to derive the corrected KK masses as Eqs. (65), (74), (83), and (90) for fermions, gauge bosons, extra dimensional components gauge bosons, and scalar bosons respectively.

Finally we estimated the corrected KK masses of the first KK mode ($\ell = 1, |m| = 1$) for each SM particle, applying the formulas in Sect. 3. The resulting corrected masses, taking $1/R = 500\,\mathrm{GeV}$ as a reference value, are summarized in Table 5 for each cut-off. We then found that the lightest KK particle is the first KK photon γ_μ^{11} as in the minimal UED case, and it can be identified as a promising DM candidate. We have also shown numerical plots of the one-loop correction to the first KK modes as a function of cut-off scale Λ in Fig. 12. We have found that the corrected masses tend to be small for even $\ell_{\max}$ compared to odd ones due to the sign factor $(-1)^{\{\ell,m\}}$ which appears in the loop diagram calculation. The quantum correction tends to be large for higher cut-off since the number of modes inside a loop becomes very large, which indicates that we cannot take the cut-off scale too large.

It would be very interesting to study the relic density of the dark matter candidate, γ_μ^{11}, with the corrected mass spectrum, which will give constraints for the S^2/Z_2 radius R and the cut-off scale Λ. Furthermore, the one-loop corrections to the mass spectrum would lead to a prediction of the experimental signature of our model, and the analysis is left for future work.

Acknowledgements

The work of N.M. was supported in part by a Grant-in-Aid from the Ministry of Education, Culture, Sports, Science, and Technology, Government of Japan (No. 24540283). The work of T.N. was supported in part by NSC Grant No. 102-2811-M-006-035. The work of J.S. was supported in part by Grants-in-Aid from the Ministry of Education, Culture, Sports, Science, and Technology, Government of Japan (Nos. 24340044 and 25105009).

Funding

Open Access funding: Funded by SCOAP[3].

Appendix A. Summary lists of vertices in our model

Here we summarize the Feynman rules for vertices in our model. The vertices including fermions are derived from gauge interactions and Yukawa interactions

$$\int \mathrm{d}x^4 \mathrm{d}\Omega g_{6a} \bar{\Psi}_\pm \Gamma^M T_i^a A_M^i \Psi_\pm, \tag{A1}$$

$$\int \mathrm{d}x^4 \mathrm{d}\Omega Y_f \bar{\Psi}_\pm H \Psi_\mp, \tag{A2}$$

where $A_{\theta,\phi}$ in Eqs. (20) and (21) are substituted. The Feynman rules for these vertices are listed in Table A1, where the non-trivial factors in these vertices are given by integrations of the mode

Table A1. The vertex factors for interactions including fermions where $Y_f = Y_{u,d,e}$.

Interaction	Vertex factor
$\Psi_{\pm\ell_1 m_1} A_{\mu\ell_2 m_2} \Psi_{\pm\ell_3 m_3}$	$\mathrm{i}\frac{g_{6a}}{R} T^a \gamma^\mu \left[I^\alpha_{\ell_1 m_1;\ell_2 m_2;\ell_3 m_3} P_{R(L)} + I^\beta_{\ell_1 m_1;\ell_2 m_2;\ell_3 m_3} P_{L(R)} \right]$
$\Psi_{\pm\ell_1 m_1} \phi_{1\ell_2 m_2} \Psi_{\pm\ell_3 m_3}$	$\mathrm{i}\frac{g_{6a}}{R} T^a \gamma_5 \left[C^\alpha_{\ell_1 m_1;\ell_2 m_2;\ell_3 m_3} P_{L(R)} + C^\beta_{\ell_1 m_1;\ell_2 m_2;\ell_3 m_3} P_{R(L)} \right]$
$\Psi_{\pm\ell_1 m_1} \phi_{2\ell_2 m_2} \Psi_{\pm\ell_3 m_3}$	$\mathrm{i}\frac{g_{6a}}{R} T^a \gamma_5 \left[\mathrm{i} C^\alpha_{\ell_1 m_1;\ell_2 m_2;\ell_3 m_3} P_{L(R)} - \mathrm{i} C^\beta_{\ell_1 m_1;\ell_2 m_2;\ell_3 m_3} P_{R(L)} \right]$
$\Psi_{\mp\ell_1 m_1} H_{\ell_2 m_2} \Psi_{\pm\ell_3 m_3}$	$\mathrm{i}\frac{Y_f}{R} \left[I^\alpha_{\ell_1 m_1;\ell_2 m_2;\ell_3 m_3} P_{R(L)} + I^\beta_{\ell_1 m_1;\ell_2 m_2;\ell_3 m_3} P_{L(R)} \right]$

Table A2. The vertex factors for interactions including Higgs bosons.

Interaction	Vertex factor
$H^\dagger_{\ell_1 m_1}(p_1) A_{\mu\ell_2 m_2} H_{\ell_3 m_3}(p_2)$	$\mathrm{i}\frac{g_{6a}}{R} T^a (p_1^\mu + p_2^\mu) J^1_{\underline{\ell_1 m_1};\ell_2 m_2;\ell_3 m_3}$
$H^\dagger_{\ell_1 m_1}(p_1) \phi_{1\ell_2 m_2} H_{\ell_3 m_3}(p_2)$	$-\frac{g_{6a}}{R} T^a \left[J^2_{\underline{\ell_1 m_1};\ell_2 m_2;\ell_3 m_3} - J^2_{\ell_3 m_3;\ell_2 m_2;\underline{\ell_1 m_1}} \right]$
$H^\dagger_{\ell_1 m_1}(p_1) \phi_{2\ell_2 m_2} H_{\ell_3 m_3}(p_2)$	$-\frac{g_{6a}}{R} T^a \left[J^3_{\underline{\ell_1 m_1};\ell_2 m_2;\ell_3 m_3} - J^3_{\ell_3 m_3;\ell_2 m_2;\underline{\ell_1 m_1}} \right]$
$A^\mu_{\ell_1 m_1} A^\nu_{\ell_2 m_2} H^\dagger_{\ell_3 m_3} H_{\ell_4 m_4}$	$2\mathrm{i}\frac{g_{6a}^2}{R^2} T^a_i T^a_j g_{\mu\nu} K^1_{\ell_1 m_1;\ell_2 m_2;\underline{\ell_3 m_3};\ell_4 m_4}$
$\phi_{1(2)\ell_1 m_1} \phi_{1(2)\ell_2 m_2} H^\dagger_{\ell_3 m_3} H_{\ell_4 m_4}$	$-2\mathrm{i}\frac{g_{6a}^2}{R^2} T^a_i T^a_j K^2_{\ell_1 m_1;\ell_2 m_2;\underline{\ell_3 m_3};\ell_4 m_4}$
$H_{\ell_1 m_1} H_{\ell_2 m_2} H_{\ell_3 m_3} H_{\ell_4 m_4}$	$-\mathrm{i}\frac{\lambda_6}{R^2} g_{\mu\nu} K^1_{\ell_1 m_1;\ell_2 m_2;\ell_3 m_3;\ell_4 m_4}$

function as Eq. (46) for $I^{\alpha(\beta)}$, and

$$C^\alpha_{\ell_1 m_1;\ell_2 m_2;\ell_3 m_3} = \int \mathrm{d}\Omega \tilde{\alpha}^*_{\ell_1 m_1} \left(\partial_\theta - \frac{\mathrm{i}}{\sin\theta} \partial_\phi \right) \tilde{Y}_{\ell_2 m_2} \tilde{\beta}_{\ell_3 m_3}, \tag{A3}$$

$$C^\beta_{\ell_1 m_1;\ell_2 m_2;\ell_3 m_3} = -\int \mathrm{d}\Omega \tilde{\beta}^*_{\ell_1 m_1} \left(\partial_\theta + \frac{\mathrm{i}}{\sin\theta} \partial_\phi \right) \tilde{Y}_{\ell_2 m_2} \tilde{\alpha}_{\ell_3 m_3}. \tag{A4}$$

The vertices for self-interactions of gauge boson are derived from the terms in the Lagrangian

$$\int \mathrm{d}x^4 \mathrm{d}\Omega \left[-\frac{1}{4} F^i_{\mu\nu} F^{i\mu\nu} + \frac{1}{2R^2} F^i_{\theta\mu} F^{i\mu}_\theta + \frac{1}{2R^2 \sin^2\theta} F^i_{\phi\mu} F^{i\mu}_\phi - \frac{1}{2R^4 \sin^2\theta} F^i_{\theta\phi} F^i_{\theta\phi} \right], \tag{A5}$$

where i is the index of the gauge group. The first term of Eq. (A5) in the bracket is expanded as

$$\begin{aligned} -\frac{1}{4} F^i_{\mu\nu} F^{i\mu\nu} = & -\frac{1}{4} (\partial_\mu A^i_\nu - \partial_\nu A^i_\mu)(\partial^\mu A^{i\nu} - \partial^\nu A^{i\mu}) \\ & - g f^{ijk} \partial_\mu A^i_\nu A^{j\mu} A^{k\nu} - \frac{1}{4} g^2 f^{ijm} f^{klm} A^i_\mu A^j_\nu A^{k\mu} A^{l\nu}, \end{aligned} \tag{A6}$$

where the second line of the right-hand side gives the three- and four-point self-interaction of the gauge boson summarized in Table A3. The second and the third terms of Eq. (A5) give interactions

between A_μ and $A_{\theta,\phi}$. By substituting $A_{\theta,\phi}$ of Eqs. (20) and (21), we obtain the interaction terms

$$\begin{aligned}
&\frac{1}{2R^2}F^i_{\theta\mu}F^{i\mu}_{\theta}+\frac{1}{2R^2\sin^2\theta}F^i_{\phi\mu}F^{i\mu}_{\phi}\supset\frac{g_{6a}}{R^2}f^{ijk}\Bigg[\frac{1}{\sin\theta}(\partial_\phi A^i_\mu\partial_\theta\phi^j_1A^{k\mu}-\partial_\theta A^i_\mu\partial_\phi\phi^j_1A^{k\mu})\\
&+\partial_\theta A^i_\mu\partial_\theta\phi^j_2A^{k\mu}+\frac{1}{\sin^2\theta}\partial_\phi A^i_\mu\partial_\phi\phi^j_2A^{k\mu}-\partial_\theta\partial_\mu\phi^i_1\partial_\theta\phi^j_1A^{k\mu}-\frac{1}{\sin^2\theta}\partial_\phi\partial_\mu\phi^i_1\partial_\phi\phi^j_1A^{k\mu}\\
&-\partial_\theta\partial_\mu\phi^i_2\partial_\theta\phi^j_2A^{k\mu}-\frac{1}{\sin^2\theta}\partial_\phi\partial_\mu\phi^i_2\partial_\phi\phi^j_2A^{k\mu}-\frac{1}{\sin\theta}(\partial_\theta\partial_\mu\phi^i_1\partial_\phi\phi^j_2A^{k\mu}+\partial_\phi\partial_\mu\phi^i_2\partial_\theta\phi^j_1A^{k\mu}\\
&-\partial_\theta\partial_\mu\phi^i_2\partial_\phi\phi^j_1A^{k\mu}-\partial_\phi\partial_\mu\phi^i_1\partial_\theta\phi^j_2A^{k\mu})\Bigg]+\frac{g^2_{6a}}{2R^2}f^{ijm}f^{klm}\Bigg[\partial_\theta\phi^i_1\partial_\theta\phi^k_1A^j_\mu A^{l\mu}\\
&+\frac{1}{\sin^2\theta}\partial_\phi\phi^i_1\partial_\phi\phi^k_1A^j_\mu A^{l\mu}+\partial_\theta\phi^i_2\partial_\theta\phi^k_2A^j_\mu A^{l\mu}+\frac{1}{\sin^2\theta}\partial_\phi\phi^i_2\partial_\phi\phi^k_2A^j_\mu A^{l\mu}\\
&+\frac{1}{\sin\theta}(\partial_\theta\phi^i_1\partial_\phi\phi^k_2A^j_\mu A^{l\mu}+\partial_\phi\phi^i_2\partial_\theta\phi^k_1A^j_\mu A^{l\mu}-\partial_\theta\phi^i_2\partial_\phi\phi^k_1A^j_\mu A^{l\mu}-\partial_\phi\phi^i_1\partial_\theta\phi^k_2A^j_\mu A^{l\mu})\Bigg],
\end{aligned}\tag{A7}$$

providing vertex factors from the third line to the seventh line in Table A3. The last term of Eq. (A5) gives interactions between the ϕ_is after substituting $A_{\theta,\phi}$ from Eqs. (20) and (21) such that

$$\begin{aligned}
&-\frac{1}{2R^4\sin^2\theta}F^i_{\theta\phi}F^i_{\theta\phi}\supset\frac{g_{6a}}{R^4}f^{ijk}\Bigg[(\hat{L}^2\phi^i_1)\left(\partial_\theta\phi^j_2\partial_\theta\phi^k_1-\frac{1}{\sin^2\theta}\partial_\phi\phi^j_1\partial_\phi\phi^k_2\right)\\
&+\frac{1}{\sin\theta}(\hat{L}^2\phi^i_1)\partial_\theta\phi^j_2\partial_\phi\phi^k_2-\frac{1}{\sin\theta}(\hat{L}^2\phi^i_1)\partial_\phi\phi^j_1\partial_\theta\phi^k_1\Bigg]\\
&-\frac{g^2_{6a}}{2R^4}f^{ijm}f^{klm}\Bigg[\frac{1}{\sin^2\theta}\partial_\phi\phi^i_1\partial_\theta\phi^j_1\partial_\phi\phi^k_1\partial_\theta\phi^l_1+\frac{1}{\sin^2\theta}\partial_\theta\phi^i_2\partial_\phi\phi^j_2\partial_\theta\phi^k_2\partial_\phi\phi^l_2\\
&-\frac{1}{\sin\theta}\partial_\theta\phi^i_2\partial_\theta\phi^j_1\partial_\phi\phi^k_1\partial_\theta\phi^l_1-\frac{1}{\sin\theta}\partial_\phi\phi^i_1\partial_\theta\phi^j_1\partial_\theta\phi^k_2\partial_\theta\phi^l_1+\frac{1}{\sin^3\theta}\partial_\phi\phi^i_1\partial_\theta\phi^j_1\partial_\phi\phi^k_1\partial_\phi\phi^l_2\\
&+\frac{1}{\sin^3\theta}\partial_\phi\phi^i_1\partial_\phi\phi^j_2\partial_\phi\phi^k_1\partial_\theta\phi^l_1+\frac{1}{\sin\theta}\partial_\theta\phi^i_2\partial_\theta\phi^j_1\partial_\theta\phi^k_2\partial_\phi\phi^l_2+\frac{1}{\sin\theta}\partial_\theta\phi^i_2\partial_\phi\phi^j_2\partial_\theta\phi^k_2\partial_\theta\phi^l_1\\
&-\frac{1}{\sin^3\theta}\partial_\theta\phi^i_2\partial_\phi\phi^j_2\partial_\phi\phi^k_1\partial_\phi\phi^l_2-\frac{1}{\sin^3\theta}\partial_\phi\phi^i_1\partial_\phi\phi^j_2\partial_\theta\phi^k_2\partial_\phi\phi^l_2+\partial_\theta\phi^i_2\partial_\theta\phi^j_1\partial_\theta\phi^k_2\partial_\theta\phi^l_1\\
&+\frac{1}{\sin^4\theta}\partial_\phi\phi^i_1\partial_\phi\phi^j_2\partial_\phi\phi^k_1\partial_\phi\phi^l_2-\frac{1}{\sin^2\theta}\partial_\theta\phi^i_2\partial_\theta\phi^j_1\partial_\phi\phi^k_1\partial_\phi\phi^l_2-\frac{1}{\sin^2\theta}\partial_\theta\phi^i_2\partial_\phi\phi^j_2\partial_\phi\phi^k_1\partial_\theta\phi^l_1\\
&-\frac{1}{\sin^2\theta}\partial_\phi\phi^i_1\partial_\theta\phi^j_1\partial_\theta\phi^k_2\partial_\phi\phi^l_2-\frac{1}{\sin^2\theta}\partial_\phi\phi^i_1\partial_\phi\phi^j_2\partial_\theta\phi^k_2\partial_\theta\phi^l_1\Bigg],
\end{aligned}\tag{A8}$$

providing vertex factors from the eighth line to the thirteenth line in Table A3. The vertex factor associated with the ghost fields c^i is also obtained from the gauge–ghost interaction in Eq. (8), and it is summarized in both the fourteenth and the fifteenth vertex factors in Table A3. The non-trivial coefficients appearing in the vertex factors in Table A3 are given by integration of spherical harmonics and their derivative with respect to the extra spatial coordinates. For three-point vertices, these

Table A3. The vertex factors for self-interactions of gauge bosons including extra-dimensional components.

Interaction	Vertex factor
$A^{i\mu}_{\ell_1 m_1}(k)A^{j\nu}_{\ell_2 m_2}(p)A^{k\rho}_{\ell_3 m_3}(q)$	$\frac{g_{6a}}{R}f_a^{ijk}\,[g^{\mu\nu}(k-p)^\rho + g^{\nu\rho}(p-q)^\mu + g^{\rho\mu}(q-k)^\nu]\,J^1_{\ell_1 m_1;\ell_2 m_2;\ell_3 m_3}$
$A^{i\mu}_{\ell_1 m_1}A^{j\nu}_{\ell_2 m_2}A^{k\rho}_{\ell_3 m_3}A^{l\sigma}_{\ell_4 m_4}$	$-\mathrm{i}\frac{g_{6a}^2}{R^2}[f_a^{ijm}f^{klm}(g^{\mu\rho}g^{\nu\sigma}-g^{\mu\sigma}g^{\nu\rho}) + f^{ikm}f^{jlm}(g^{\mu\nu}g^{\rho\sigma}-g^{\mu\sigma}g^{\nu\rho})$ $+f^{ilm}f^{jkm}(g^{\mu\nu}g^{\rho\sigma}-g^{\mu\rho}g^{\nu\sigma})]K^1_{\ell_1 m_1;\ell_2 m_2;\ell_3 m_3;\ell_4 m_4}$
$A^{i\mu}_{\ell_1 m_1}A^{j\nu}_{\ell_2 m_2}\phi^k_{1\ell_3 m_3}$	$-\mathrm{i}\frac{g_{6a}}{R^2}f^{ijk}g^{\mu\nu}J^4_{\ell_1 m_1;\ell_2 m_2;\ell_3 m_3}$
$A^{i\mu}_{\ell_1 m_1}A^{j\nu}_{\ell_2 m_2}\phi^k_{2\ell_3 m_3}$	$-\mathrm{i}\frac{g_{6a}}{R^2}f^{ijk}g^{\mu\nu}J^5_{\ell_1 m_1;\ell_2 m_2;\ell_3 m_3}$
$\phi^i_{1(2)\ell_1 m_1}(p)\phi^j_{1(2)\ell_2 m_2}(q)A^{k\mu}_{\ell_3 m_3}$	$\frac{g_{6a}}{R}f^{ijk}(q-p)^\mu J^6_{\ell_1 m_1;\ell_2 m_2;\ell_3 m_3}$
$\phi^i_{1\ell_1 m_1}(p)\phi^j_{2\ell_2 m_2}(q)A^{k\mu}_{\ell_3 m_3}$	$\frac{g_{6a}}{R}f^{ijk}(q-p)^\mu J^7_{\ell_1 m_1;\ell_2 m_2;\ell_3 m_3}$
$\phi^i_{1\ell_1 m_1}(p)\phi^j_{2\ell_2 m_2}(q)A^{k\mu}_{\ell_3 m_3}A^{lv}_{\ell_4 m_4}$	$\mathrm{i}\frac{g_{6a}^2}{R^2}g^{\mu\nu}(f^{ikm}f^{jlm}+f^{ilm}f^{jkm})K^3_{\ell_1 m_1;\ell_2 m_2;\ell_3 m_3;\ell_4 m_4}$
$\phi^i_{1\ell_1 m_1}(p)\phi^j_{1\ell_2 m_2}(q)\phi^k_{2\ell_3 m_3}$	$-\mathrm{i}\frac{g_{6a}}{R^2}f^{ijk}J^8_{\ell_1 m_1;\ell_2 m_2;\ell_3 m_3}$
$\phi^i_{2\ell_1 m_1}(p)\phi^j_{2\ell_2 m_2}(q)\phi^k_{1\ell_3 m_3}$	$\mathrm{i}\frac{g_{6a}}{R^2}f^{ijk}J^9_{\ell_1 m_1;\ell_2 m_2;\ell_3 m_3}$
$\phi^i_{1\ell_1 m_1}\phi^j_{1\ell_2 m_2}\phi^k_{1\ell_3 m_3}$	$-\mathrm{i}\frac{g_{6a}}{R^2}f^{ijk}J^{10}_{\ell_1 m_1;\ell_2 m_2;\ell_3 m_3}$
$\phi^i_{1(2)\ell_1 m_1}\phi^j_{1(2)\ell_2 m_2}\phi^k_{1(2)\ell_3 m_3}\phi^l_{1(2)\ell_4 m_4}$	$-\mathrm{i}\frac{g_{6a}^2}{R^2}\Big[(f^{ijm}f^{klm}+f^{kjm}f^{ilm})K^4_{\ell_1 m_1;\ell_2 m_2;\ell_3 m_3;\ell_4 m_4}$ $-(f^{ijm}f^{klm}+f^{ikm}f^{jlm})K^4_{\ell_2 m_2;\ell_1 m_1;\ell_3 m_3;\ell_4 m_4}$ $+(f^{ikm}f^{jlm}-f^{kjm}f^{ilm})K^4_{\ell_1 m_1;\ell_3 m_3;\ell_2 m_2;\ell_4 m_4}\Big]$
$\phi^i_{1(2)\ell_1 m_1}\phi^j_{2(1)\ell_2 m_2}\phi^k_{2(1)\ell_3 m_3}\phi^l_{2(1)\ell_4 m_4}$	$\pm\mathrm{i}\frac{g_{6a}^2}{R^2}\Big[(f^{ijm}f^{klm}+f^{ikm}f^{jlm})K^5_{\ell_1 m_1;\ell_2 m_2;\ell_3 m_3;\ell_4 m_4}$ $-(f^{ijm}f^{klm}-f^{ilm}f^{jkm})K^5_{\ell_1 m_1;\ell_2 m_2;\ell_4 m_4;\ell_3 m_3}$ $-(f^{ilm}f^{jkm}+f^{ikm}f^{jlm})K^5_{\ell_1 m_1;\ell_4 m_4;\ell_3 m_3;\ell_2 m_2}\Big]$
$\phi^i_{1\ell_1 m_1}\phi^j_{1\ell_2 m_2}\phi^k_{2\ell_3 m_3}\phi^l_{2\ell_4 m_4}$	$\mathrm{i}\frac{g_{6a}^2}{R^2}\Big[(f^{ikm}f^{jlm}+f^{jkm}f^{ilm})K^6_{\ell_1 m_1;\ell_2 m_2;\ell_3 m_3;\ell_4 m_4}$ $+(f^{ijm}f^{klm}-f^{ilm}f^{jkm})K^4_{\ell_2 m_2;\ell_1 m_1;\ell_3 m_3;\ell_4 m_4}$ $-(f^{ijm}f^{klm}+f^{ikm}f^{jlm})K^4_{\ell_1 m_1;\ell_2 m_2;\ell_3 m_3;\ell_4 m_4}\Big]$
$c^i_{\ell_1 m_1}(p)A^{j\mu}_{\ell_2 m_2}c^k_{\ell_3 m_3}$	$-\frac{g_{6a}}{R}f^{ijk}p^\mu J^1_{\underline{\ell_1 m_1};\ell_2 m_2;\ell_3 m_3}$
$c^i_{\ell_1 m_1}(p)\phi^j_{2\ell_2 m_2}c^k_{\ell_3 m_3}$	$\frac{g_{6a}}{R^2}\xi f^{ijk}J^{11}_{\underline{\ell_1 m_1};\ell_2 m_2;\ell_3 m_3}$

coefficients are given by

$$J^1_{\ell_1 m_1;\ell_2 m_2;\ell_3 m_3} = \int \mathrm{d}\Omega Y_{\ell_1 m_1}Y_{\ell_2 m_2}Y_{\ell_3 m_3}, \tag{A9}$$

$$J^2_{\ell_1 m_1;\ell_2 m_2;\ell_3 m_3} = \int \mathrm{d}\Omega \frac{1}{\sin\theta}\left[-\partial_\theta Y_{\ell_1 m_1}\partial_\phi \tilde{Y}_{\ell_2 m_2}Y_{\ell_3 m_3} + \partial_\phi Y_{\ell_1 m_1}\partial_\theta \tilde{Y}_{\ell_2 m_2}Y_{\ell_3 m_3}\right], \tag{A10}$$

$$J^3_{\ell_1 m_1;\ell_2 m_2;\ell_3 m_3} = \int \mathrm{d}\Omega \left[\partial_\theta Y_{\ell_1 m_1}\partial_\theta \tilde{Y}_{\ell_2 m_2}Y_{\ell_3 m_3} + \frac{1}{\sin^2\theta}\partial_\phi Y_{\ell_1 m_1}\partial_\phi \tilde{Y}_{\ell_2 m_2}Y_{\ell_3 m_3}\right], \tag{A11}$$

$$J^4_{\ell_1 m_1;\ell_2 m_2;\ell_3 m_3} = \int \mathrm{d}\Omega \frac{1}{\sin\theta}\big[(\partial_\phi Y_{\ell_1 m_1}Y_{\ell_2 m_2} - Y_{\ell_1 m_1}\partial_\phi Y_{\ell_2 m_2})\partial_\theta \tilde{Y}_{\ell_3 m_3} - (\partial_\theta Y_{\ell_1 m_1}Y_{\ell_2 m_2} - Y_{\ell_1 m_1}\partial_\phi Y_{\ell_2 m_2})\partial_\phi \tilde{Y}_{\ell_3 m_3}\big], \tag{A12}$$

$$J^5_{\ell_1 m_1;\ell_2 m_2;\ell_3 m_3} = \int \mathrm{d}\Omega\Big[(\partial_\theta Y_{\ell_1 m_1} Y_{\ell_2 m_2} - Y_{\ell_1 m_1}\partial_\theta Y_{\ell_2 m_2})\partial_\theta \tilde{Y}_{\ell_3 m_3} + \frac{1}{\sin^2\theta}(\partial_\phi Y_{\ell_1 m_1} Y_{\ell_2 m_2} - Y_{\ell_1 m_1}\partial_\phi Y_{\ell_2 m_2})\partial_\phi \tilde{Y}_{\ell_3 m_3}\Big], \tag{A13}$$

$$J^6_{\ell_1 m_1;\ell_2 m_2;\ell_3 m_3} = \int \mathrm{d}\Omega \left[\partial_\theta \tilde{Y}_{\ell_1 m_1}\partial_\theta \tilde{Y}_{\ell_2 m_2} + \frac{1}{\sin^2\theta}\partial_\phi \tilde{Y}_{\ell_1 m_1}\partial_\phi \tilde{Y}_{\ell_2 m_2}\right] Y_{\ell_3 m_3}, \tag{A14}$$

$$J^7_{\ell_1 m_1;\ell_2 m_2;\ell_3 m_3} = \int \mathrm{d}\Omega \frac{1}{\sin\theta}\left[\partial_\theta \tilde{Y}_{\ell_1 m_1}\partial_\phi \tilde{Y}_{\ell_2 m_2} - \partial_\phi \tilde{Y}_{\ell_1 m_1}\partial_\theta \tilde{Y}_{\ell_2 m_2}\right] Y_{\ell_3 m_3}, \tag{A15}$$

$$J^8_{\ell_1 m_1;\ell_2 m_2;\ell_3 m_3} = \int \mathrm{d}\Omega\Big[\hat{L}^2 \tilde{Y}_{\ell_1 m_1}\left(\partial_\theta \tilde{Y}_{\ell_2 m_2}\partial_\theta \tilde{Y}_{\ell_3 m_3} + \frac{1}{\sin^2\theta}\partial_\phi \tilde{Y}_{\ell_2 m_2}\partial_\phi \tilde{Y}_{\ell_3 m_3}\right) - \hat{L}^2 \tilde{Y}_{\ell_2 m_2}\left(\partial_\theta \tilde{Y}_{\ell_1 m_1}\partial_\theta \tilde{Y}_{\ell_3 m_3} + \frac{1}{\sin^2\theta}\partial_\phi \tilde{Y}_{\ell_1 m_1}\partial_\phi \tilde{Y}_{\ell_3 m_3}\right)\Big], \tag{A16}$$

$$J^9_{\ell_1 m_1;\ell_2 m_2;\ell_3 m_3} = \int \mathrm{d}\Omega \frac{1}{\sin\theta}\left[\partial_\theta \tilde{Y}_{\ell_1 m_1}\partial_\phi \tilde{Y}_{\ell_2 m_2} - \partial_\phi \tilde{Y}_{\ell_1 m_1}\partial_\theta \tilde{Y}_{\ell_2 m_2}\right]\hat{L}^2 \tilde{Y}_{\ell_3 m_3}, \tag{A17}$$

$$J^{10}_{\ell_1 m_1;\ell_2 m_2;\ell_3 m_3} = \int \mathrm{d}\Omega \frac{1}{\sin\theta}\Big[\hat{L}^2 \tilde{Y}_{\ell_1 m_1}\left(\partial_\phi \tilde{Y}_{\ell_2 m_2}\partial_\theta \tilde{Y}_{\ell_3 m_3} - \partial_\theta \tilde{Y}_{\ell_2 m_2}\partial_\phi \tilde{Y}_{\ell_3 m_3}\right) + \hat{L}^2 \tilde{Y}_{\ell_2 m_2}\left(\partial_\theta \tilde{Y}_{\ell_1 m_1}\partial_\phi \tilde{Y}_{\ell_3 m_3} - \partial_\phi \tilde{Y}_{\ell_1 m_1}\partial_\theta \tilde{Y}_{\ell_3 m_3}\right) + \hat{L}^2 \tilde{Y}_{\ell_3 m_3}\left(\partial_\phi \tilde{Y}_{\ell_1 m_1}\partial_\theta \tilde{Y}_{\ell_2 m_2} - \partial_\theta \tilde{Y}_{\ell_1 m_1}\partial_\phi \tilde{Y}_{\ell_2 m_2}\right)\Big], \tag{A18}$$

$$J^{11}_{\ell_1 m_1;\ell_2 m_2;\ell_3 m_3} = \int \mathrm{d}\Omega Y_{\ell_1 m_1}\hat{L}^2 Y_{\ell_2 m_2} Y_{\ell_3 m_3}, \tag{A19}$$

where we adopt the convention that we put an underline for indices ℓm of $Y^*_{\ell m}$. The coefficients for four-point vertices are also given by

$$K^1_{\ell_1 m_1;\ell_2 m_2;\ell_3 m_3;\ell_4 m_4} = \int \mathrm{d}\Omega Y_{\ell_1 m_1} Y_{\ell_2 m_2} Y_{\ell_3 m_3} Y_{\ell_4 m_4}, \tag{A20}$$

$$K^2_{\ell_1 m_1;\ell_2 m_2;\ell_3 m_3;\ell_4 m_4} = \int \mathrm{d}\Omega \left[\partial_\theta \tilde{Y}_{\ell_1 m_1}\partial_\theta \tilde{Y}_{\ell_2 m_2} + \frac{1}{\sin^2\theta}\partial_\phi \tilde{Y}_{\ell_1 m_1}\partial_\phi \tilde{Y}_{\ell_2 m_2}\right] Y_{\ell_3 m_3} Y_{\ell_4 m_4}, \tag{A21}$$

$$K^3_{\ell_1 m_1;\ell_2 m_2;\ell_3 m_3;\ell_4 m_4} = \int \mathrm{d}\Omega \frac{1}{\sin\theta}\left[\partial_\theta \tilde{Y}_{\ell_1 m_1}\partial_\phi \tilde{Y}_{\ell_2 m_2} - \partial_\phi \tilde{Y}_{\ell_1 m_1}\partial_\theta \tilde{Y}_{\ell_2 m_2}\right] Y_{\ell_3 m_3} Y_{\ell_4 m_4}, \tag{A22}$$

$$K^4_{\ell_1 m_1;\ell_2 m_2;\ell_3 m_3;\ell_4 m_4} = \int \mathrm{d}\Omega \frac{1}{\sin^2\theta}\big(\partial_\phi \tilde{Y}_{\ell_1 m_1}\partial_\theta \tilde{Y}_{\ell_2 m_2}\partial_\phi \tilde{Y}_{\ell_3 m_3}\partial_\theta \tilde{Y}_{\ell_4 m_4} + \partial_\theta \tilde{Y}_{\ell_1 m_1}\partial_\phi \tilde{Y}_{\ell_2 m_2}\partial_\theta \tilde{Y}_{\ell_3 m_3}\partial_\phi \tilde{Y}_{\ell_4 m_4}\big), \tag{A23}$$

$$K^5_{\ell_1 m_1;\ell_2 m_2;\ell_3 m_3;\ell_4 m_4} = \int \mathrm{d}\Omega \frac{1}{\sin\theta}\big(\partial_\theta \tilde{Y}_{\ell_1 m_1}\partial_\theta \tilde{Y}_{\ell_2 m_2}\partial_\theta \tilde{Y}_{\ell_3 m_3}\partial_\phi \tilde{Y}_{\ell_4 m_4} - \frac{1}{\sin^2\theta}\partial_\phi \tilde{Y}_{\ell_1 m_1}\partial_\phi \tilde{Y}_{\ell_2 m_2}\partial_\phi \tilde{Y}_{\ell_3 m_3}\partial_\theta \tilde{Y}_{\ell_4 m_4}\big), \tag{A24}$$

$$K^6_{\ell_1 m_1;\ell_2 m_2;\ell_3 m_3;\ell_4 m_4} = -\int \mathrm{d}\Omega\big(\partial_\theta \tilde{Y}_{\ell_1 m_1}\partial_\theta \tilde{Y}_{\ell_2 m_2}\partial_\theta \tilde{Y}_{\ell_3 m_3}\partial_\theta \tilde{Y}_{\ell_4 m_4} + \frac{1}{\sin^4\theta}\partial_\phi \tilde{Y}_{\ell_1 m_1}\partial_\phi \tilde{Y}_{\ell_2 m_2}\partial_\phi \tilde{Y}_{\ell_3 m_3}\partial_\phi \tilde{Y}_{\ell_4 m_4}\big). \tag{A25}$$

Table A4. The one-loop contributions for correction to KK masses of fermions. The summation symbols $\{\sum_{\ell_1=0}^{\ell_{\max}}, \sum_{\ell_2=0}^{\ell_{\max}}, \sum_{m_1=-\ell_1}^{\ell_1}\}$ and the overall factor $(T_a)^2 g_{6a}^2/64\pi^2 R^2((Y_{u,d,e})^2/64\pi^2 R^2)$ for the fermion(Higgs) loop are omitted for all contributions in the third column. Also, the $\ln(\Lambda^2/\mu^2)$ factor is omitted for boundary contributions in the third column. The subscripts fA_μ etc. show the propagating particles inside the loop.

Diagram	Coefficients	
Fig. 1	$\Sigma_{\rm bulk}^{fA_\mu,R(L)}$	$\int_0^1 d\alpha \int_0^{\Lambda^2} \frac{2\alpha x dx}{[x+\Delta]^2}(-1)^{m_1+m} I^{\alpha(\beta)}_{\ell_1 m_1;\ell_2 m_1-m;\ell' m} I^{\alpha(\beta)}_{\ell m;\ell_2 m-m_1;\ell_1 m_1}$
	$\tilde{\Sigma}_{\rm bulk}^{fA_\mu,R(L)}$	$\int_0^1 d\alpha \int_0^{\Lambda^2} \frac{4x dx}{[x+\Delta]^2}(-1)^{m_1+m} M_{\ell_1} I^{\beta(\alpha)}_{\ell_1 m_1;\ell_2 m_1-m;\ell' m} I^{\alpha(\beta)}_{\ell m;\ell_2 m-m_1;\ell_1 m_1}$
	$\Sigma_{\rm bound}^{fA_\mu,R(L)}$	$(-1)^{m_1+m+\ell_2} I^{\alpha(\beta)}_{\ell_1 m_1;\ell_2-m_1+m;\ell' 2m_1-m} I^{\alpha(\beta)}_{\ell m;\ell_2 m-m_1;\ell_1 m_1}$
	$\tilde{\Sigma}_{\rm bound}^{fA_\mu,R(L)}$	$(-1)^{m_1+m+\ell_2} 4 M_{\ell_1} I^{\beta(\alpha)}_{\ell_1 m_1;\ell_2-m_1+m;\ell' 2m_1-m} I^{\alpha(\beta)}_{\ell m;\ell_2 m-m_1;\ell_1 m_1}$
Fig. 1	$\Sigma_{\rm bulk}^{f\phi_1,R(L)}$	$-\int_0^1 d\alpha \int_0^{\Lambda^2} \frac{\alpha x dx}{[x+\Delta]^2}(-1)^{m_1+m} C^{\alpha(\beta)}_{\ell_1 m_1;\ell_2 m_1-m;\ell' m} C^{\beta(\alpha)}_{\ell m;\ell_2 m-m_1;\ell_1 m_1}$
	$\tilde{\Sigma}_{\rm bulk}^{f\phi_1,R(L)}$	$\int_0^1 d\alpha \int_0^{\Lambda^2} \frac{x dx}{[x+\Delta]^2}(-1)^{m_1+m} M_{\ell_1} C^{\beta(\alpha)}_{\ell_1 m_1;\ell_2 m_1-m;\ell' m} C^{\beta(\alpha)}_{\ell m;\ell_2 m-m_1;\ell_1 m_1}$
	$\Sigma_{\rm bound}^{f\phi_1,R(L)}$	$-(-1)^{m_1+m+\ell_2} \frac{1}{2} C^{\alpha(\beta)}_{\ell_1 m_1;\ell_2-m_1+m;\ell' 2m_1-m} C^{\beta(\alpha)}_{\ell m;\ell_2 m-m_1;\ell_1 m_1}$
	$\tilde{\Sigma}_{\rm bound}^{f\phi_1,R(L)}$	$(-1)^{m_1+m+\ell_2} M_{\ell_1} C^{\beta(\alpha)}_{\ell_1 m_1;\ell_2-m_1+m;\ell' 2m_1-m} C^{\beta(\alpha)}_{\ell m;\ell_2 m-m_1;\ell_1 m_1}$
Fig. 1	$\Sigma_{\rm bulk}^{f\phi_2,R(L)}$	$-\int_0^1 d\alpha \int_0^{\Lambda^2} \frac{\alpha x dx}{[x+\Delta]^2}(-1)^{m_1+m} C^{\alpha(\beta)}_{\ell_1 m_1;\ell_2 m_1-m;\ell' m} C^{\beta(\alpha)}_{\ell m;\ell_2 m-m_1;\ell_1 m_1}$
	$\tilde{\Sigma}_{\rm bulk}^{f\phi_2,R(L)}$	$-\int_0^1 d\alpha \int_0^{\Lambda^2} \frac{x dx}{[x+\Delta]^2}(-1)^{m_1+m} M_{\ell_1} C^{\beta(\alpha)}_{\ell_1 m_1;\ell_2 m_1-m;\ell' m} C^{\beta(\alpha)}_{\ell m;\ell_2 m-m_1;\ell_1 m_1}$
	$\Sigma_{\rm bound}^{f\phi_2,R(L)}$	$-(-1)^{m_1+m+\ell_2} \frac{1}{2} C^{\alpha(\beta)}_{\ell_1 m_1;\ell_2-m_1+m;\ell' 2m_1-m} C^{\beta(\alpha)}_{\ell m;\ell_2 m-m_1;\ell_1 m_1}$
	$\tilde{\Sigma}_{\rm bound}^{f\phi_2,R(L)}$	$-(-1)^{m_1+m+\ell_2} M_{\ell_1} C^{\beta(\alpha)}_{\ell_1 m_1;\ell_2-m_1+m;\ell' 2m_1-m} C^{\beta(\alpha)}_{\ell m;\ell_2 m-m_1;\ell_1 m_1}$
Fig. 2	$\Sigma_{\rm bulk}^{H,R(L)}$	$\int_0^1 d\alpha \int_0^{\Lambda^2} \frac{\alpha x dx}{[x+\Delta]^2}(-1)^{m_1+m} I^{\beta(\alpha)}_{\ell_1 m_1;\ell_2 m_1-m;\ell' m} I^{\beta(\alpha)}_{\ell m;\ell_2 m-m_1;\ell_1 m_1}$
	$\tilde{\Sigma}_{\rm bulk}^{fH,R(L)}$	$\int_0^1 d\alpha \int_0^{\Lambda^2} \frac{x dx}{[x+\Delta]^2}(-1)^{m_1+m} M_{\ell_1} I^{\alpha(\beta)}_{\ell_1 m_1;\ell_2 m_1-m;\ell' m} I^{\beta(\alpha)}_{\ell m;\ell_2 m-m_1;\ell_1 m_1}$
	$\Sigma_{\rm bound}^{fH,R(L)}$	$(-1)^{m_1+m+\ell_2} \frac{1}{2} I^{\beta(\alpha)}_{\ell_1 m_1;\ell_2-m_1+m;\ell' 2m_1-m} I^{\beta(\alpha)}_{\ell m;\ell_2 m-m_1;\ell_1 m_1}$
	$\tilde{\Sigma}_{\rm bound}^{fH,R(L)}$	$(-1)^{m_1+m+\ell_2} M_{\ell_1} I^{\alpha(\beta)}_{\ell_1 m_1;\ell_2-m_1+m;\ell' 2m_1-m} I^{\beta(\alpha)}_{\ell m;\ell_2 m-m_1;\ell_1 m_1}$

The vertices including the Higgs field are derived from the interactions

$$\int dx^4 d\Omega \left[(D^M H)^\dagger (D_M H) - \mu^2 H^\dagger H - \frac{\lambda_6}{4}(H^\dagger H)^2 \right], \tag{A26}$$

which has the same structure as in the SM. The Feynman rules of these interactions are listed in Table A2, where the non-trivial coefficients in the vertex factors have already been given above.

Appendix B. One-loop calculations

Here we list the one-loop corrections to the KK masses for fermions, gauge bosons, and a Higgs boson.

Table A5. The contributions from fermion and Higgs boson loops for correction to the KK masses of the gauge boson. The summation symbols and the log divergence are omitted, as in Table A4. The overall factor $Tr[T_i^a T_j^a] g_{6a}^2/64\pi^2 R^2$ is also omitted for each expression. A coefficient providing zero contribution is omitted.

Diagram	Coefficients	
Fig. 3	$\Pi^{ff}_{\rm bulk}$	$-\int_0^1 d\alpha \int_0^{\Lambda^2} \frac{x dx}{[x+\Delta]^2}(-1)^m 4\alpha(1-\alpha)\left(\delta_{m,m'}+(-1)^{\ell'}\delta_{-m,m'}\right)\times$ $[I^{\alpha}_{\ell_1 m_1;\ell' m;\ell_2 m_1-m} I^{\alpha}_{\ell_2 m_1-m;\ell-m;\ell_1 m_1} + I^{\beta}_{\ell_1 m_1;\ell',m;\ell_2 m_1-m} I^{\beta}_{\ell_2 m_1-m;\ell-m;\ell_1 m_1}]$
	$\tilde{\Pi}^{ff}_{\rm bulk}$	$-\int_0^1 d\alpha \int_0^{\Lambda^2} \frac{x dx}{[x+\Delta]^2}(-1)^m \Big[(x-2\alpha(1-\alpha)p^2)\left(\delta_{m,m'}+(-1)^{\ell'}\delta_{-m,m'}\right)\times$ $\left[I^{\alpha}_{\ell_1 m_1;\ell' m;\ell_2 m_1-m} I^{\alpha}_{\ell_2 m_1-m;\ell-m;\ell_1 m_1} + I^{\beta}_{\ell_1 m_1;\ell' m;\ell_2 m_1-m} I^{\beta}_{\ell_2 m_1-m;\ell-m;\ell_1 m_1}\right]$ $+2M_{\ell_1}M_{\ell_2}\left(\delta_{m,m'}-(-1)^{\ell'}\delta_{-m,m'}\right)\times$ $\left[I^{\alpha}_{\ell_1 m_1;\ell' m;\ell_2 m_1-m} I^{\beta}_{\ell_2 m_1-m;\ell-m;\ell_1 m_1} + I^{\beta}_{\ell_1 m_1;\ell' m;\ell_2 m_1-m} I^{\alpha}_{\ell_2 m_1-m;\ell-m;\ell_1 m_1}\right]\Big]$
	$\Pi^{ff}_{\rm bound}$	$-(-1)^{\ell_2+m_1}\frac{2}{3}\left(\delta_{2m_1,m+m'}+(-1)^{\ell'}\delta_{2m_1,m-m'}\right)\left[I^{\alpha}_{\ell_1 m_1;\ell' 2m_1-m;\ell_2 m-m_1} I^{\alpha}_{\ell_2 m_1-m;\ell-m;\ell_1 m_1}\right.$ $\left.-I^{\beta}_{\ell_1 m_1;\ell' 2m_1-m;\ell_2 m-m_1} I^{\beta}_{\ell_2 m_1-m;\ell-m;\ell_1 m_1}\right]$
	$\tilde{\Pi}^{ff}_{\rm bound}$	$(-1)^{\ell_2+m_1}\Big[(M^2_{\ell_1}+M^2_{\ell_2})\left(\delta_{2m_1,m+m'}+(-1)^{\ell'}\delta_{2m_1,m-m'}\right)\left[I^{\alpha}_{\ell_1 m_1;\ell' 2m_1-m;\ell_2 m-m_1}\right.$ $\left.\times I^{\alpha}_{\ell_2 m_1-m;\ell-m;\ell_1 m_1} - I^{\beta}_{\ell_1 m_1;\ell' 2m_1-m;\ell_2 m-m_1} I^{\beta}_{\ell_2 m_1-m;\ell-m;\ell_1 m_1}\right]$ $-2M_{\ell_1}M_{\ell_2}\left(\delta_{2m_1,m+m'}-(-1)^{\ell'}\delta_{2m_1,m-m'}\right)\left[I^{\alpha}_{\ell_1 m_1;\ell' 2m_1-m;\ell_2 m-m_1} I^{\beta}_{\ell_2 m_1-m;\ell-m;\ell_1 m_1}\right.$ $\left.-I^{\beta}_{\ell_1 m_1;\ell' 2m_1-m;\ell_2 m-m_1} I^{\alpha}_{\ell_2 m_1-m;\ell-m;\ell_1 m_1}\right]\Big]$
Fig. 4	$\Pi^{HH}_{\rm bulk}$	$-\int_0^1 d\alpha \int_0^{\Lambda^2} \frac{x dx}{[x+\Delta]^2}(1-4\alpha(1-\alpha))\left(\delta_{m,m'}+(-1)^{\ell'}\delta_{-m,m'}\right) J^1_{\ell_1 -m_1;\ell' m;\ell_2 m_1-m}$ $\times J^1_{\ell_2 m-m_1;\ell-m;\ell_1 m_1}$
	$\tilde{\Pi}^{HH}_{\rm bulk}$	$-\int_0^1 d\alpha \int_0^{\Lambda^2} \frac{x dx}{[x+\Delta]^2}(x-(1-4\alpha(1-\alpha))p^2)\left(\delta_{m,m'}+(-1)^{\ell'}\delta_{-m,m'}\right)$ $\times J^1_{\ell_1 -m_1;\ell' m;\ell_2 m_1-m} J^1_{\ell_2 m-m_1;\ell-m;\ell_1 m_1}$
	$\Pi^{HH}_{\rm bound}$	$-\frac{1}{3}(-1)^{\ell_2}\left(\delta_{2m_1,m+m'}+(-1)^{\ell'}\delta_{2m_1,m-m'}\right) J^1_{\ell_1 -m_1;\ell' 2m_1-m;\ell_2 -m_1+m} J^1_{\ell_2 m-m_1;\ell-m;\ell_1 m_1}$
	$\tilde{\Pi}^{HH}_{\rm bound}$	$(M^2_{\ell_1}+M^2_{\ell_2})(-1)^{\ell_2}\left(\delta_{2m_1,m+m'}+(-1)^{\ell'}\delta_{2m_1,m-m'}\right) J^1_{\ell_1 -m_1;\ell' 2m_1-m;\ell_2 -m_1+m}$ $\times J^1_{\ell_2 m-m_1;\ell-m;\ell_1 m_1}$
Fig. 5	$\tilde{\Pi}^{H}_{\rm bulk}$	$\int_0^{\Lambda^2} \frac{4x dx}{x+M^2_{\ell_1}}(-1)^{m+m_1}\delta_{m,m'} K^1_{\ell-m;\ell_1 m_1;\ell_1 -m_1;\ell' m'}$
	$\tilde{\Pi}^{H}_{\rm bound}$	$-4M^2_{\ell_1}(-1)^{\ell_1+m+m_1}\delta_{2m_1,m-m'} K^1_{\ell-m;\ell_1 m_1;\ell_1 m_1;\ell' m'}$

B.1. One-loop corrections to KK masses of fermions

For fermions, the corresponding one-loop diagrams are shown in Figs. 1 and 2, and the contributions from each diagram are expressed as Eqs. (52) and (53). We have calculated a diagram in Fig. 1, Sect. 3, for four-dimensional components of a gauge boson inside a loop and obtained Eqs. (54)–(57), which are summarized in the first part of Table A4. The contribution from ϕ_i to the diagram in Fig. 1 is obtained by using $\bar{\Psi}\phi_i\Psi$ vertices in Table A1 and the ϕ_i propagator Eq. (39). We then obtain the second and third parts of Table A4.

Figure 2 can be calculated in the same way by using the Yukawa coupling constants in Table A1 and the scalar boson propagator Eq. (42):

$$
\begin{aligned}
-\mathrm{i}\Sigma^{\mathrm{Fig.2}}(p;\ell m;\ell' m') = \frac{1}{4R^2}\sum_{\ell_1=0}^{\ell_{\max}}\sum_{\ell_2=0}^{\ell_{\max}}\sum_{m_1=-\ell_1}^{\ell_1}\sum_{m_1'=-\ell_1}^{\ell_1}\int_\Lambda \frac{\mathrm{d}^4k}{(2\pi)^4} \\
\times\Bigg[\frac{\mathrm{i}}{(p-k)^2-M_{\ell_2}^2}(\delta_{m_1-m,m_1'-m'}+(-1)^{\ell_2}\delta_{-(m_1-m),m_1'-m'}) \\
\times(\mathrm{i}Y_f)[I^{\alpha}_{\ell_1 m_1';\ell_2 m_1'-m';\ell' m'}P_R+I^{\beta}_{\ell_1 m_1';\ell_2 m_1'-m';\ell' m'}P_L] \\
\times\frac{\mathrm{i}}{\not{k}+\mathrm{i}\gamma_5 M_{\ell_1}}(\delta_{m_1,m_1'}+(-1)^{\ell_1+m_1}\delta_{-m_1,m_1'}\gamma_5) \\
\times(\mathrm{i}Y_f)[I^{\alpha}_{\ell m;\underline{\ell_2 m_1-m};\ell_1 m_1}P_L+I^{\beta}_{\ell m;\underline{\ell_2 m_1-m};\ell_1 m_1}P_R]\Bigg],
\end{aligned}
\tag{B1}
$$

where Y_f is the corresponding Yukawa coupling constant in six dimensions. The right-hand side is expressed as the case of Fig. 1 and the results are summarized in the fourth part of Table A4.

B.2. One-loop corrections to KK masses of four-dimensional components of gauge bosons

For gauge bosons, the corresponding one-loop diagrams are shown in Figs. 3–7, and they are calculated as in the fermion case. Figure 3 for four-dimensional components of gauge bosons can be obtained by using the relevant propagators of fermion Eq. (33) and $\bar{\Psi}A_\mu\Psi$ vertices in Table A1:

$$
\begin{aligned}
\mathrm{i}\Pi_{\mu\nu}^{\mathrm{Fig.3}}(p;\ell m,\ell' m') = -\frac{1}{4R^2}\sum_{\ell_1=0}^{\ell_{\max}}\sum_{\ell_2=0}^{\ell_{\max}}\sum_{m_1=-\ell_1}^{\ell_1}\sum_{m_1'=-\ell_1}^{\ell_1}\int_\Lambda\frac{\mathrm{d}^4k}{(2\pi)^4} \\
\times\mathrm{Tr}\Bigg[(\mathrm{i}g_{6a}T_a\gamma_\mu)\Big[I^{\alpha}_{\ell_1 m_1';\ell' m';\ell_2 m_1'-m'}P_R+I^{\beta}_{\ell_1 m_1';\ell' m';\ell_2 m_1'-m'}P_L\Big] \\
\times\frac{\mathrm{i}}{\not{k}+\mathrm{i}\gamma_5 M_{\ell_1}}(\delta_{m_1,m_1'}\mp(-1)^{\ell_1+m_1}\delta_{-m_1,m_1'}\gamma_5) \\
\times(\mathrm{i}g_{6a}T_a\gamma_\nu)\Big[I^{\alpha}_{\ell_2 m_1-m;\underline{\ell m};\ell_1 m_1}P_R+I^{\beta}_{\ell_2 m_1-m;\underline{\ell m};\ell_1 m_1}P_L\Big] \\
\times\frac{\mathrm{i}}{\not{k}-\not{p}+\mathrm{i}\gamma_5 M_{\ell_2}}(\delta_{m_1-m,m_1'-m'}\mp(-1)^{\ell_2+m_1+m}\delta_{-(m_1-m),m_1'-m'}\gamma_5)\Bigg],
\end{aligned}
\tag{B2}
$$

where the sign $\pm$ corresponds to $\Psi_+^{(\pm\gamma_5)}$ in the loop. Taking the sum over m_1', the products of the Kronecker delta become m-conserving $\{\delta_{m,m'},\delta_{-m,m'}\}$ and m-violating $\{\delta_{2m_1,m+m'},\delta_{2m_1,m-m'}\}$, and we separate the bulk and the boundary contribution as in the fermion case, $\mathrm{i}\Pi_{\mu\nu}^{\mathrm{Fig.3}}(p;\ell m,\ell' m') = \mathrm{i}\Pi_{\mu\nu}^{\mathrm{Fig.3\ bulk}}(p;\ell m,\ell' m') + \mathrm{i}\Pi_{\mu\nu}^{\mathrm{Fig.3\ bound}}(p;\ell m,\ell' m')$. After combining denominators with the Feynman parameter and carrying out Wick rotation, a bulk contribution is estimated with Euclidean four-momentum integration with cut-off Λ and a boundary contribution is estimated taking the leading log-divergent part as in Eq. (51). After some calculations, we can express it in the form of Eqs. (66) and (67), where each coefficient is given in the first part of Table A5.

Figure 4 is calculated by making use of the propagator of scalar boson Eq. (42) and the $H^\dagger A_\mu H$ vertex in Table A2 such that

$$
\begin{aligned}
&\mathrm{i}\Pi_{\mu\nu}^{\mathrm{Fig.4}}(p;\ell m;\ell' m') \\
&= \frac{1}{4R^2}\sum_{\ell_1=0}^{\ell_{\max}}\sum_{\ell_2=0}^{\ell_{\max}}\sum_{m_1=-\ell_1}^{\ell_1}\sum_{m_1'=-\ell_1}^{\ell_1}\int\frac{\mathrm{d}^4k}{(2\pi)^4}J^1_{\underline{\ell_1 m_1'};\ell' m';\ell_2 m_1'-m'}J^1_{\underline{\ell_2 m_1-m};\underline{\ell m};\ell_1,m_1} \\
&\times\left[\{\mathrm{i}g_{6a}T_a(2k_\mu-p_\mu)\}\frac{\mathrm{i}}{k^2-M_{\ell_1}^2}\left(\delta_{m_1,m_1'}+(-1)^{\ell_1}\delta_{-m_1,m_1'}\right)\right. \\
&\left.\times\{\mathrm{i}g_{6a}T_a(2k_\nu-p_\nu)\}\frac{\mathrm{i}}{(k-p)^2-M_{\ell_2}^2}\left(\delta_{m_1-m,m_1'-m'}+(-1)^{\ell_2}\delta_{-(m_1-m),m_1'-m'}\right)\right], \qquad \text{(B3)}
\end{aligned}
$$

which is also expressed as the form of Eqs. (66) and (67), and the explicit form of each coefficient is summarized in the second part of Table A5.

Figure 5 is calculated by making use of the propagator of the scalar boson Eq. (42) and the $H^\dagger H A_\mu A^\mu$ vertex in Table A2 such that

$$
\begin{aligned}
\mathrm{i}\Pi_{\mu\nu}^{\mathrm{Fig.\ 5}}(\ell m;\ell' m') &= \frac{1}{2R^2}\sum_{\ell_1=0}^{\ell_{\max}}\sum_{m_1=-\ell_1}^{\ell_1}\sum_{m_1'=-\ell_1}^{\ell_1}\int\frac{\mathrm{d}^4k}{(2\pi)^4}(2\mathrm{i}g_{6a}^2T_a^2g_{\mu\nu})\frac{\mathrm{i}}{k^2-M_{\ell_1}^2} \\
&\times K^1_{\underline{\ell,m};\ell_1,m_1;\underline{\ell_1,m_1'};\ell',m'}[\delta_{m_1,m_1'}+(-1)^{\ell_1}\delta_{-m_1,m_1'}]\delta_{m'-m_1'+m_1-m,0}, \qquad \text{(B4)}
\end{aligned}
$$

which is expressed in the form of Eqs. (66) and (67), and the explicit form of each coefficient is summarized in the third part of Table A5.

Figure 6 for two virtual A_μ is calculated by making use of the propagator of A_μ Eq. (36) and the $(A_\mu)^3$ vertex in Table A3 such that

$$
\begin{aligned}
&\mathrm{i}\Pi_{\mu\nu}^{\mathrm{Fig.6(A_\mu A_\mu)}}(p;\ell m;\ell' m') \\
&= \frac{1}{2}\sum_{\ell_1=0}^{\ell_{\max}}\sum_{\ell_2=0}^{\ell_{\max}}\sum_{m_1=-\ell_1}^{\ell_1}\sum_{m_1'=-\ell_1}^{\ell_1}\int\frac{\mathrm{d}^4k}{(2\pi)^4}\frac{-\mathrm{i}}{k^2-M_{\ell_1}^2}g_{\alpha\beta}\frac{-\mathrm{i}}{(k+p)^2-M_{\ell_2}^2}g_{\rho\sigma} \\
&\times\tfrac{1}{2}[\delta_{m_1m_1'}+(-1)^{\ell_1}\delta_{-m_1m_1'}]\tfrac{1}{2}[\delta_{m_1-m,m_1'-m'}+(-1)^{\ell_2}\delta_{-(m_1-m),m_1'-m'}] \\
&\times\frac{g_{6a}}{R}f^{ikl}[g^{\mu\alpha}(p-k)^\rho+g^{\alpha\rho}(p+2k)^\mu+g^{\rho\mu}(-2p-k)^\alpha] \\
&\times\frac{g_{6a}}{R}f^{jkl}[g^{\beta\nu}(p-k)^\sigma+g^{\nu\sigma}(-2p-k)^\beta+g^{\sigma\beta}(p+2k)^\nu] \\
&\times J^1_{\ell' m';\underline{\ell_1 m_1'};\ell_2 m_1'-m'}J^1_{\underline{\ell m};\ell_1 m_1;\underline{\ell_2 m_1-m}}, \qquad \text{(B5)}
\end{aligned}
$$

which is expressed in the form of Eqs. (66) and (67), and the explicit form of each coefficient is summarized in the first part of Table B1. Figure 6 for one virtual A_μ and one virtual ϕ_i is calculated in the same way by making use of the propagators of A_μ in Eq. (36) and ϕ_i in Eq. (39), and the $(A_\mu)^2\phi_i$ vertex in Table A3. The results are summarized in the fourth part of Table B1. Figure 6 for two virtual ϕ_i is also calculated by making use of the propagator of ϕ_i Eq. (39) and the $A_\mu(\phi_i)^2$ vertex in Table A3, and the results are summarized in the sixth part of Table B1.

Table B1. The contributions from the gauge boson loop with self-interactions for correction to the KK masses of the gauge boson. The summation symbols and the log divergence factor are omitted, as in Table A4. The overall factor $C_2(G)g_{6a}^2/64\pi^2R^2$ is also omitted where $C_2(G)$ is obtained as $f^{lmi}f^{lmj} = C_2(G)\delta^{ij}$ for the corresponding gauge group G.

Diagram	Coefficients	
Fig. 6	$\Pi^{A_\mu A_\mu}_{\rm bulk}$	$\int_0^1 d\alpha \int_0^{\Lambda^2} dx \frac{-x}{2[x+\Delta]^2}[2(1-2\alpha)^2 - 2(1+\alpha)(2-\alpha)](\delta_{mm'} + (-1)^{\ell'}\delta_{-mm'}) \times J^1_{\ell' m;\underline{\ell_1 m_1};\ell_2 m_1 - m} J^1_{\underline{\ell m};\ell_1 m_1;\underline{\ell_2 m_1 - m}}$
	$\tilde{\Pi}^{A_\mu A_\mu}_{\rm bulk}$	$\int_0^1 d\alpha \int_0^{\Lambda^2} dx \frac{x}{2[x+\Delta]^2}\Big[[(2-\alpha)^2 + 3(\alpha^2-1) + 2(1-2\alpha)^2]p^2 - 9x/2\Big] (\delta_{mm'} + (-1)^{\ell'}\delta_{-mm'}) J^1_{\ell' m;\underline{\ell_1 m_1};\ell_2 m_1 - m} J^1_{\underline{\ell m};\ell_1 m_1;\underline{\ell_2 m_1 - m}}$
	$\Pi^{A_\mu A_\mu}_{\rm bound}$	$(-1)^{l_2}\frac{11}{6}(\delta_{2m_1,m+m'} + (-1)^{\ell'}\delta_{2m_1,m-m'})\ J^1_{\ell' 2m_1 - m;\underline{\ell_1 m_1};\ell_2 m - m_1} J^1_{\underline{\ell m};\ell_1 m_1;\underline{\ell_2 m_1 - m}}$
	$\tilde{\Pi}^{A_\mu A_\mu}_{\rm bound}$	$-\Big[\frac{1}{4}p^2 - \frac{9}{4}(M^2_{l_1} + M^2_{l_2})\Big](-1)^{\ell_2}(\delta_{2m_1,m+m'} + (-1)^{\ell'}\delta_{2m_1,m-m'}) J^1_{\ell' 2m_1 - m;\underline{\ell_1 m_1};\ell_2 m - m_1} J^1_{\underline{\ell m};\ell_1 m_1;\underline{\ell_2 m_1 - m}}$
Fig.7	$\tilde{\Pi}^{A_\mu}_{\rm bulk}$	$\int_0^1 d\alpha \int_0^{\Lambda^2} dx \frac{6x}{[x+\Delta']^2}[x - (1-\alpha)^2 p^2]\delta_{mm'} K^1_{\ell' m;\underline{\ell m};\ell_1 m_1;\underline{\ell_1 m_1}}$
	$\tilde{\Pi}^{A_\mu}_{\rm bound}$	$-6\ln\Big(\frac{\Lambda^2}{\mu^2}\Big) M^2_{\ell_1}(-1)^{\ell_1}\delta_{2m_1,m-m'} K^1_{\ell' - 2m_1 + m;\underline{\ell m};\ell_1 m_1;\underline{\ell_1 - m_1}}$
Fig. 4	$\Pi^{c}_{\rm bulk}$	$-\int_0^1 d\alpha \int_0^{\Lambda^2} dx \frac{x}{[x+\Delta]^2}\alpha(1-\alpha)(\delta_{mm'} + (-1)^{\ell'}\delta_{-mm'})\ J^1_{\underline{\ell_1 m_1};\ell' m;\ell_2 m_1 - m} \times J^1_{\underline{\ell_2 m_1 - m};\underline{\ell m};l_1 m_1}$
	$\tilde{\Pi}^{cc}_{\rm bulk}$	$\int_0^1 d\alpha \int_0^{\Lambda^2} dx \frac{x}{[x+\Delta]^2}\Big(\frac{x}{4} + \alpha(1-\alpha)p^2\Big)(\delta_{mm'} + (-1)^{\ell'}\delta_{-mm'})\ J^1_{\underline{\ell_1 m_1};\ell' m;\ell_2 m_1 - m} \times J^1_{\underline{\ell_2 m_1 - m};\underline{\ell m};\ell_1 m_1}$
	$\Pi^{cc}_{\rm bound}$	$-(-1)^{\ell_2}\frac{1}{6}(\delta_{2m_1,m+m'} + (-1)^{\ell'}\delta_{2m_1,m-m'})\ J^1_{\underline{\ell_1 m_1};\ell' 2m_1 - m;\ell_2 m - m_1} J^1_{\underline{\ell_2 m_1 - m};\underline{\ell m};\ell_1 m_1}$
	$\tilde{\Pi}^{cc}_{\rm bound}$	$(-1)^{\ell_2}\frac{1}{4}\Big(p^2 - M^2_{l_1} - M^2_{l_2}\Big)(\delta_{2m_1,m+m'} + (-1)^{\ell'}\delta_{2m_1,m-m'})\ J^1_{\underline{\ell_1 m_1};\ell' 2m_1 - m;\ell_2 m - m_1} \times J^1_{\underline{\ell_2 m_1 - m};\underline{\ell m};\ell_1 m_1}$
Fig. 6	$\tilde{\Pi}^{A_\mu \phi_1(\phi_2)}_{\rm bulk}$	$-\frac{1}{R^2}\int_0^1 d\alpha \int_0^{\Lambda^2} dx \frac{x}{[x+\Delta]^2}(\delta_{mm'} + (-1)^{\ell'}\delta_{-mm'}) J^{4(5)}_{\ell' m;\underline{\ell_1 m_1};\ell_2 m_1 - m} J^{4(5)}_{\underline{\ell m};\ell_1 m_1;\underline{\ell_2 m_1 - m}}$
	$\tilde{\Pi}^{A_\mu \phi_1(\phi_2)}_{\rm bound}$	$-\frac{(-1)^{\ell_2}}{R^2}(\delta_{2m_1,m+m'} + (-1)^{\ell'}\delta_{2m_1,m-m'}) J^{4(5)}_{\ell' 2m_1 - m;\underline{\ell_1 m_1};\ell_2 m - m_1} J^{4(5)}_{\underline{\ell m};\ell_1 m_1;\underline{\ell_2 m_1 - m}}$
Fig. 7	$\tilde{\Pi}^{\phi_i}_{\rm bulk}$	$\int_0^{\Lambda^2} dx \frac{2x}{x + M^2_{\ell_1}}\delta_{mm'} K^2_{\underline{\ell_1 m_1};\ell_1 m_1;\ell' m;\underline{\ell m}}$
	$\tilde{\Pi}^{\phi_i}_{\rm bound}$	$-2M^2_{\ell_1}(-1)^{\ell_1}\delta_{2m_1,m-m'} K^2_{\underline{\ell_1,-m_1};\ell_1 m_1;\ell' - 2m_1 + m;\underline{\ell m}}$
Fig. 6	$\Pi^{\phi_i \phi_i(\phi_1 \phi_2)}_{\rm bulk}$	$-\int_0^1 d\alpha \int_0^{\Lambda^2} dx \frac{x}{[x+\Delta]^2}\Big(1 - 4\alpha(1-\alpha)\Big) J^{6(7)}_{\ell_2 m_1 - m;\underline{\ell_1 m_1};\ell' m} \times J^{6(7)}_{\underline{\ell_2 m_1 - m};\ell_1 m_1;\underline{\ell m}}(\delta_{mm'} + (-1)^{\ell'}\delta_{-mm'})$

continued.

Table B1. continued.

Diagram	Coefficients
	$\bar{\Pi}^{\phi_i\phi_i(\phi_1\phi_2)}_{\rm bulk}$ $-\int_0^1 {\rm d}\alpha \int_0^{\Lambda^2} {\rm d}x \frac{x}{[x+\Delta]^2}\left(x+[4\alpha(1-\alpha)-1]p^2\right) J^{6(7)}_{\ell_2 m_1-m;\underline{\ell_1 m_1};\ell' m} \times J^{6(7)}_{\underline{\ell_2 m_1-m};\ell_1 m_1;\underline{\ell m}}(\delta_{mm'}+(-1)^{\ell'}\delta_{-mm'})$
	$\Pi^{\phi_i\phi_i(\phi_1\phi_2)}_{\rm bound}$ $-(-1)^{l_2}\frac{1}{3} J^{6(7)}_{\ell_2 m-m_1;\underline{\ell_1 m_1};\ell' 2m_1-m} J^{6(7)}_{\underline{\ell_2 m_1-m};\ell_1 m_1;\underline{\ell m}}(\delta_{2m_1,m+m'}+(-1)^{\ell'}\delta_{2m_1,m-m'})$
	$\bar{\Pi}^{\phi_i\phi_i(\phi_1\phi_2)}_{\rm bound}$ $(-1)^{\ell_2}\left(M^2_{\ell_1}+M^2_{\ell_2}\right) J^{6(7)}_{\ell_2 m-m_1;\underline{\ell_1 m_1};\ell' 2m_1-m} \times J^{6(7)}_{\underline{\ell_2 m_1-m};\ell_1 m_1;\underline{\ell m}}(\delta_{2m_1,m+m'}+(-1)^{\ell'}\delta_{2m_1,m-m'})$

Figure 7 for virtual A_μ is calculated by making use of the propagator of A_μ in Eq. (36) and the $(A_\mu)^4$ vertex in Table A3 such that

$$
\begin{aligned}
&{\rm i}\Pi^{{\rm Fig.7(A}_\mu{\rm)}}_{\mu\nu}(p;\ell m;\ell' m') \\
&= \frac{1}{2}\sum_{\ell_1=0}^{\ell_{\max}}\sum_{m_1=-\ell_1}^{\ell_1}\sum_{m_1'=-\ell_1}^{\ell_1}\int\frac{{\rm d}^4k}{(2\pi)^4}\frac{-{\rm i}}{k^2-M^2_{\ell_1}} g_{\sigma\rho}\delta^{kl} \\
&\times\left(-{\rm i}\frac{g^2_{6a}}{R^2}\right)[f^{ijm}f^{klm}(g^{\mu\rho}g^{\nu\sigma}-g^{\mu\sigma}g^{\nu\rho})+f^{ikm}f^{jlm}(g^{\mu\nu}g^{\rho\sigma}-g^{\mu\sigma}g^{\nu\rho}) \\
&+ f^{ilm}f^{jkm}(g^{\mu\nu}g^{\rho\sigma}-g^{\mu\rho}g^{\nu\sigma})] \\
&\times\frac{1}{2}[\delta_{m_1m_1'}+(-1)^{\ell_1}\delta_{-m_1m_1'}]\delta_{m'-m_1'+m_1-m,0}K^1_{\ell' m';\underline{\ell m};\ell_1 m_1;\underline{\ell_1 m_1'}},
\end{aligned}
\tag{B6}
$$

which is expressed in the form of Eqs. (66) and (67) and the explicit form of each coefficient is summarized in the second part of Table B1. Figure 7 for virtual ϕ_i is calculated in the same way by making use of the propagator of ϕ_i in Eq. (39) and the $(A_\mu)^2(\phi_i)^2$ vertex in Table A3. The results are summarized in the fifth part of Table B1.

Figure 4 for the ghost contribution is calculated by making use of the propagator of the scalar boson in Eq. (42) and the $\bar{c}cA_\mu$ vertex in Table A3 such that

$$
\begin{aligned}
{\rm i}\Pi^{{\rm Fig.4(cc)}}_{\mu\nu}(p;\ell m;\ell' m') = (-1)&\sum_{\ell_1=0}^{\ell_{\max}}\sum_{\ell_2=0}^{\ell_{\max}}\sum_{m_1=-\ell_1}^{\ell_1}\sum_{m_1'=-\ell_1}^{\ell_1}\int\frac{{\rm d}^4k}{(2\pi)^4}\frac{\rm i}{k^2-M^2_{\ell_1}}\frac{\rm i}{(k+p)^2-M^2_{\ell_2}} \\
&\times\frac{g^2_{6a}}{R^2}f^{ilk}(k+p)^\mu f^{kjl}k^\nu J^1_{\ell' m';\underline{\ell_1 m_1'};\ell_2 m_1'-m'}J^1_{\underline{\ell m};\ell_1 m_1;\underline{\ell_2 m_1-m}} \\
&\times\frac{1}{2}[\delta_{m_1m_1'}+(-1)^{\ell_1}\delta_{-m_1m_1'}]\frac{1}{2}[\delta_{m_1-m,m_1'-m'}+(-1)^{\ell_2}\delta_{-(m_1-m),m_1'-m'}],
\end{aligned}
\tag{B7}
$$

which is expressed in the form of Eqs. (66) and (67), and the explicit form of each coefficient is summarized in the third part of Table B1.

B.3. One-loop corrections to KK masses of the extra-dimensional components of gauge bosons

Here we calculate one-loop corrections to the $\phi_1\phi_1$ term. Figure 3 for the extra-dimensional components of gauge bosons ϕ_1 can be obtained by making use of the propagator of the fermion in Eq. (33)

Table B2. The contributions from fermions and the Higgs boson loop for correction to the KK masses of the extra components of gauge bosons. The summation symbols and the log divergence are omitted, as in Table A4. The overall factor $\mathrm{Tr}[T_i^a T_j^a] g_{6a}^2/64\pi^2 R^2$ is also omitted for each expression.

Diagram		Coefficients
Fig. 3	$\Theta^{(i)ff}_{\rm bulk}$	$-\int_0^1 \mathrm{d}\alpha \int_0^{\Lambda^2} \frac{x\,\mathrm{d}x}{[x+\Delta_M]^2}(-1)^m \Big[\frac{6x+2\Delta_M}{x+\Delta_M}\alpha(1-\alpha)\big(\delta_{m,m'}+(-1)^{\ell'}\delta_{-m,m'}\big) \times \big[C^{\alpha}_{\ell_1 m_1;\ell' m;\ell_2 m_1-m} C^{\beta}_{\ell_2 m_1-m;\ell-m;\ell_1 m_1} + C^{\beta}_{\ell_1 m_1;\ell' m;\ell_2 m_1-m} C^{\alpha}_{\ell_2 m_1-m;\ell-m;\ell_1 m_1}\big] - 4M_{\ell_1}M_{\ell_2}\frac{\alpha(1-\alpha)}{x+\Delta_M}\big(\delta_{m,m'}-(-1)^{\ell'}\delta_{-m,m'}\big)\big[C^{\alpha}_{\ell_1 m_1;\ell' m;\ell_2 m_1-m} C^{\alpha}_{\ell_2 m_1-m;\ell-m;\ell_1 m_1} + C^{\beta}_{\ell_1 m_1;\ell' m;\ell_2 m_1-m} C^{\beta}_{\ell_2 m_1-m;\ell-m;\ell_1 m_1}\big] \Big]$
	$\tilde{\Theta}^{(i)ff}_{\rm bulk}$	$\int_0^1 \mathrm{d}\alpha \int_0^{\Lambda^2} \frac{x\,\mathrm{d}x}{[x+\Delta_M]^2}(-1)^m \Big[2x\big(\delta_{m,m'}+(-1)^{\ell'}\delta_{-m,m'}\big) \times \big[C^{\alpha}_{\ell_1 m_1;\ell' m;\ell_2 m_1-m} C^{\beta}_{\ell_2 m_1-m;\ell-m;\ell_1 m_1} + C^{\beta}_{\ell_1 m_1;\ell' m;\ell_2 m_1-m} C^{\alpha}_{\ell_2 m_1-m;\ell-m;\ell_1 m_1}\big] - 2M_{\ell_1}M_{\ell_2}\big(\delta_{m,m'}-(-1)^{\ell'}\delta_{-m,m'}\big) \times \big[C^{\alpha}_{\ell_1 m_1;\ell' m;\ell_2 m_1-m} C^{\alpha}_{\ell_2 m_1-m;\ell-m;\ell_1 m_1} + C^{\beta}_{\ell_1 m_1;\ell' m;\ell_2 m_1-m} C^{\beta}_{\ell_2 m_1-m;\ell-m;\ell_1 m_1}\big] \Big]$
	$\Theta^{(i)ff}_{\rm bound}$	$-(-1)^{\ell_2+m_1}\Big[\big(\delta_{2m_1,m+m'}+(-1)^{\ell'}\delta_{2m_1,m-m'}\big)\big[C^{\alpha}_{\ell_1 m_1;\ell' 2m_1-m;\ell_2 m-m_1} C^{\beta}_{\ell_2 m_1-m;\ell-m;\ell_1 m_1} - C^{\beta}_{\ell_1 m_1;\ell' 2m_1-m;\ell_2 m-m_1} C^{\alpha}_{\ell_2 m_1-m;\ell-m;\ell_1 m_1}\big]\Big]$
	$\tilde{\Theta}^{(i)ff}_{\rm bound}$	$-(-1)^{\ell_2+m_1}\Big[(M_{\ell_1}^2+M_{\ell_2}^2)\big(\delta_{2m_1,m+m'}+(-1)^{\ell'}\delta_{2m_1,m-m'}\big)\big[C^{\alpha}_{\ell_1 m_1;\ell' 2m_1-m;\ell_2 m-m_1} \times C^{\beta}_{\ell_2 m_1-m;\ell-m;\ell_1 m_1} - C^{\beta}_{\ell_1 m_1;\ell' 2m_1-m;\ell_2 m-m_1} C^{\alpha}_{\ell_2 m_1-m;\ell-m;\ell_1 m_1}\big] + 2M_{\ell_1}M_{\ell_2}\big(\delta_{2m_1,m+m'}-(-1)^{\ell'}\delta_{2m_1,m-m'}\big)\big[C^{\alpha}_{\ell_1 m_1;\ell' 2m_1-m;\ell_2 m-m_1} C^{\alpha}_{\ell_2 m_1-m;\ell-m;\ell_1 m_1} - C^{\beta}_{\ell_1 m_1;\ell' 2m_1-m;\ell_2 m-m_1} C^{\beta}_{\ell_2 m_1-m;\ell-m;\ell_1 m_1}\big]\Big]$
Fig. 4	$\Theta^{(1(2))HH}_{\rm bulk}$	$-\frac{1}{R^2}\int_0^1 \mathrm{d}\alpha \int_0^{\Lambda^2} \frac{x\,\mathrm{d}x}{[x+\Delta_M]^2}\frac{2\alpha(1-\alpha)}{x+\Delta_M}\big(\delta_{m,m'}+(-1)^{\ell'}\delta_{-m,m'}\big)\times \{J^{2(3)}_{\ell_1-m_1;\ell' m;\ell_2 m_1-m} - J^{2(3)}_{\ell_2 m_1-m;\ell' m;\ell_1-m_1}\}\{J^{2(3)}_{\ell_2 m-m_1;\ell-m;\ell_1 m_1} - J^{2(3)}_{\ell_1 m_1;\ell-m;\ell_2 m-m_1}\}$
	$\tilde{\Theta}^{(1(2))HH}_{\rm bulk}$	$\frac{1}{R^2}\int_0^1 \mathrm{d}\alpha \int_0^{\Lambda^2} \frac{x\,\mathrm{d}x}{[x+\Delta_M]^2}\big(\delta_{m,m'}+(-1)^{\ell'}\delta_{-m,m'}\big)\times \{J^{2(3)}_{\ell_1-m_1;\ell' m;\ell_2 m_1-m} - J^{2(3)}_{\ell_2 m_1-m;\ell' m;\ell_1-m_1}\}\{J^{2(3)}_{\ell_2 m-m_1;\ell-m;\ell_1 m_1} - J^{2(3)}_{\ell_1 m_1;\ell-m;\ell_2 m-m_1}\}$
	$\tilde{\Theta}^{(1(2))HH}_{\rm bound}$	$\frac{(-1)^{\ell_2}}{R^2}\big(\delta_{2m_1,m+m'}+(-1)^{\ell'}\delta_{2m_1,m-m'}\big)\times \{J^{2(3)}_{\ell_1-m_1;\ell' 2m_1-m;\ell_2 m-m_1} - J^{2(3)}_{\ell_2 m-m_1;\ell' 2m_1-m;\ell_1-m_1}\}\{J^{2(3)}_{\ell_2 m-m_1;\ell-m;\ell_1 m_1} - J^{2(3)}_{\ell_1 m_1;\ell-m;\ell_2 m-m_1}\}$
Fig. 5	$\tilde{\Theta}^{(i)H}_{\rm bulk}$	$\int_0^{\Lambda^2} \frac{4x\,\mathrm{d}x}{x+M_{\ell_1}^2}(-1)^{m+m_1}\delta_{m,m'}K^2_{\ell-m;\ell' m;\ell_1-m_1;\ell_1 m_1}$
	$\tilde{\Theta}^{(i)H}_{\rm bound}$	$-4M_{\ell_1}^2(-1)^{\ell_1+m-m_1}\delta_{2m_1,m-m'}K^2_{\ell-m;\ell' m';\ell_1 m_1;\ell_1-m_1}$

and the $\bar{\Psi}\phi_i\Psi$ vertex in Table A1, such that

$$\mathrm{i}\Theta^{(i)}_{\mathrm{Fig.3}}(p;\ell m,\ell' m') = -\frac{1}{4R^2}\sum_{\ell_1=0}^{\ell_{\max}}\sum_{\ell_2=0}^{\ell_{\max}}\sum_{m_1=-\ell_1}^{\ell_1}\sum_{m_1'=-\ell_1}^{\ell_1}\int_\Lambda \frac{\mathrm{d}^4k}{(2\pi)^4} \times \mathrm{Tr}\Big[(\mathrm{i}g_{6a}T^a\gamma_5)\Big[C^{\alpha}_{\ell_1 m_1';\ell' m';\ell_2 m_1'-m'}P_L + C^{\beta}_{\ell_1 m_1';\ell' m';\ell_2 m_1'-m'}P_R\Big]$$

Table B3. The contributions from the gauge boson loop with self-interactions for correction to the $\phi_1\phi_1$ terms for the KK masses of the extra components of gauge bosons. The summation symbols and the log divergence factor are omitted, as in Table A4. The overall factor $C_2(G)g_{6a}^2/64\pi^2R^2$ is also omitted.

Diagram	Coefficients	
Fig. 6	$\Theta^{(1)A_\mu\phi_1(\phi_2)}_{\rm bulk}$	$\int_0^1 d\alpha \int_0^{\Lambda^2} dx \frac{x[(3\alpha^2-4\alpha+1)x+(\alpha-1)^2\Delta_M]}{[x+\Delta_M]^2(x+\Delta_M)}(\delta_{mm'}+(-1)^{\ell'}\delta_{-mm'})$ $J^{6(7)}_{\ell' m;\underline{\ell_1 m_1};\ell_2 m_1-m}\, J^{6(7)}_{\underline{\ell m};\ell_1 m_1;\underline{\ell_2 m_1-m}}$
	$\tilde\Theta^{(1)A_\mu\phi_1(\phi_2)}_{\rm bulk}$	$\int_0^1 d\alpha \int_0^{\Lambda^2} dx \frac{x^2}{[x+\Delta_M]^2}(\delta_{mm'}+(-1)^{\ell'}\delta_{-mm'}) J^{6(7)}_{\ell' m;\underline{\ell_1 m_1};\ell_2 m_1-m} J^{6(7)}_{\underline{\ell m};\ell_1 m_1;\underline{\ell_2 m_1-m}}$
	$\tilde\Theta^{(1)A_\mu\phi_1(\phi_2)}_{\rm bound}$	$-(M_{l_1}^2+M_{l_2}^2)(-1)^{\ell_2}(\delta_{2m_1,m+m'}+(-1)^{\ell'}\delta_{2m_1,m-m'}) J^{6(7)}_{\ell' 2m_1-m;\underline{\ell_1 m_1};\ell_2 m-m_1}$ $\times J^{6(7)}_{\underline{\ell m};\ell_1 m_1;\underline{\ell_2 m_1-m}}$
Fig. 7	$\tilde\Theta^{(1)A_\mu}_{\rm bulk}$	$\int_0^{\Lambda^2} dx \frac{8x}{x+M_{\ell_1}^2}\delta_{mm'} K^2_{\underline{\ell m};\ell' m;\underline{\ell_1 m_1};\ell_1 m_1}$
	$\tilde\Theta^{(1)A_\mu}_{\rm bound}$	$-8M_{l_1}^2(-1)^{l_1}\delta_{2m_1,m-m'} K^2_{\underline{l m};l'-2m_1+m;\underline{l_1-m_1};l_1 m_1}$
Fig. 6	$\Theta^{(1)A_\mu A_\mu}_{\rm bulk}$	$\frac{1}{R^2}\int_0^1 d\alpha \int_0^{\Lambda^2} dx \frac{4x}{[x+\Delta_M]^2}\frac{2\alpha(1-\alpha)}{x+\Delta_M}(\delta_{mm'}+(-1)^{\ell'}\delta_{-mm'}) J^4_{\ell_2 m_1-m;\underline{\ell_1 m_1};\ell' m}$ $\times J^4_{\underline{\ell_2 m_1-m};\ell_1 m_1;\underline{\ell m}}$
	$\tilde\Theta^{(1)A_\mu A_\mu}_{\rm bulk}$	$-\frac{1}{R^2}\int_0^1 d\alpha \int_0^{\Lambda^2} dx \frac{4x}{[x+\Delta_M]^2}(\delta_{mm'}+(-1)^{\ell'}\delta_{-mm'}) J^4_{\ell_2 m_1-m;;\underline{\ell_1 m_1};\ell' m}$ $\times J^4_{\underline{\ell_2 m_1-m};\ell_1 m_1;\underline{\ell m}}$
	$\tilde\Theta^{(1)A_\mu A_\mu}_{\rm bound}$	$-\frac{4}{R^2}(-1)^{\ell_2}(\delta_{2m_1,m+m'}+(-1)^{\ell'}\delta_{2m_1,m-m'}) J^4_{\ell_2 m-m_1;\underline{\ell_1 m_1};\ell' 2m_1-m} J^4_{\underline{\ell_2 m_1-m};\ell_1 m_1;\underline{\ell m}}$
Fig. 6	$\Theta^{(1)\phi_1\phi_1}_{\rm bulk}$	$\frac{1}{R^2}\int_0^1 d\alpha \int_0^{\Lambda^2} dx \frac{x}{[x+\Delta_M]^2}\frac{\alpha(1-\alpha)}{x+\Delta_M}(\delta_{mm'}+(-1)^{\ell'}\delta_{-mm'}) J^{10}_{\ell' m;\ell_2 m_1-m;\underline{\ell_1 m_1}}$ $\times J^{10}_{\underline{\ell_2 m_1-m};\ell_1 m_1;\underline{\ell m}}$
	$\tilde\Theta^{(1)\phi_1\phi_1}_{\rm bulk}$	$-\frac{1}{R^2}\int_0^1 d\alpha \int_0^{\Lambda^2} dx \frac{x}{2[x+\Delta_M]^2}(\delta_{mm'}+(-1)^{\ell'}\delta_{-mm'}) J^{10}_{\ell' m;\ell_2 m_1-m;\underline{\ell_1 m_1}}$ $\times J^{10}_{\underline{\ell_2 m_1-m};\ell_1 m_1;\underline{\ell m}}$
	$\tilde\Theta^{(1)\phi_1\phi_1}_{\rm bound}$	$-\frac{1}{2R^2}(-1)^{\ell_2}(\delta_{2m_1,m+m'}+(-1)^{\ell'}\delta_{2m_1,m-m'}) J^{10}_{\ell' 2m_1-m;\ell_2 m-m_1;\underline{\ell_1 m_1}} J^{10}_{\underline{\ell_2 m_1-m};\ell_1 m_1;\underline{\ell m}}$
Fig. 6	$\Theta^{(1)\phi_2\phi_2}_{\rm bulk}$	$\frac{1}{R^2}\int_0^1 d\alpha \int_0^{\Lambda^2} dx \frac{x}{[x+\Delta_M]^2}\frac{\alpha(1-\alpha)}{x+\Delta_M}(\delta_{mm'}+(-1)^{\ell'}\delta_{-mm'}) J^9_{\ell_2 m_1-m;\underline{\ell_1 m_1};\ell' m}$ $\times J^9_{\underline{\ell_2 m_1-m};\ell_1 m_1;\underline{\ell m}}$
	$\tilde\Theta^{(1)\phi_2\phi_2}_{\rm bulk}$	$-\frac{1}{R^2}\int_0^1 d\alpha \int_0^{\Lambda^2} dx \frac{x}{2[x+\Delta_M]^2}(\delta_{mm'}+(-1)^{\ell'}\delta_{-mm'}) J^9_{\ell_2 m_1-m;\underline{\ell_1 m_1};\ell' m}$ $\times J^9_{\underline{\ell_2 m_1-m};\ell_1 m_1;\underline{\ell m}}$
	$\tilde\Theta^{(1)\phi_2\phi_2}_{\rm bound}$	$-\frac{1}{2R^2}(-1)^{\ell_2}(\delta_{2m_1,m+m'}+(-1)^{\ell'}\delta_{2m_1,m-m'}) J^9_{\ell_2 m-m_1;\underline{\ell_1 m_1};\ell' 2m_1-m} J^9_{\underline{\ell_2 m_1-m};\ell_1 m_1;\underline{\ell m}}$
Fig. 6	$\Theta^{(1)\phi_1\phi_2}_{\rm bulk}$	$\frac{1}{R^2}\int_0^1 d\alpha \int_0^{\Lambda^2} dx \frac{x}{[x+\Delta_M]^2}\frac{\alpha(1-\alpha)}{x+\Delta_M}(\delta_{mm'}+(-1)^{\ell'}\delta_{-mm'}) J^8_{\ell' m;\underline{\ell_1 m_1};\ell_2 m_1-m}$ $\times J^8_{\underline{\ell m};\ell_1 m_1;\underline{\ell_2 m_1-m}}$

continued.

Table B3. continued.

Diagram	Coefficients	
	$\tilde{\Theta}^{(1)\phi_1\phi_2}_{\rm bulk}$	$-\frac{1}{R^2}\int_0^1 {\rm d}\alpha \int_0^{\Lambda^2} {\rm d}x \frac{x}{2[x+\Delta_M]^2}(\delta_{mm'}+(-1)^{\ell'}\delta_{-mm'})J^8_{\ell' m;\underline{\ell_1 m_1};\ell_2 m_1-m} \times J^8_{\underline{\ell m};\ell_1 m_1;\underline{\ell_2 m_1-m}}$
	$\tilde{\Theta}^{(1)\phi_1\phi_2}_{\rm bound}$	$-\frac{1}{2R^2}(-1)^{\ell_2}(\delta_{2m_1,m+m'}+(-1)^{\ell'}\delta_{2m_1,m-m'})J^8_{\ell' 2m_1-m;\underline{\ell_1 m_1};\ell_2 m-m_1}J^8_{\underline{\ell m};\ell_1 m_1;\underline{\ell_2 m_1-m}}$
Fig. 7	$\tilde{\Theta}^{(1)\phi_1}_{\rm bulk}$	$\int_0^{\Lambda^2}{\rm d}x\frac{x}{x+M^2_{\ell_1}}\delta_{mm'}\left(2K^4_{\ell' m;\underline{\ell_1 m_1};\underline{\ell m};\ell_1 m_1}-K^4_{\underline{\ell m};\ell' m;\underline{\ell_1 m_1};\ell_1 m_1}-K^4_{\ell' m;\underline{\ell m};\underline{\ell_1 m_1};\ell_1 m_1}\right)$
	$\tilde{\Theta}^{(1)\phi_1}_{\rm bound}$	$-M^2_{\ell_1}\delta_{2m_1,m-m'}\left(2K^4_{\ell'-2m_1+m;\underline{\ell_1-m_1};\underline{\ell m};\ell_1 m_1}-K^4_{\underline{\ell m};\ell'-2m_1+m;\underline{\ell_1-m_1};\ell_1 m_1} - K^4_{\ell'-2m_1+m;\underline{\ell m};\underline{\ell_1-m_1};\ell_1 m_1}\right)$
Fig. 7	$\tilde{\Theta}^{(1)\phi_2}_{\rm bulk}$	$-\int_0^{\Lambda^2}{\rm d}x\frac{x}{x+M^2_{\ell_1}}\delta_{mm'}\left(2K^6_{\ell' m;\underline{\ell m};\underline{\ell_1 m_1};\ell_1 m_1}-K^4_{\underline{\ell m};\ell' m;\underline{\ell_1 m_1};\ell_1 m_1}-K^4_{\ell' m;\underline{\ell m};\underline{\ell_1 m_1};\ell_1 m_1}\right)$
	$\tilde{\Theta}^{(1)\phi_2}_{\rm bound}$	$M^2_{\ell_1}\delta_{2m_1,m-m'}\left(2K^6_{\ell'-2m_1+m;\underline{\ell m};\underline{\ell_1-m_1};\ell_1 m_1}-K^4_{\underline{\ell m};\ell'-2m_1+m;\underline{\ell_1-m_1};\ell_1 m_1} - K^4_{\ell'-2m_1+m;\underline{\ell m};\underline{\ell_1-m_1};\ell_1 m_1}\right)$

$$\times\frac{\rm i}{\not k+{\rm i}\gamma_5 M_{\ell_1}}(\delta_{m_1,m_1'}\mp(-1)^{\ell_1+m_1}\delta_{-m_1,m_1'}\gamma_5)\times \times({\rm i}g_{6a}T^a\gamma_5)\Big[C^{\alpha}_{\ell_2 m_1-m;\underline{\ell m};\ell_1 m_1}P_L+C^{\beta}_{\ell_2 m_1-m;\underline{\ell m};\ell_1 m_1}P_R\Big] \times\frac{\rm i}{\not k-\not p+{\rm i}\gamma_5 M_{\ell_2}}(\delta_{m_1-m,m_1'-m'}\mp(-1)^{\ell_2+m_1+m}\delta_{-(m_1-m),m_1'-m'}\gamma_5)\Big], \tag{B8}$$

where the $\pm$ sign corresponds to $\Psi_+^{(\pm\gamma_5)}$ in the loop. After taking the sum over m_1', it is separated into bulk and boundary contributions as in the previous cases. We then arrange the terms in the form of Eqs. (75) and (76), and each coefficient is given in the first line of Table B2. In arranging the terms, we expanded the denominator of Eq. (B34) to extract the terms proportional to p^2 such as

$$\frac{1}{[\not k+{\rm i}\gamma_5 M_{\ell_1}][\not k-\not p+{\rm i}\gamma_5 M_{\ell_2}]}\to\int_0^1{\rm d}\alpha\frac{1}{[k_E^2+(1-\alpha)M^2_{\ell_1}+\alpha M^2_{\ell_2}-\alpha(1-\alpha)p^2]^2} =\frac{1}{k_E^2+\Delta_M}\Big[1+\frac{2\alpha(1-\alpha)}{k_E^2+\Delta_M}p^2+O(p^4)\Big], \tag{B9}$$

where $\Delta_M=(1-\alpha)M^2_{\ell_1}+\alpha M^2_{\ell_2}$, and k_E is a Euclidean momentum.

Figure 4 is calculated in the same manner by making use of the propagator of the scalar boson in Eq. (42) and the $H^\dagger H\phi_i$ vertex in Table A2 such that

$${\rm i}\Theta^{\rm Fig.4}(p;\ell m;\ell' m') =\frac{1}{4R^4}\sum_{\ell_1=0}^{\ell_{\rm max}}\sum_{\ell_2=0}^{\ell_{\rm max}}\sum_{m_1=-\ell_1}^{\ell_1}\sum_{m_1'=-\ell_1}^{\ell_1}\int\frac{{\rm d}^4k}{(2\pi)^4}g_{6a}T_a\frac{-{\rm i}}{k^2-M^2_{\ell_1}}(\delta_{m_1,m_1'}+(-1)^{\ell_1}\delta_{-m_1,m_1'})$$

Table B4. The contributions from the gauge boson loop with self-interactions for correction to the $\phi_2\phi_2$ terms for the KK masses of the extra components of gauge bosons. The summation symbols and the log divergence factor are omitted, as in Table A4. The overall factor $C_2(G)g_{6a}^2/64\pi^2R^2$ is also omitted.

Diagram	Coefficients	
Fig. 6	$\Theta^{(2)A_\mu\phi_1}_{\rm bulk}$	$\displaystyle\int_0^1 d\alpha\int_0^{\Lambda^2} dx\,\frac{x[(3\alpha^2-4\alpha+1)x+(\alpha-1)^2\Delta_M]}{[x+\Delta_M]^2(x+\Delta_M)}(\delta_{mm'}+(-1)^{\ell'}\delta_{-mm'})$ $\times J^7_{\underline{\ell_1 m_1};\ell' m;\ell_2 m_1-m}J^7_{\ell_1 m_1;\underline{\ell m};\underline{\ell_2 m_1-m}}$
	$\tilde\Theta^{(2)A_\mu\phi_1}_{\rm bulk}$	$\displaystyle\int_0^1 d\alpha\int_0^{\Lambda^2} dx\,\frac{-x^2}{[x+\Delta_M]^2}(\delta_{mm'}+(-1)^{\ell'}\delta_{-mm'})J^7_{\underline{\ell_1 m_1};\ell' m;\ell_2 m_1-m}J^7_{\ell_1 m_1;\underline{\ell m};\underline{\ell_2 m_1-m}}$
	$\tilde\Theta^{(2)A_\mu\phi_1}_{\rm bound}$	$-(M_{l_1}^2+M_{l_2}^2)(-1)^{l_2}(\delta_{2m_1,m+m'}+(-1)^{l'}\delta_{2m_1,m-m'})$ $\times J^7_{\underline{\ell_1 m_1};\ell' 2m_1-m;\ell_2 m-m_1}J^7_{\ell_1 m_1;\underline{\ell m};\underline{\ell_2 m_1-m}}$
Fig. 6	$\Theta^{(2)A_\mu\phi_2}_{\rm bulk}$	$\displaystyle\int_0^1 d\alpha\int_0^{\Lambda^2} dx\,\frac{x[(3\alpha^2-4\alpha+1)x+(\alpha-1)^2\Delta_M]}{[x+\Delta_M]^2(x+\Delta_M)}(\delta_{mm'}+(-1)^{\ell'}\delta_{-mm'})$ $\times J^6_{\ell' m;\underline{\ell_1 m_1};\ell_2 m_1-m}J^6_{\underline{\ell m};\ell_1 m_1;\underline{\ell_2 m_1-m}}$
	$\tilde\Theta^{(2)A_\mu\phi_2}_{\rm bulk}$	$\displaystyle\int_0^1 d\alpha\int_0^{\Lambda^2} dx\,\frac{-x^2}{[x+\Delta_M]^2}(\delta_{mm'}+(-1)^{\ell'}\delta_{-mm'})J^6_{\ell' m;\underline{\ell_1 m_1};\ell_2 m_1-m}J^6_{\underline{\ell m};\ell_1 m_1;\underline{\ell_2 m_1-m}}$
	$\tilde\Theta^{(2)A_\mu\phi_2}_{\rm bound}$	$-(M_{l_1}^2+M_{l_2}^2)(-1)^{l_2}(\delta_{2m_1,m+m'}+(-1)^{l'}\delta_{2m_1,m-m'})$ $\times J^6_{\ell' 2m_1-m;\underline{\ell_1 m_1};\ell_2 m-m_1}J^6_{\underline{\ell m};\ell_1 m_1;\underline{\ell_2 m_1-m}}$
Fig. 7	$\tilde\Theta^{(2)A_\mu}_{\rm bulk}$	$\displaystyle\int_0^{\Lambda^2} dx\,\frac{8x}{x+M_{\ell_1}^2}\delta_{mm'}K^2_{\underline{\ell m};\ell' m;\underline{\ell_1 m_1};\ell_1 m_1}$
	$\tilde\Theta^{(2)A_\mu}_{\rm bound}$	$-8M_{\ell_1}^2(-1)^{\ell_1}\delta_{2m_1,m-m'}K^2_{\underline{\ell m};\ell'-2m_1+m;\underline{\ell_1-m_1};\ell_1 m_1}$
Fig. 6	$\Theta^{(2)A_\mu A_\mu}_{\rm bulk}$	$\displaystyle\frac{1}{R^2}\int_0^1 d\alpha\int_0^{\Lambda^2} dx\,\frac{4x}{[x+\Delta_M]^2}\frac{2\alpha(1-\alpha)}{x+\Delta_M}(\delta_{mm'}+(-1)^{\ell'}\delta_{-mm'})$ $\times J^5_{\ell_2 m_1-m;\underline{\ell_1 m_1};\ell' m}J^5_{\underline{\ell_2 m_1-m};\ell_1 m_1;\underline{\ell m}}$
	$\tilde\Theta^{(2)A_\mu A_\mu}_{\rm bulk}$	$\displaystyle-\frac{1}{R^2}\int_0^1 d\alpha\int_0^{\Lambda^2} dx\,\frac{4x}{[x+\Delta_M]^2}(\delta_{mm'}+(-1)^{\ell'}\delta_{-mm'})$ $\times J^5_{\ell_2 m_1-m;\underline{\ell_1 m_1};\ell' m}J^5_{\underline{\ell_2 m_1-m};\ell_1 m_1;\underline{\ell m}}$
	$\tilde\Theta^{(2)A_\mu A_\mu}_{\rm bound}$	$\displaystyle-\frac{4}{R^2}(-1)^{\ell_2}(\delta_{2m_1,m+m'}+(-1)^{\ell'}\delta_{2m_1,m-m'})J^5_{\ell_2 m-m_1;\underline{\ell_1 m_1};\ell' 2m_1-m}J^5_{\underline{\ell_2 m_1-m};\ell_1 m_1;\underline{\ell m}}$
Fig. 6	$\Theta^{(2)\phi_1\phi_1}_{\rm bulk}$	$\displaystyle\frac{1}{R^2}\int_0^1 d\alpha\int_0^{\Lambda^2} dx\,\frac{x}{[x+\Delta_M]^2}\frac{\alpha(1-\alpha)}{x+\Delta_M}(\delta_{mm'}+(-1)^{\ell'}\delta_{-mm'})$ $\times J^8_{\ell_2 m_1-m;\underline{\ell_1 m_1};\ell' m}J^8_{\underline{\ell_2 m_1-m};\ell_1 m_1;\underline{\ell m}}$
	$\tilde\Theta^{(2)\phi_1\phi_1}_{\rm bulk}$	$\displaystyle-\frac{1}{R^2}\int_0^1 d\alpha\int_0^{\Lambda^2} dx\,\frac{x}{2[x+\Delta_M]^2}(\delta_{mm'}+(-1)^{\ell'}\delta_{-mm'})$ $\times J^8_{\ell_2 m_1-m;\underline{\ell_1 m_1};\ell' m}J^8_{\underline{\ell_2 m_1-m};\ell_1 m_1;\underline{\ell m}}$
	$\tilde\Theta^{\phi_1\phi_1}_{\rm bound}$	$\displaystyle-\frac{1}{2R^2}(-1)^{\ell_2}(\delta_{2m_1,m+m'}+(-1)^{\ell'}\delta_{2m_1,m-m'})J^8_{\ell_2 m-m_1;\underline{\ell_1 m_1};\ell' 2m_1-m}J^8_{\underline{\ell_2 m_1-m};\ell_1 m_1;\underline{\ell m}}$

(*continued.*)

Table B4. continued.

Diagram	Coefficients	
Fig. 6	$\mathrm{i}\Theta^{(2)\phi_2\phi_2}_{\mathrm{bulk}}$	$\frac{1}{R^2}\int_0^1 \mathrm{d}\alpha \int_0^{\Lambda^2} \mathrm{d}x \frac{x}{[x+\Delta_M]^2}\frac{\alpha(1-\alpha)}{x+\Delta_M}(\delta_{mm'}+(-1)^{\ell'}\delta_{-mm'})$ $\times J^9_{\ell' m;\underline{\ell_1 m_1};\ell_2 m_1-m} J^9_{\underline{\ell m};\ell_1 m_1;\underline{\ell_2 m_1-m}}$
	$\tilde{\Theta}^{(2)\phi_2\phi_2}_{\mathrm{bulk}}$	$-\frac{1}{R^2}\int_0^1 \mathrm{d}\alpha \int_0^{\Lambda^2} \mathrm{d}x \frac{x}{2[x+\Delta_M]^2}(\delta_{mm'}+(-1)^{\ell'}\delta_{-mm'})$ $\times J^9_{\ell' m;\underline{\ell_1 m_1};\ell_2 m_1-m} J^9_{\underline{\ell m};\ell_1 m_1;\underline{\ell_2 m_1-m}}$
	$\tilde{\Theta}^{(2)\phi_2\phi_2}_{\mathrm{bound}}$	$-\frac{1}{2R^2}(-1)^{\ell_2}(\delta_{2m_1,m+m'}+(-1)^{\ell'}\delta_{2m_1,m-m'}) J^9_{\ell' 2m_1-m;\underline{\ell_1 m_1};\ell_2 m-m_1} J^9_{\underline{\ell m};\ell_1 m_1;\underline{\ell_2 m_1-m}}$
Fig. 7	$\tilde{\Theta}^{(2)\phi_1}_{\mathrm{bulk}}$	$\int_0^{\Lambda^2} \mathrm{d}x \frac{x}{x+M^2_{\ell_1}}\delta_{mm'}\left(2K^4_{\ell' m;\underline{\ell_1 m_1};\underline{\ell m};\ell_1 m_1}-K^4_{\underline{\ell m};\ell' m;\underline{\ell_1 m_1};\ell_1 m_1}-K^4_{\ell' m;\underline{\ell m};\underline{\ell_1 m_1};\ell_1 m_1}\right)$
	$\tilde{\Theta}^{(2)\phi_1}_{\mathrm{bound}}$	$-M^2_{\ell_1}\delta_{2m_1,m-m'}\Big(2K^4_{\ell'-2m_1+m;\underline{\ell_1-m_1};\underline{\ell m};\ell_1 m_1}-K^4_{\underline{\ell m};\ell'-2m_1+m;\underline{\ell_1-m_1};\ell_1 m_1}$ $-K^4_{\ell'-2m_1+m;\underline{\ell m};\underline{\ell_1-m_1};\ell_1 m_1}\Big)$
Fig. 7	$\tilde{\Theta}^{(2)\phi_2}_{\mathrm{bulk}}$	$-\int_0^{\Lambda^2} \mathrm{d}x \frac{x}{x+M^2_{l_1}}\delta_{mm'}\left(2K^6_{\underline{\ell_1 m_1};\ell_1 m_1;\ell' m;\underline{\ell m}}-K^4_{\ell_1 m_1;\underline{\ell_1 m_1};\ell' m;\underline{\ell m}}-K^4_{\underline{\ell_1 m_1};\ell_1 m_1;\ell' m;\underline{\ell m}}\right)$
	$\tilde{\Theta}^{(2)\phi_2}_{\mathrm{bound}}$	$M^2_{\ell_1}\delta_{2m_1,m-m'}\Big(2K^6_{\underline{\ell_1-m_1};\ell_1 m_1;\ell'-2m_1+m;\underline{\ell m}}-K^4_{\ell_1 m_1;\underline{\ell_1-m_1};\ell'-2m_1+m;\underline{\ell m}}$ $-K^4_{\underline{\ell_1-m_1};\ell_1 m_1;\ell'-2m_1+m;\underline{\ell m}}\Big)$

$$\times g_{6a}T_a\frac{-\mathrm{i}}{(k-p)^2-M^2_{\ell_2}}\left(\delta_{m_1-m,m'_1-m'}+(-1)^{\ell_2}\delta_{-(m_1-m),m'_1-m'}\right)$$
$$\times [J^2_{\underline{\ell_1,m'_1};\ell',m';\ell_2,m'_1-m'}-J^2_{\ell_2,m'_1-m';\ell',m';\underline{\ell_1,m'_1}}]$$
$$\times [J^2_{\underline{\ell_2,m_1-m};\underline{\ell,m};\ell_1,m_1}-J^2_{(\ell_1,m_1);\underline{\ell,m};\underline{\ell_2,m_1-m}}], \tag{B10}$$

which is expressed in the form of Eqs. (75) and (76), and each coefficient is summarized in the second part of Table B2.

Figure 5 is calculated in the same manner by making use of the propagator of the scalar boson in Eq. (42) and the $H^\dagger H(\phi_i)^2$ vertex in Table A2 such that

$$\mathrm{i}\Theta^{\mathrm{Fig.5}}(\ell,m,\ell',m') = \frac{1}{2R^2}\sum_{\ell_1=0}^{\ell_{\max}}\sum_{m_1=-\ell_1}^{\ell_1}\sum_{m'_1=-\ell_1}^{\ell_1}\int\frac{\mathrm{d}^4k}{(2\pi)^4}2\mathrm{i}(g_{6a}T_a)^2\frac{\mathrm{i}}{k^2-M^2_{\ell_1}}$$
$$\times K^2_{\underline{\ell_1,m'_1};\ell',m';\underline{\ell,m};\ell_1,m_1}[\delta_{m_1,m'_1}+(-1)^{\ell_1}\delta_{-m_1,m'_1}]\delta_{m'-m'_1+m_1-m,0}, \tag{B11}$$

which is expressed in the form of Eqs. (75) and (76), and each coefficient is summarized in the third part of Table B2.

Table B5. The contributions from the gauge boson loop with self-interactions for correction to the $\phi_1\phi_2$ terms for the KK masses of the extra components of gauge bosons. The summation symbols and the log divergence factor are omitted, as in Table A4. The overall factor $C_2(G)g_{6a}^2/64\pi^2R^2$ is also omitted.

Diagram	Coefficients	
Fig. 6	$\Theta^{(12)\phi_1\phi_1}_{\rm bulk}$	$\frac{1}{R^2}\int_0^1 d\alpha\int_0^{\Lambda^2} dx \frac{x}{[x+\Delta_M]^2}\frac{\alpha(1-\alpha)}{x+\Delta_M}(\delta_{mm'}+(-1)^{\ell'}\delta_{-mm'})$ $\times J^{10}_{\ell_2 m_1-m;\underline{\ell_1 m_1};\ell' m} J^{8}_{\underline{\ell_2 m_1-m};\ell_1 m_1;\underline{\ell m}}$
	$\tilde\Theta^{(12)\phi_1\phi_1}_{\rm bulk}$	$-\frac{1}{R^2}\int_0^1 d\alpha\int_0^{\Lambda^2} dx \frac{x}{2[x+\Delta_M]^2}(\delta_{mm'}+(-1)^{\ell'}\delta_{-mm'})$ $\times J^{10}_{\ell_2 m_1-m;\underline{\ell_1 m_1};\ell' m} J^{8}_{\underline{\ell_2 m_1-m};\ell_1 m_1;\underline{\ell m}}$
	$\tilde\Theta^{(12)\phi_1\phi_1}_{\rm bound}$	$-\frac{1}{2R^2}(-1)^{\ell_2}(\delta_{2m_1,m+m'}+(-1)^{l'}\delta_{2m_1,m-m'})J^{10}_{\ell_2 m-m_1;\underline{\ell_1 m_1};\ell' 2m_1-m} J^{8}_{\underline{\ell_2 m_1-m};\ell_1 m_1;\underline{\ell m}}$
Fig. 6	$\Theta^{(12)\phi_1\phi_2}_{\rm bulk}$	$-\frac{1}{R^2}\int_0^1 d\alpha\int_0^{\Lambda^2} dx \frac{x}{[x+\Delta_M]^2}\frac{\alpha(1-\alpha)}{x+\Delta_M}(\delta_{mm'}+(-1)^{\ell'}\delta_{-mm'})$ $\times J^{8}_{\ell' m;\ell_2 m_1-m;\underline{\ell_1 m_1}} J^{9}_{\underline{\ell m};\ell_1 m_1;\underline{\ell_2 m_1-m}}$
	$\tilde\Theta^{(12)\phi_1\phi_2}_{\rm bulk}$	$\frac{1}{R^2}\int_0^1 d\alpha\int_0^{\Lambda^2} dx \frac{x}{2[x+\Delta_M]^2}(\delta_{mm'}+(-1)^{\ell'}\delta_{-mm'})J^{8}_{\ell' m;\ell_2 m_1-m;\underline{\ell_1 m_1}} J^{9}_{\underline{\ell m};\ell_1 m_1;\underline{\ell_2 m_1-m}}$
	$\tilde\Theta^{(12)\phi_1\phi_2}_{\rm bound}$	$\frac{1}{2R^2}(-1)^{\ell_2}(\delta_{2m_1,m+m'}+(-1)^{l'}\delta_{2m_1,m-m'})J^{8}_{\ell' 2m_1-m;\ell_2 m-m_1;\underline{\ell_1 m_1}} J^{9}_{\underline{\ell m};\ell_1 m_1;\underline{\ell_2 m_1-m}}$
Fig. 7	$\tilde\Theta^{(12)\phi_1}_{\rm bulk}$	$-\frac{1}{R^2}\int_0^1 d\alpha\int_0^{\Lambda^2} dx \frac{1}{x+M^2_{\ell_1}}\Big[K^{5}_{\underline{\ell m};\ell' m;\ell_1 m_1;\underline{\ell_1 m_1}}+K^{5}_{\underline{\ell m};\ell' m;\underline{\ell_1 m_1};\ell_1 m_1}$ $-2K^{5}_{\underline{\ell m};\underline{\ell_1 m_1};\ell_1 m_1;\ell' m}\Big]\delta_{mm'}$
	$\tilde\Theta^{(12)\phi_1}_{\rm bound}$	$\frac{1}{R^2}\Big[K^{5}_{\underline{\ell m};\ell' m-2m_1;\ell_1 m_1;\underline{\ell_1-m_1}}+K^{5}_{\underline{\ell m};\ell' m-2m_1;\underline{\ell_1-m_1};\ell_1 m_1}$ $-2K^{5}_{\underline{\ell m};\underline{\ell_1-m_1};\ell_1 m_1;\ell' m-2m_1}\Big]\delta_{2m_1,m-m'}$
Fig. 7	$\tilde\Theta^{(12)\phi_2}_{\rm bulk}$	$\frac{1}{R^2}\int_0^1 d\alpha\int_0^{\Lambda^2} dx \frac{1}{x+M^2_{\ell_1}}\Big[K^{5}_{\underline{\ell m};\ell' m;\ell_1 m_1;\underline{\ell_1 m_1}}+K^{5}_{\underline{\ell m};\ell' m;\underline{\ell_1 m_1};\ell_1 m_1}$ $-2K^{5}_{\underline{\ell m};\underline{\ell_1 m_1};\ell_1 m_1;\ell' m}\Big]\delta_{mm'}$
	$\tilde\Theta^{(12)\phi_2}_{\rm bound}$	$-\frac{1}{R^2}\Big[K^{5}_{\underline{\ell m};\ell' m-2m_1;\ell_1 m_1;\underline{\ell_1-m_1}}+K^{5}_{\underline{\ell m};\ell' m-2m_1;\underline{\ell_1-m_1};\ell_1 m_1}$ $-2K^{5}_{\underline{\ell m};\underline{\ell_1-m_1};\ell_1 m_1;\ell' m-2m_1}\Big]\delta_{2m_1,m-m'}$

Figure 6 for two virtual A_μ is calculated by making use of the propagator of A_μ in Eq. (36) and the $(A_\mu)^2\phi_1$ vertex in Table A3 such that

$$
\begin{aligned}
&i\Theta^{\text{Fig.6}(A_\mu A_\mu)}(p;\ell m;\ell' m') \\
&= \sum_{\ell_1=0}^{\ell_{\max}}\sum_{\ell_2=0}^{\ell_{\max}}\sum_{m_1=-\ell_1}^{\ell_1}\sum_{m_1'=-\ell_1}^{\ell_1}\int\frac{d^4k}{(2\pi)^4}\frac{-i}{k^2-M^2_{\ell_1}}\frac{-i}{(k+p)^2-M^2_{\ell_2}}g_{\mu\nu} \\
&\times\frac{1}{2}[\delta_{m_1 m_1'}+(-1)^{\ell_1}\delta_{-m_1 m_1'}]\frac{1}{2}[\delta_{m_1-m,m_1'-m'}+(-1)^{\ell_2}\delta_{-(m_1-m),m_1'-m'}] \\
&\times\frac{g_{6a}}{R}f^{kil}(-k-p)^\mu\frac{g_{6a}}{R}f^{kjl}(-k-p)^\nu J^{6}_{\ell' m';\underline{\ell_1 m_1'};\ell_2 m_1'-m'} J^{6}_{\underline{\ell m};\ell_1 m_1;\underline{\ell_2 m_1-m}},
\end{aligned}
\tag{B12}
$$

Table B6. The contributions from the Higgs boson and gauge boson loops for correction to the KK masses of the Higgs boson. The summation symbols and the log divergence factor are omitted, as in Table A4. The overall factors $(T_a)^2 g_{6a}^2/64\pi^2 R^2$ and $\lambda_6/64\pi^2 R^2$ are also omitted for loops with gauge interaction and Higgs–self interaction respectively.

Diagram	Coefficients	
Fig. 8	$\Xi^{A_\mu H}_{\rm bulk}$	$\int_0^1 d\alpha \int_0^{\Lambda^2} \frac{-x dx}{[x+\Delta_M]^2}\left((\alpha+1)^2 - \frac{2\alpha(1-\alpha)x}{x+\Delta_M}\right)[\delta_{m,m'} + (-1)^{\ell'}\delta_{m,-m'}]$ $\times J^1_{\underline{\ell_1 m_1};\ell_2 m_1 - m;\ell' m} J^1_{\underline{\ell m};\underline{\ell_2 m_1 - m};\ell_1 m_1}$
	$\tilde{\Xi}^{A_\mu H}_{\rm bulk}$	$-\int_0^1 d\alpha \int_0^{\Lambda^2} dx \frac{x^2}{[x+\Delta_M]^2}[\delta_{m,m'} + (-1)^{\ell'}\delta_{m,-m'}] J^1_{\underline{\ell_1 m_1};\ell_2 m_1 - m;\ell' m} J^1_{\underline{\ell m};\underline{\ell_2 m_1 - m};\ell_1 m_1}$
	$\Xi^{A_\mu H}_{\rm bound}$	$-2(-1)^{\ell_2}[\delta_{2m_1,m+m'} + (-1)^{\ell'}\delta_{2m_1,m-m'}] J^1_{\underline{\ell_1 m_1};\ell_2 m - m_1;\ell' 2m_1 - m} J^1_{\underline{\ell m};\underline{\ell_2 m_1 - m};\ell_1 m_1}$
	$\tilde{\Xi}^{A_\mu H}_{\rm bound}$	$(M_{\ell_1}^2 + M_{\ell_2}^2)(-1)^{\ell_2}[\delta_{2m_1,m+m'} + (-1)^{\ell'}\delta_{2m_1,m-m'}] J^1_{\underline{\ell_1 m_1};\ell_2 m - m_1;\ell' 2m_1 - m} J^1_{\underline{\ell m};\underline{\ell_2 m_1 - m};\ell_1 m_1}$
Fig. 8	$\Xi^{\phi_{1(2)} H}_{\rm bulk}$	$-\frac{1}{R^2}\int_0^1 d\alpha \int_0^{\Lambda^2} dx \frac{x}{[x+\Delta_M]^2}\frac{2\alpha(1-\alpha)}{x+\Delta_M}[\delta_{m,m'} - (-1)^{\ell'}\delta_{-m,m'}]$ $\times\left[J^{2(3)}_{\underline{\ell_1 m_1};\ell_2 m_1 - m;\ell' m} - J^{2(3)}_{\underline{\ell' m};\ell_2 m_1 - m;\underline{\ell_1 m_1}}\right]\left[J^{2(3)}_{\underline{\ell m};\underline{\ell_2 m_1 - m};\ell_1 m_1} - J^{2(3)}_{\ell_1 m_1;\underline{\ell_2 m_1 - m};\underline{\ell m}}\right]$
	$\tilde{\Xi}^{\phi_{1(2)} H}_{\rm bulk}$	$\frac{1}{R^2}\int_0^1 d\alpha \int_0^{\Lambda^2} dx \frac{x}{[x+\Delta_M]^2}[\delta_{m,m'} - (-1)^{l'}\delta_{-m,m'}]$ $\times [J^2_{\underline{\ell_1 m_1};\ell_2 m_1 - m;\ell' m} - J^2_{\underline{\ell' m};\ell_2 m_1 - m;\underline{\ell_1 m_1}}][J^{2(3)}_{\underline{\ell m};\underline{\ell_2 m_1 - m};\ell_1 m_1} - J^{2(3)}_{\ell_1 m_1;\underline{\ell_2 m_1 - m};\underline{\ell m}}]$
	$\tilde{\Xi}^{\phi_{1(2)} H}_{\rm bound}$	$\frac{(-1)^{\ell_2}}{R^2}[\delta_{2m_1,m+m'} - (-1)^{\ell'}\delta_{2m_1,m-m'}]\left[J^{2(3)}_{\underline{\ell_1 m_1};\ell_2 m - m_1;\ell' 2m_1 - m} - J^{2(3)}_{\ell' 2m_1 - m;\ell_2 m - m_1;\underline{\ell_1 m_1}}\right]$ $\times\left[J^{2(3)}_{\underline{\ell m};\underline{\ell_2 m_1 - m};\ell_1 m_1} - J^{2(3)}_{\ell_1 m_1;\underline{\ell_2 m_1 - m};\underline{\ell m}}\right]$
Fig. 9	$\tilde{\Xi}^{A_\mu}_{\rm bulk}$	$\int_0^{\Lambda^2} \frac{8x dx}{x+M_{\ell_1}^2} K^1_{\underline{\ell_1 m_1};\ell_1 m_1;\underline{\ell m};\ell' m}\delta_{m,m'}$
	$\tilde{\Xi}^{A_\mu}_{\rm bound}$	$-(-1)^{\ell_1} 8M_{\ell_1}^2 K^1_{\underline{\ell_1 m_1};\ell_1 - m_1;\underline{\ell m};\ell' m'}\delta_{2m_1,m'-m}$
Fig. 9	$\tilde{\Xi}^{\phi_i}_{\rm bulk}$	$\int_0^{\Lambda^2} \frac{2x dx}{x+M_{\ell_1}^2} K^2_{\underline{\ell_1 m_1};\ell_1 m_1;\underline{\ell m};\ell' m}\delta_{m,m'}$
	$\tilde{\Xi}^{\phi_i}_{\rm bound}$	$-(-1)^{\ell_1} 2M_{\ell_1}^2 K^2_{\underline{\ell_1 m_1};\ell_1 - m_1;\underline{\ell m};\ell' m'}\delta_{2m_1,m'-m}$
Fig. 11	$\tilde{\Xi}^{H}_{\rm bulk}$	$\int_0^{\Lambda^2} \frac{2x dx}{x+M_{\ell_1}^2} K^1_{\underline{\ell_1 m_1};\ell_1 m_1;\underline{\ell m};\ell' m}\delta_{m,m'}$
	$\tilde{\Xi}^{H}_{\rm bound}$	$-(-1)^{\ell_1} 2M_{\ell_1}^2 K^1_{\underline{\ell_1 m_1};\ell_1 - m_1;\underline{\ell m};\ell' m'}\delta_{2m_1,m'-m}$

which is expressed in the form of Eqs. (75) and (76), and each coefficient is summarized in the third part of Table B3. Figure 6 for one virtual A_μ and one virtual ϕ_i is calculated in the same way by making use of the propagator of A_μ in Eq. (36), that of ϕ_i in Eq. (39), and the $(A_\mu)^2\phi_i$ vertex in Table A3. The results are summarized in the first part of Table B3. Figure 6 for two virtual ϕ_i is calculated by making use of the propagator of ϕ_i in Eq. (39) and the $(\phi_i)^4$ vertex in Table A3, and the results are summarized in the fourth, fifth, and sixth parts of Table B3.

Table B7. The contributions from the fermion loop for correction to the KK masses of the Higgs boson. The summation symbols and the log divergence factor are omitted, as in Table A4. The overall factor $Y_f^2/64\pi^2R^2$ is also omitted.

Diagram	Coefficients	
Fig. 10	$\Xi^{ff}_{\rm bulk}$	$\int_0^1 \mathrm{d}\alpha \int_0^{\Lambda^2} \mathrm{d}x \frac{2x}{[x+\Delta_M]^2}\Big[\Big(\alpha(1-\alpha)+\frac{2\alpha(1-\alpha)x}{x+\Delta_M}\Big)[\delta_{m,m'}+(-1)^{l'}\delta_{-m,m'}]$ $\times (I^{\alpha}_{\ell_1 m_1;\ell' m;\ell_2 m_1-m} I^{\alpha}_{\ell_2 m_1-m;\underline{\ell m};\ell_1 m_1} + I^{\beta}_{\ell_1 m_1;\ell' m;\ell_2 m_1-m} I^{\beta}_{\ell_2 m_1-m;\underline{\ell m};\ell_1 m_1})$ $+ M_{l_1} M_{l_2} \frac{2\alpha(1-\alpha)}{x+\Delta_M}[\delta_{m,m'}+(-1)^{\ell'}\delta_{-m,m'}]$ $\times (I^{\alpha}_{\ell_1 m_1;\ell' m;\ell_2 m_1-m} I^{\beta}_{\ell_2 m_1-m;\underline{\ell m};\ell_1 m_1} + I^{\beta}_{\ell_1 m_1;\ell' m;\ell_2 m_1-m} I^{\alpha}_{\ell_2 m_1-m;\underline{\ell m};\ell_1 m_1})\Big]$
	$\tilde{\Xi}^{ff}_{\rm bulk}$	$-\int_0^1 \mathrm{d}\alpha \int_0^{\Lambda^2} \mathrm{d}x \frac{2x}{[x+\Delta_M]^2}\big[x[\delta_{m,m'}+(-1)^{l'}\delta_{-m,m'}]$ $\times (I^{\alpha}_{\ell_1 m_1;\ell' m;\ell_2 m_1-m} I^{\alpha}_{\ell_2 m_1-m;\underline{\ell m};\ell_1 m_1} + I^{\beta}_{\ell_1 m_1;\ell' m;\ell_2 m_1-m} I^{\beta}_{\ell_2 m_1-m;\underline{\ell m};\ell_1 m_1})$ $+ M_{\ell_1} M_{\ell_2}[\delta_{m,m'}+(-1)^{\ell'}\delta_{-m,m'}]$ $\times (I^{\alpha}_{\ell_1 m_1;\ell' m;\ell_2 m_1-m} I^{\beta}_{\ell_2 m_1-m;\underline{\ell m};\ell_1 m_1} + I^{\beta}_{\ell_1 m_1;\ell' m;\ell_2 m_1-m} I^{\alpha}_{\ell_2 m_1-m;\underline{\ell m};\ell_1 m_1})\big]$
	$\Xi^{ff}_{\rm bound}$	$-(-1)^{\ell_2+m_1+m}[\delta_{2m_1,m+m'}+(-1)^{\ell'}\delta_{2m_1,m-m'}]$ $\times (I^{\alpha}_{\ell_1 m_1;\ell' 2m_1-m;\ell_2 m-m_1} I^{\alpha}_{\ell_2 m_1-m;\underline{\ell m};\ell_1 m_1} - I^{\beta}_{\ell_1 m_1;\ell' 2m_1-m;\ell_2 m-m_1} I^{\beta}_{\ell_2 m_1-m;\underline{\ell m};\ell_1 m_1})$
	$\tilde{\Xi}^{ff}_{\rm bound}$	$-2\big[(M^2_{\ell_1}+M^2_{\ell_2})(-1)^{\ell_2+m_1+m}[\delta_{2m_1,m+m'}+(-1)^{\ell'}\delta_{2m_1,m-m'}]$ $\times \big(I^{\alpha}_{\ell_1 m_1;\ell' 2m_1-m;\ell_2 m-m_1} I^{\alpha}_{\ell_2 m_1-m;\underline{\ell m};\ell_1 m_1} - I^{\beta}_{\ell_1 m_1;\ell' 2m_1-m;\ell_2 m-m_1} I^{\beta}_{\ell_2 m_1-m;\underline{\ell m};\ell_1 m_1}\big)$ $- M_{\ell_1} M_{\ell_2}(-1)^{\ell_2+m_1+m}[\delta_{2m_1,m+m'}-(-1)^{\ell'}\delta_{2m_1,m-m'}]$ $\times \big(I^{\alpha}_{\ell_1 m_1;\ell' 2m_1-m;\ell_2 m-m_1} I^{\beta}_{\ell_2 m_1-m;\underline{\ell m};\ell_1 m_1} - I^{\beta}_{\ell_1 m_1;\ell' 2m_1-m;\ell_2 m-m_1} I^{\alpha}_{\ell_2 m_1-m;\underline{\ell m};\ell_1 m_1}\big)\big]$

Figure 7 for virtual A_μ is calculated by applying the propagator of A_μ in Eq. (36) and the $(A_\mu)^2(\phi_i)^2$ vertex in Table A3 such that

$$\begin{aligned}
\mathrm{i}\Theta^{\mathrm{Fig.7}(A_\mu)}(p;\ell m;\ell' m') = \frac{1}{2}\sum_{\ell_1=0}^{\ell_{\max}}\sum_{\ell_2=0}^{\ell_{\max}}\sum_{m_1=-\ell_1}^{\ell_1}\sum_{m_1'=-\ell_1}^{\ell_1}\int\frac{\mathrm{d}^4k}{(2\pi)^4}\frac{-\mathrm{i}}{k^2-M^2_{\ell_1}}g_{\sigma\rho}\delta^{kl} \\
\times \mathrm{i}\frac{g^2_{6a}}{R^2}g^{\rho\sigma}[f^{ikm}f^{jlm}+f^{ilm}f^{jkm}] \\
\times \frac{1}{2}[\delta_{m_1 m_1'}+(-1)^{\ell_1}\delta_{-m_1 m_1'}]\delta_{m'-m_1'+m_1-m,0}K^2_{\underline{\ell m};\ell' m';\underline{\ell_1 m_1'};\ell_1 m_1},
\end{aligned} \tag{B13}$$

which is expressed in the form of Eqs. (75) and (76), and each coefficient is summarized in the second part of Table B3. Figure 7 for virtual ϕ_i is calculated in the same way by making use of the propagator of ϕ_i in Eq. (39) and the $(\phi_i)^4$ vertex in Table A3, and the results are summarized in the seventh and eighth parts of Table B3.

The one-loop corrections to the $\phi_2\phi_2$ term and off-diagonal $\phi_1\phi_2$ term are carried out in the same way, and the results are summarized in Tables B4 and B5 respectively.

B.4. One-loop corrections to the KK mass of the Higgs boson

For the Higgs boson, the corresponding one-loop diagrams are shown in Figs. 8–11. These diagrams are calculated as in the previous cases. Figure 11 for virtual A_μ can be obtained by making use of

the propagators in Eq. (42) and the $H^\dagger H A_\mu$ vertex in Table A2, such that

$$\begin{aligned}
\mathrm{i}\Xi_{\mathrm{Fig.11}}(p;\ell m,\ell' m') = \frac{1}{4R^2}\sum_{\ell_1=0}^{\ell_{\max}}\sum_{\ell_2=0}^{\ell_{\max}}\sum_{m_1=-\ell_1}^{\ell_1}\sum_{m_1'=-\ell_1}^{\ell_1}\int\frac{\mathrm{d}^4k}{(2\pi)^4}\\
\times \mathrm{i}g_{6a}T^a(p+k)^\mu J^1_{\underline{\ell_1 m_1'};\ell_2 m_1'-m';\ell' m'}\\
\times\frac{\mathrm{i}}{k^2-M_{\ell_1}^2}[\delta_{m_1-m,m_1'-m'}+(-1)^{\ell_2}\delta_{-m_1+m,m_1'-m'}]\\
\times \mathrm{i}g_{6a}T^a(p+k)_\mu J^1_{\underline{\ell m};\underline{\ell_2 m_1-m};\ell_1 m_1}\\
\times\frac{-\mathrm{i}}{(p-k)^2-M_{\ell_2}^2}[\delta_{m_1,m_1'}+(-1)^{\ell_1}\delta_{-m_1,m_1'}].
\end{aligned}\tag{B14}$$

After summing over m_1', it is separated into the bulk and the boundary contribution as in the previous cases. We then arrange the terms in the form of Eqs. (84) and (85) using Eq. (B35) to extract terms proportional to p^2, and each coefficient is given in the first part of Table B6. Figure 11 for one virtual ϕ_i is calculated in the same way by applying the propagator of ϕ_i in Eq. (39), the propagator of the scalar boson in Eq. (42), and the $H^\dagger H\phi_i$ vertex in Table A2, and the results are summarized in the second part of Table B6.

Figure 10 for virtual A_μ is calculated by making use of the propagator of A_μ in Eq. (36) and the $H^\dagger H(A_\mu)^2$ vertex in Table A2 such that

$$\begin{aligned}
\mathrm{i}\Xi^{\mathrm{Fig.9}(A_\mu)}(p;\ell m;\ell' m') = \mathrm{i}\frac{g_{6a}^2}{R^2}T_a^2 g_{\mu\nu}g^{\mu\nu}\sum_{\ell_1=0}^{\ell_{\max}}\sum_{m_1=-\ell_1}^{\ell_1}\sum_{m_1'=-\ell_1}^{\ell_1}\int\frac{\mathrm{d}^4k}{(2\pi)^4}K^1_{\underline{\ell_1 m_1};\ell_1 m_1';\underline{\ell m};\ell' m'}\\
\times\frac{1}{2}\frac{-\mathrm{i}}{k^2-M_{\ell_1}^2}[\delta_{m_1,m_1'}+(-1)^{\ell_1}\delta_{-m_1,m_1'}]\delta_{m+m_1,-m,m_1'},
\end{aligned}\tag{B15}$$

which is expressed in the form of Eqs. (84) and (85), and each coefficient is summarized in the third part of Table B6. Figure 10 for virtual ϕ_i is calculated in the same way by applying the propagator of ϕ_i in Eq. (39) and the $H^\dagger H(\phi_i)^2$ vertex in Table A2, and the results are summarized in the fourth part of Table B6.

Figure 8 is calculated in the same manner by making use of the propagator of the scalar boson in Eq. (42) and the $(H^\dagger H)^2$ vertex in Table A2 such that

$$\begin{aligned}
\mathrm{i}\Xi^{\mathrm{Fig.11}}(p;\ell m;\ell' m') = \frac{-\mathrm{i}\lambda_6}{2R^2}\sum_{\ell_1=0}^{\ell_{\max}}\sum_{m_1=-\ell_1}^{\ell_1}\sum_{m_1'=-\ell_1}^{\ell_1}\int\frac{\mathrm{d}^4k}{(2\pi)^4}K^1_{\underline{\ell_1 m_1};\ell_1 m_1';\underline{\ell m};\ell' m'}\\
\times\frac{\mathrm{i}\delta_{m+m_1,m'+m_1'}}{k^2-M_{\ell_1}^2}[\delta_{m_1,m_1'}+(-1)^{\ell_1}\delta_{-m_1,m_1'}],
\end{aligned}\tag{B16}$$

which is expressed in the form of Eqs. (84) and (85), and each coefficient is summarized in the fifth part of Table B6.

Figure 9 is calculated by making use of the propagator of the scalar boson in Eq. (42) and the $\Psi\Psi H$ vertex in Table A2 such that

$$
\begin{aligned}
\mathrm{i}\Xi^{\mathrm{Fig.10}}(p;\ell m;\ell' m') = -\frac{(Y_f)^2}{4R^4}\sum_{\ell_1=0}^{\ell_{\max}}\sum_{\ell_2=0}^{\ell_{\max}}\sum_{m_1=-\ell_1}^{\ell_1}\sum_{m_1'=-\ell_1}^{\ell_1}\int\frac{\mathrm{d}^4k}{(2\pi)^4}\\
\times\mathrm{Tr}\Big[(I^{\alpha}_{\ell_1 m_1';\ell' m';\ell_2 m_1'-m'}P_L + I^{\beta}_{\ell_1 m_1';\ell' m';\ell_2 m_1'-m'}P_R)\frac{\mathrm{i}}{\gamma^\mu k_\mu + \mathrm{i}\gamma^5 M_{\ell_1}}\\
\times(\delta_{m_1,m_1'} \mp (-1)^{\ell_1+m_1}\delta_{-m_1,m_1'}\gamma^5)(I^{\alpha}_{\ell_2 m_1-m;\underline{\ell m};\ell_1 m_1}P_L + I^{\beta}_{\ell_2 m_1-m;\underline{\ell m};\ell_1 m_1}P_R)\\
\times\frac{\mathrm{i}}{\gamma^\mu(k_\mu-p_\mu)+\mathrm{i}\gamma^5 M_{\ell_2}}(\delta_{m_1-m,m_1'-m'} \mp (-1)^{\ell_2+m_1+m}\delta_{-(m_1-m),m_1'-m'}\gamma^5)\Big],
\end{aligned}
\tag{B17}
$$

which is expressed as in the previous case and the result is summarized in Table B7.

References

[1] T. Appelquist, H. C. Cheng, and B. A. Dobrescu, Phys. Rev. D **64**, 035002 (2001).
[2] I. Antoniadis, Phys. Lett. B **246**, 377 (1990).
[3] K. Agashe, N. G. Deshpande, and G. H. Wu, Phys. Lett. B **511**, 85 (2001).
[4] K. Agashe, N. G. Deshpande, and G. H. Wu, Phys. Lett. B **514**, 309 (2001).
[5] T. Appelquist and B. A. Dobrescu, Phys. Lett. B **516**, 85 (2001).
[6] T. Appelquist and H. U. Yee, Phys. Rev. D **67**, 055002 (2003).
[7] J. F. Oliver, J. Papavassiliou, and A. Santamaria, Phys. Rev. D **67**, 056002 (2003).
[8] D. Chakraverty, K. Huitu, and A. Kundu, Phys. Lett. B **558**, 173 (2003).
[9] A. J. Buras, M. Spranger, and A. Weiler, Nucl. Phys. B **660**, 225 (2003).
[10] P. Colangelo, F. De Fazio, R. Ferrandes, and T. N. Pham, Phys. Rev. D **73**, 115006 (2006).
[11] I. Gogoladze and C. Macesanu, Phys. Rev. D **74**, 093012 (2006).
[12] H. C. Cheng, J. L. Feng, and K. T. Matchev, Phys. Rev. Lett. **89**, 211301 (2002).
[13] G. Servant and T. M. P. Tait, Nucl. Phys. B **650**, 391 (2003).
[14] M. Kakizaki, S. Matsumoto, Y. Sato, and M. Senami, Phys. Rev. D **71**, 123522 (2005).
[15] S. Matsumoto and M. Senami, Phys. Lett. B **633**, 671 (2006).
[16] F. Burnell and G. D. Kribs, Phys. Rev. D **73**, 015001 (2006).
[17] M. Kakizaki, S. Matsumoto, and M. Senami, Phys. Rev. D **74**, 023504 (2006).
[18] K. Kong and K. T. Matchev, JHEP **0601**, 038 (2006).
[19] S. Matsumoto, J. Sato, M. Senami, and M. Yamanaka, Phys. Rev. D **76**, 043528 (2007).
[20] A. K. Datta, K. Kong, and K. T. Matchev, Phys. Rev. D **72**, 096006 (2005); **72**, 119901 (2005) [erratum].
[21] S. Matsumoto, J. Sato, M. Senami, and M. Yamanaka, Phys. Rev. D **80**, 056006 (2009).
[22] S. Matsumoto, J. Sato, M. Senami, and M. Yamanaka, Phys. Lett. B **647**, 466 (2007).
[23] B. A. Dobrescu and E. Poppitz, Phys. Rev. Lett. **87**, 031801 (2001).
[24] T. Appelquist, B. A. Dobrescu, E. Ponton, and H. U. Yee, Phys. Rev. Lett. **87**, 181802 (2001).
[25] N. Maru, T. Nomura, J. Sato, and M. Yamanaka, Nucl. Phys. B **830**, 414 (2010).
[26] H. Dohi and K.-y. Oda, Phys. Lett. B **692**, 114 (2010).
[27] N. Maru, T. Nomura, J. Sato, and M. Yamanaka, Eur. Phys. J. C **66**, 283 (2010).
[28] K. Nishiwaki, JHEP **1205**, 111 (2012).
[29] K. Nishiwaki, K.-y. Oda, N. Okuda, and R. Watanabe, Phys. Lett. B **707**, 506 (2012).
[30] T. Kakuda, K. Nishiwaki, K.-y. Oda, and R. Watanabe, Phys. Rev. D **88**, 035007 (2013).
[31] D. Kapetanakis and G. Zoupanos, Phys. Rept. **219**, 1 (1992).
[32] T. Nomura and J. Sato, Nucl. Phys. B **811**, 109 (2009) [arXiv:0810.0898 [hep-ph]].
[33] S. Bauman and K. R. Dienes, Phys. Rev. D **85**, 125011 (2012) [arXiv:1112.5631 [hep-ph]].
[34] S. Bauman and K. R. Dienes, Phys. Rev. D **77**, 125005 (2008) [arXiv:0712.3532 [hep-th]].
[35] S. Bauman and K. R. Dienes, Phys. Rev. D **77**, 125006 (2008) [arXiv:0801.4110 [hep-th]].
[36] H. C. Cheng, K. T. Matchev, and M. Schmaltz, Phys. Rev. D **66**, 036005 (2002).
[37] T. Ohlsson and S. Riad, Phys. Lett. B **718**, 1002 (2013) [arXiv:1208.6297 [hep-ph]].

[38] A. Lichnerowicz, Bull. Soc. Math. Fr. **92**, 11 (1964).
[39] A.A. Abrikosov, arXiv:hep-th/0212134.
[40] Z. Horvath, L.Palla, E. Cremmer, and J. Scherk, Nucl. Phys. B **127**, 57 (1977).
[41] S. Randjbar-Daemi, A. Salam, and J.A. Strathdee, Nucl. Phys. B **214**, 491 (1983).
[42] N. S. Manton, Nucl. Phys. B **158**, 141 (1979).
[43] S. Randjbar-Daemi and R. Percacci, Phys. Lett. B **117**, 41 (1982).
[44] H. Dohi, T. Kakuda, K. Nishiwaki, K.-y. Oda, and N. Okuda, arXiv:1406.1954 [hep-ph].
[45] H. Georgi, A. K. Grant, and G. Hailu, Phys. Lett. B **506**, 207 (2001).